UNIVERSITA' DEGLI STUDI DI PADOVA
FACOLTA' DI INGEGNERIA

Corso di laurea magistrale in ingegneria energetica

Tesi di Laurea

SIMULATION OF AN EXPERIMENTAL ORC UNIT FED BY THE WASTE HEAT OF AN ONBOARD MARINE DIESEL ENGINE

Relatore
Andrea Lazzaretto

Laureando
Luca Bortolami

Anno accademico 2015/2016

Summary

ABSTRACT

Nowadays low temperature heat sources are considered one of the main research fields in the energy sector. This thesis aims to determine the best operating conditions of the experimental ORC located in the laboratory of the National Technical University of Athens (NTUA). The searched operating conditions corresponds to those that maximizes the total recovery efficiency and, therefore, the net electrical power.

The test rig reproduces a 3 kW sized ORC system used to recover the waste heat from a Diesel internal combustion engine cooling system. The actual heat source consists in a hot water stream produced in a gas boiler having a mass flow rate of 1,5 kg/s, a temperature of 90°C and a pressure of 2,5 bar. Both the expander and the pump are volumetric devices, the former is a scroll expander while the latter is a diaphragm pump.

The ORC system and its components are modelled to evaluate the system behaviour under different operating configurations and to find the best ones. Particular effort is spent to build a detailed model of the scroll expander in order to minimize the difference between the simulations results and experimental data.

Results show the convenience in changing the nominal conditions of the system because that the actual design point is very far from the operating condition that maximized the net power output. As expected, the expander pressure ratio and working fluid mass flow rate of the are the main variables that affect the performances of the cycle. The possible problems related to different values of these two variables are studied in the final part of the work.

ABSTRACT

Le fonti a medio-basse temperature stanno acquisendo sempre maggiore importanza in questi ultimi anni e gli ORC si stanno dimostrando adatti a sfruttare questa categoria di fonti energetiche. Lo scopo di questo lavoro è lo studio di un impianto ORC come WHRS accoppiato ad un motore Diesel a bordo di una nave al fine di individuare le migliori condizioni operative. L'obiettivo è quello di massimizzare l'output elettrico avendo come input una portata d'acqua di 1,5 kg/s con una temperatura di 90°C e una pressione di 2,5 bar. Nelle condizioni di design l'impianto produce una potenza elettrica netta di 3 kW.
Il comportamento dell'impianto in diverse condizioni di lavoro è stato analizzato tramite l'utilizzo di modelli EES. Inoltre, è stato realizzato e calibrato un modello dettagliato dell'espansore scroll, in quanto elemento fondamentale per le prestazioni dell'intero ciclo.

Tramite i risultati ottenuti, è stata valutata la possibilità di cambiare il punto di design. In particolare, il rapporto di pressione e la portata di massa del fluido di lavoro si sono rivelate le variabili che influenzano maggiormente le prestazioni e la potenza elettrica netta. Tuttavia, questi cambiamenti possono comportare delle difficoltà e problematiche nella gestione dell'impianto. Tali problematiche sono state analizzate nella parte finale di questo lavoro.

1 INTRODUCTION

In these years, the research of renewables energies has grown, especially for medium and low powers. Low temperature sources, mainly waste heat from industrial or mechanical processes have been considered accurately due to the fact that they are easy to use and economically convenient. Among the analysed technologies, Organic Rankine Cycles are a viable option for low temperature sources. In fact, organic fluids present lower levels of critical pressures and temperatures and, therefore, they are suitable to exploit low temperature heat. Traditional technologies, like Rankine Steam Cycle, have revealed some economical and efficiency disadvantages. Waste heat can be recovered using waste heat recovery systems.
Several types of different WHRSs are already available on the market. Depending on the level of complexity desired, the actual electrical power consumption on-board, the rotational speed for the ship biggest possible in order to ensure the lowest possible fuel consumption for the basic performance of the ship [1], the possibilities are the following:

- ST-PT – Steam Turbine-Power Turbine generator unit

- STG – Steam Turbine Generator unit

- PTG – Power Turbine Generator unit

As a general rule we can consider the following separation:

Main engine power > 25,000 kW → Combined ST and PT

Main engine power < 25,000 kW → PTG or STG

Main engine power < 15,000 kW → PTG or ORC

The marine sector has shown interest for this type of power plants in these years. For large ships, the fuel expenses constitute about 30-55% of the total operational costs, depending on the type of vessel [2]. The goal is to reduce fuel expenses and to respect new efficiency regulations, e.g. the EEDI -Energy Efficiency Design Index [3].

The international regulations are changing towards stricter limits about emissions of CO2 and oxides of sulphur and nitrogen (SOx and NOx). Many studies have been carried out in order to lower the fuel consumption. Besides, some researches have been focused on advanced combustion technologies, such as the HCCI [4] [5], the lean combustion [6], and the stratified combustion [7], in order to achieve a higher overall efficiency and reduce overall emissions. Nevertheless, these technologies have reached a quite matured stage, and it is hard to achieve further improvements by using these solutions. Consequently, an alternative must be found: a valuable alternative approach to improve overall energy efficiency is to use the waste heat [8]. The steam Rankine cycle is focused on higher temperature WHR mainly from the exhaust gases of the main engines of a ship, while the ORC/Kalina cycles are more suitable for smaller engines like the marine auxiliary ones, while at the same time they can also be used for WHR from lower temperature heat sources (e.g. the jacket water of diesel engines). However, optimisation results suggest that the Kalina cycles present no significant advantages compared to the ORC[9].

Even though the energy efficiency of 50% is relatively high, the primary objective for the shipowner is still to lower ship operational costs further, as the total fuel consumption of the ship is still the main target. Large marine diesel engines are particularly well suited to be coupled with a WHR system [10] as the engine loses a large part of the fuel energy to the environment, mainly with the exhaust gases (up to 25% of the input energy) and the jacket water (up to 5.1% of the input energy [11]). Nevertheless, both of these heat sources, originating from the main engine, are used for covering the internal heating needs of a ship (e.g. heavy fuel oil pre-heating, fresh water generation, exhaust gas boiler), while the respective ones from the auxiliary engines remain unused. Several researchers have proposed WHR systems for main marine diesel engines [9] [10] [11] [12] [13] [14] while only a few studies have been carried out about whr systems for the auxiliary engines [15].

Other studies have been carried out on WHRS from marine diesel engines. Song et al. [16] realized a thermodynamic analysis of an ORC WHRS for marine diesel engines. Pedersen et al. [17] studied accurately the major waste heat sources available on ships and compared different technologies for their potential and suitability for marine use. A similar work has been fulfilled by Baldi et al. [18] in which they focused more on the different optimization procedures for WHRS for marine engines. A general study of an ORC for ICE waste heat recovery has been conducted by Depcik et al. [19], focusing on the importance of the selection of the working fluid and the expander.

The expander is a crucial component of the ORC. The choice of the expander strongly depends on the operating conditions and even on the size of the installation

Scroll machine is a volumetric machine, widely studied and used for the ORC application, thanks to its reduced number of moving parts, low price, reliability and broad availability at a wide power output range as studied on [20]. Moreover, this

technology is very well-known in compressor mode due to its extensive use in refrigeration and air-conditioning industry. Numerous scroll expander prototypes have been tested for different fluids but their use has mainly been limited to experimental work.
Yanagisawa et al. [21] carried out an experimental study on an oil-free scroll-type air expander. From their work it could be observed that the performance is heavily reduced by the mechanical loss, but leakage losses become important as the rotational speed decreases. The maximal values of volumetric and isentropic effectiveness were respectively 76% and 60%. Zanelli et al. [20] carried out an experimental investigation on a hermetic scroll expander-generator fed with refrigerant R134a. The machine produced a power ranging from 1.0 to 3.5 kW with a maximal isentropic effectiveness of 65%. Kane et al. [22] designed, built and tested a prototype of hybrid solar thermal power plant associating solar collectors, cogeneration engines and two superposed ORC, equipped with hermetic scroll expanders. Manzagol et al [23] studied a cryogenic scroll expander used for a 10 L/h helium liquefier. The expander was tested on a Brayton cycle refrigerator and reached an isentropic effectiveness of 50-60% for supply gas conditions of 35K and 7 bar. Gao et al. [24] studied an ORC with scroll expanders of different displacements for a given heat source temperature of 105°C. With a displacement of 66 ml/r the results show that the isentropic efficiency fluctuates over a small range from 0.62 to 0.7. Another scroll expander with a displacement of 86 ml/r is used to investigate how scroll expander displacement influences the performance of the ORC system. Under the same operating conditions as used previously, the isentropic efficiency decreases from 0.7 to 0.41 when the inlet pressure of the expander increases.

The aim of this work is the study and simulation of the ORC system and in particular of the expander so as to find the best working conditions, and, besides, discuss possible further developments. The simulations are made considering the components that are available now at the laboratory of the NTUA in Athens. As said above, the ORC cycle exploits the waste heat of the auxiliary engines and only a few works have been achieved about WHRS for the auxiliary engines.
The selection of the expander and the working conditions are explained.

2 THE MARINE ORC PROTOTYPE THE METODOLOGY

In this chapter the marine ORC prototype studied in this work and the methodology used are described. The selection of the expander and the simplifying hypothesis are justified.

2.1 THE MARINE ORC PROTOTYPE

In this paragraph the marine ORC prototype studied in this work is described. The description is reported from [15].

The marine ORC prototype unit is based on a conventional low-temperature subcritical Organic Rankine Cycle using R134a as working fluid. This experimental unit has been designed as a waste heat recovery system for the jacket water of marine diesel auxiliary internal combustion engines (ICEs). In order to simulate the operating characteristics of such engines, the heat input is in the order of 90kWth at a low-temperature (90°C), and is supplied by a natural gas boiler via an intermediate plate heat exchanger (evaporator). The boiler thermal output is adjustable and thus part load operation can be simulated as well. A schematic diagram of the unit is presented in Figure 1.

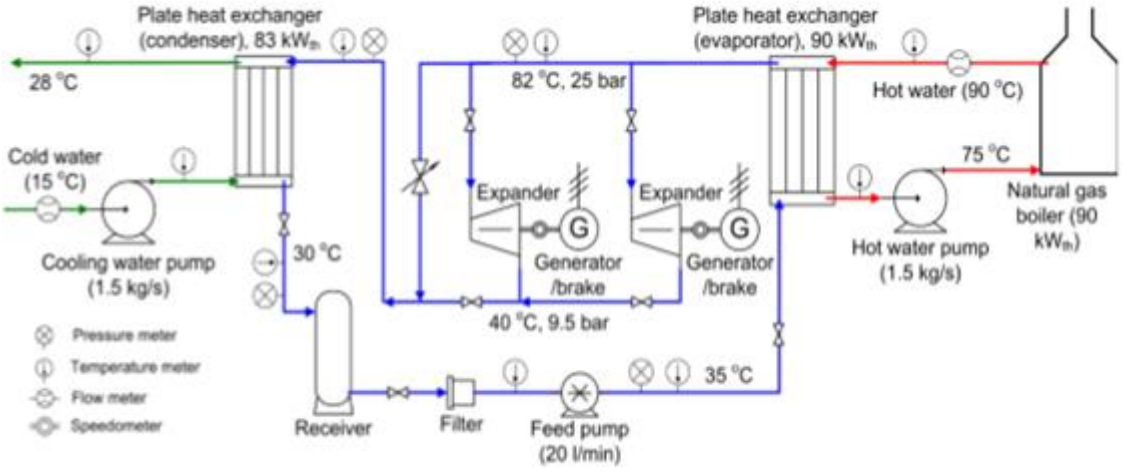

Fig. 1: Schematic diagram of the ORC prototype unit, [15]

The hot water circuit provides the heat input into the cycle. The pressure of the water in the hot circuit is 2,5 bar and the mass flow rate is 1.5 kg/s.

Both of the heat exchangers in the evaporation and the condensation are plate heat exchangers. This kind of exchangers use metal plates to allow the transfer of the heat between two fluids. The main advantages are:

- their compactness: they present a larger exchange surface with the same volume compared to the conventional heat exchangers
- their flexibility: adding plates is sufficient to supply an improved necessity

This kind of heat exchangers is a viable option for power plants that present low level of temperature and pressure, usually up to 250 °C and 25-28 bar.

The cycle is fed by a receiver (feed tank) at an average pressure of 9.5 bar and an average temperature of 30 °C. These parameters are controlled by the cold water flow in the condenser, which is adjusted by a regulatory valve. The mass flow rate is 1,5 kg/s. The powers of the two pumps involved in evaporation and condensation are considered constant even though it varies as the mass flow rate changes. However, the modification of the mass flow rate is limited and it affects little the powers.

The feed pump is a positive displacement multi-diaphragm pump that subsequently raises the pressure of the fluid at about 22-25 bar, depending on the operational conditions, and leads it to the evaporator. At a nominal speed of 960rpm a flow rate of 20lt/min (1,5 kg/s) is achieved. The rotational speed of the pump is controlled by a frequency drive. As a result, the refrigerant mass flow rate can be adjusted according to the unit load and the desired superheating temperature of the vapour, given the fact that the delivered volume flow rate of diaphragm pumps is a linear function of their rotational speed.

Before entering the pump, the working fluid passes through a sub-cooler, that lowers the temperature at the inlet conditions of the pump of about 2°C. The sub-cooler has been introduced in a second moment so as to avoid the cavitation in the pump.

The high pressure vapour is expanded in two parallel scroll expanders, while a by-pass section controlled by an electromagnetic valve can alternatively lead the flow directly to the condenser. These expanders are two open-drive scroll compressors in reverse operation.

Finally, the expanded vapour is led to the condenser (plate heat exchanger), the condensate returns to the feed tank, and the cycle starts over. The ORC unit produces about 3 kWel of net electrical power, at a design cycle pressure of 25bar and a temperature of 82°C.

Various instruments have been mounted at all key-points of the cycle (Figure 1), in order to evaluate the performance of the different components of the ORC unit. Thermocouples and pressure transducers record the thermodynamic procedure; an electromagnetic flow-meter supervises the hot water volume flow rate and two tachometers the scrolls‟ actual rotational speed. All important parameters regarding the

electrical motors of both the pump and the generators, such as the consumed/produced active power are retrieved by the respective frequency drives.

It is noted that the automatic control of the system (including the frequency drives), the measurements and the data logging is materialised with the use of an industrial PLC (Programmable Logic Controller) and a SCADA (Supervisory Control and Data Acquisition) environment, which constitutes an important step towards the standardization and commercialization of such micro-scale units.

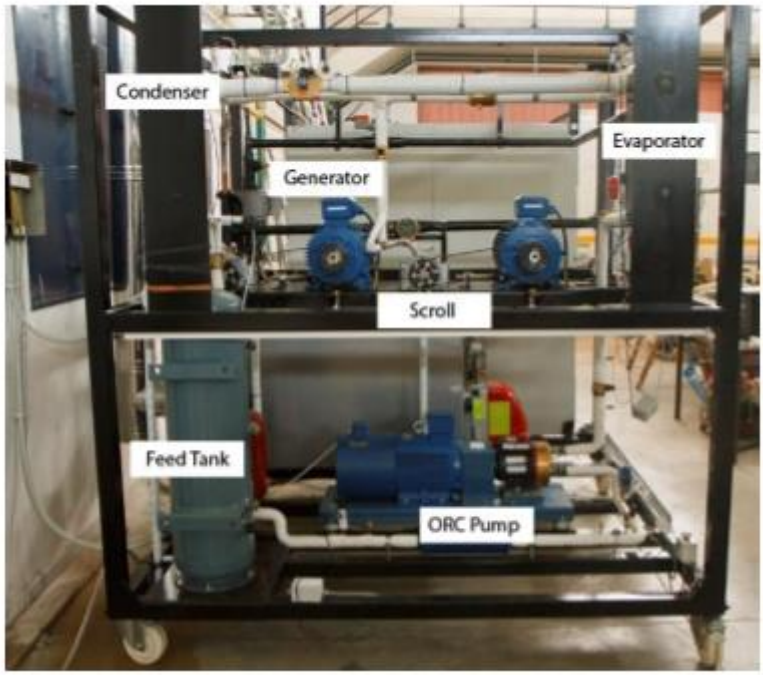

Fig. 2: Picture of the ORC unit, Athens

2.2 SELECTION OF THE EXPANDER

In this section, the selection of the expander made for the ORC cycle described above is justified. Many possibilities are taken into account. The expander has a crucial role in the overall system performance and selection of this component must be considered accurately.

There are two main types of machines: the volumetric (displacement) and the turbo (dynamic) type.

The second type, such as radial turbines and axial turbines, is usually the most suitable option for output power of at least 50 kW. Some recent researches have considered and tested turbine expanders in small-scale ORC systems[25-27]. Nevertheless, this solution does not appear suitable for small scale systems as the one studied in this work, especially due to the exponential increasing of rotational speed with the decrease of the scale. Besides, this type of machine was excluded very soon owing to its great cost and the limited availability.

Therefore, different volumetric machines could have been considered. The volumetric expanders are characterized by lower flow rates, higher pressure ratios, and much lower rotational speed compared to the turbomachines. The pressure drop is caused by the decrease in an area of expansion chamber along the flow length. The built-in volume ratio of the expander is the ratio between expansion chambers at the beginning and at the end of the process.

Currently, most of expanders used for low grade heat and waste heat recovery systems are obtained from modified compressors due to the fact that the volumetric expander market is not mature yet unlike the compressor market.
There are many factors that affect the selection of the most suitable expander, such as efficiency, power range, reliability, rotational speed, cost and availability.

There are two types of volumetric machines: reciprocating machines and rotative machines. The first type includes the piston expanders while the second one includes vane expanders, screw expanders and scroll expanders.

- Piston expanders

Reciprocating pistons can be classified into radial piston expanders and axial piston expanders. The axial type is compact in size and less noisy than the radial ones.

Piston expanders can operate at temperatures (almost 600°C) and pressures (100 bar) higher compared to the rotative expanders. The internal volume ratio is higher too, in fact it varies from 6 to 14. They present low speed (600-2000 rpm) so that they can be directly attached to the generator. The highest isentropic efficiency reported in literature is 76% [28] but in most cases its value is less than 50%.

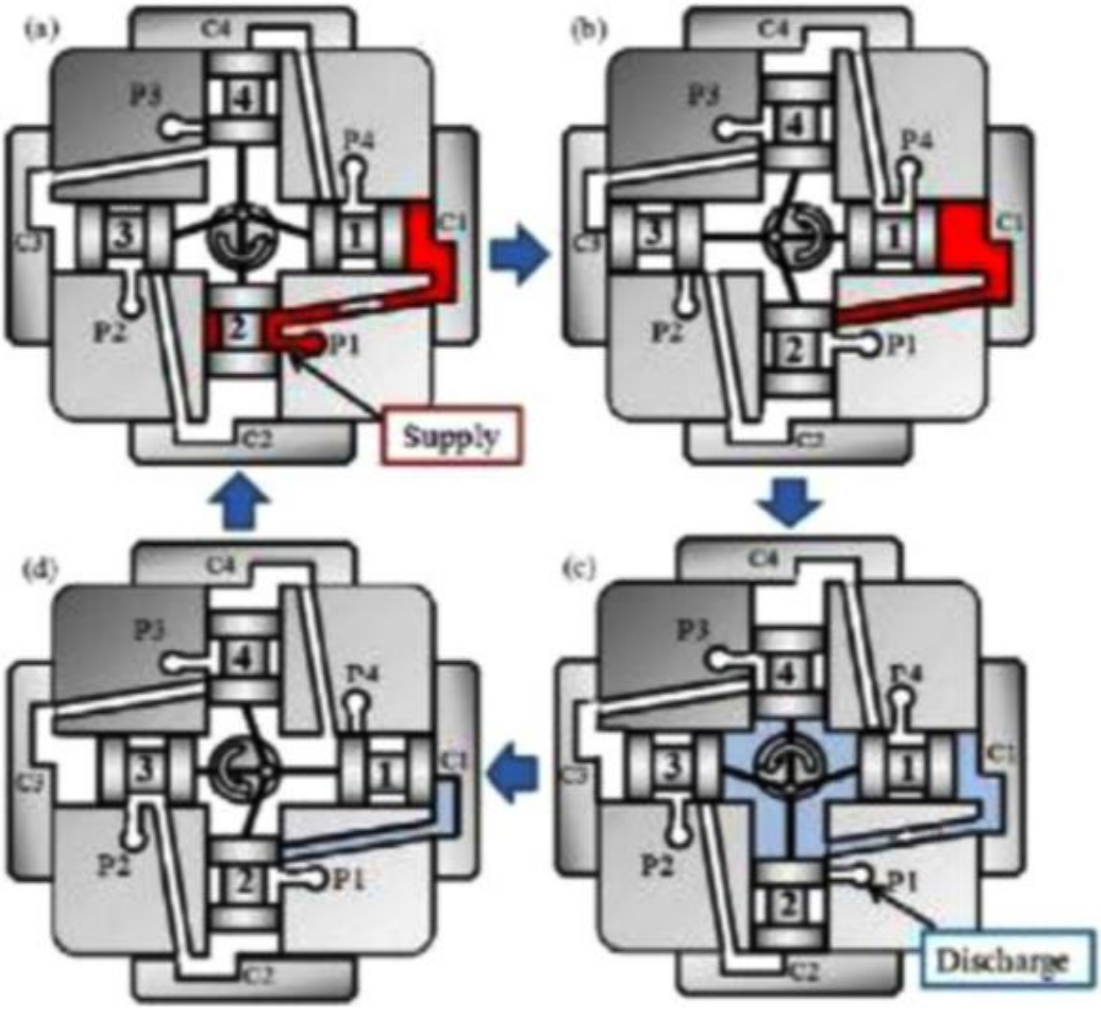

Figure 3: Scheme of the piston expander

- Vane expander

They have a simple structure and a limited cost. Besides, they present a good volumetric efficiency and they can operate at relatively high temperatures (150°C) and pressures(80 bar). The built-in ranges usually from 2 to 8. In literature, the maximum isentropic efficiency that can be found is 71% [29-30]. They present low rotational speed, 1500-3000 rpm so that they can be directly attached to the generator.

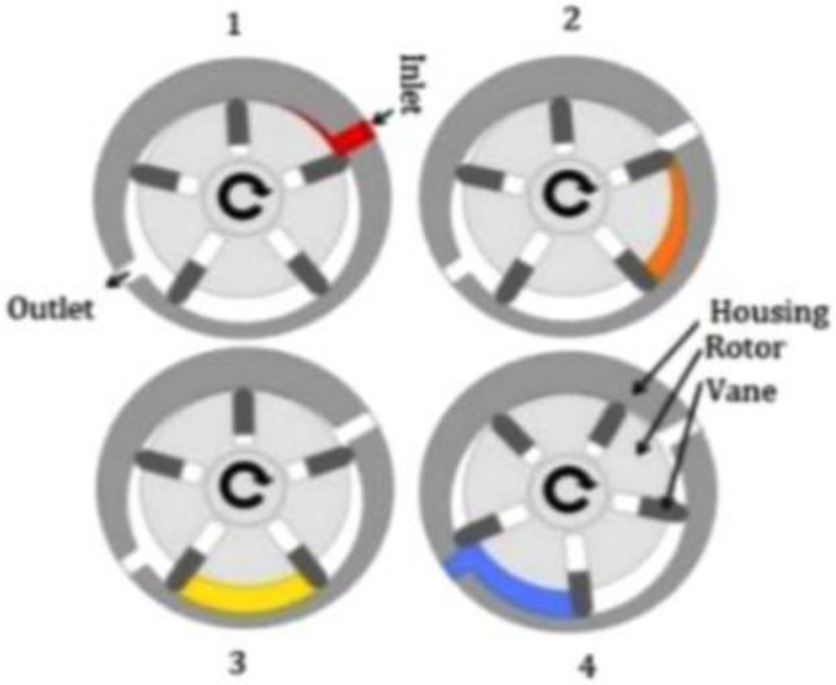

Figure 4: Scheme of the vane expander

- Screw expanders

This kind of expanders present simple structure, good values of temperatures and pressures and a wide range of capacities and sizes. However, they are characterized by a relatively high cost. Furthermore, they are not recommended for sizes less than 10 kW owing to leakage losses. Therefore, this type of expanders has been excluded.

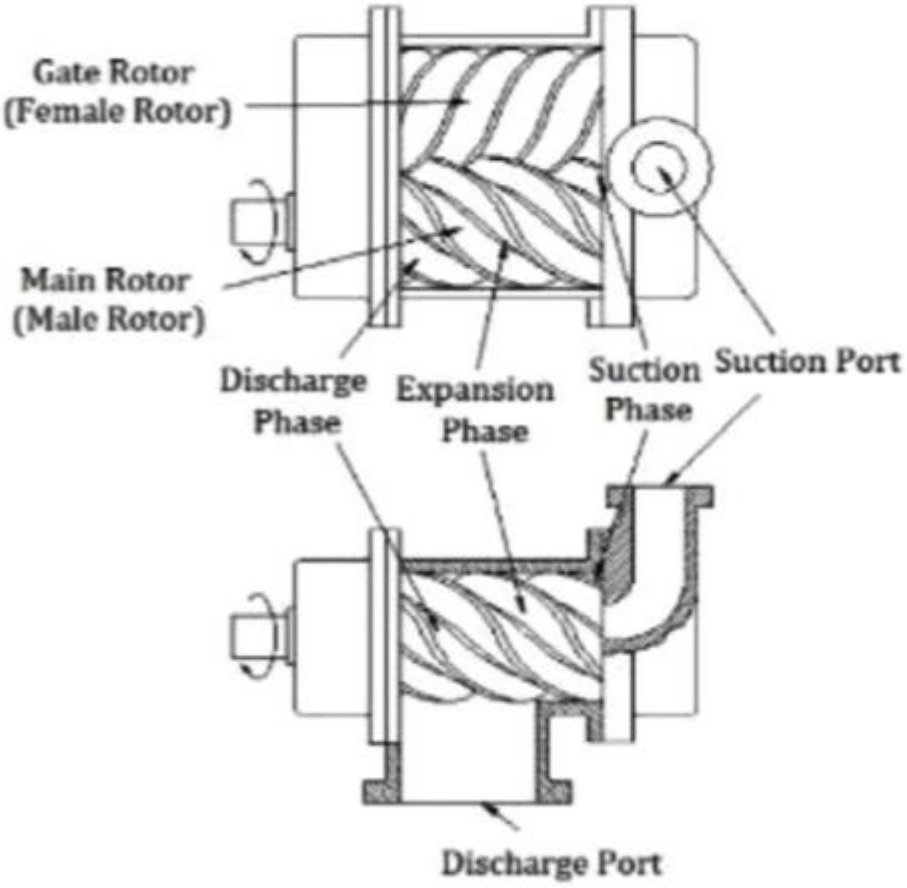

Figure 5: Scheme of the screw expander

- Scroll expander

Currently, most of scroll expanders used for small-scale applications are scroll compressors used in reverse. Scroll expander consists of two spirals, an orbiting scroll and a fixed scroll. They can operate at pressures around 80 bar and temperature up to 200-250°C. The built-in volume ratio ranges from 1,5 to 5. The highest value of isentropic efficiency in literature is 83% [31] even though most cases present a value around 65-70%. The rotational speed varies usually from 1000 to 4000 rpm.

There are three types of scroll expander: hermetic scroll expander, semi-hermetic scroll expander and open-drive scroll expander.

In the hermetic type the components and the motor drive are assembled with a common shaft and welded into a steel container, which cannot be opened for repair. To operate a hermetic scroll compressor in reverse as expander, the compressor shell must be cut open to remove check valves that prevent high pressure fluid backflow.

Semi-hermetic scroll expanders present relatively compact structure compared to the hermetic type and they can be modified into an expander by only removing the reed valve.

In the open-drive scroll type the electric motor is not assembled inside the shell and the machine is driven by automotive engine shaft through the external belt pulley. In compressor mode it consists of the compressor itself and an external clutch. The clutch engages and disengages the power transmission. In reverse mode, the belt pulley and clutch assembly acts as a convenient connection control between the expander and the electric generator, especially for expander experimental investigations.

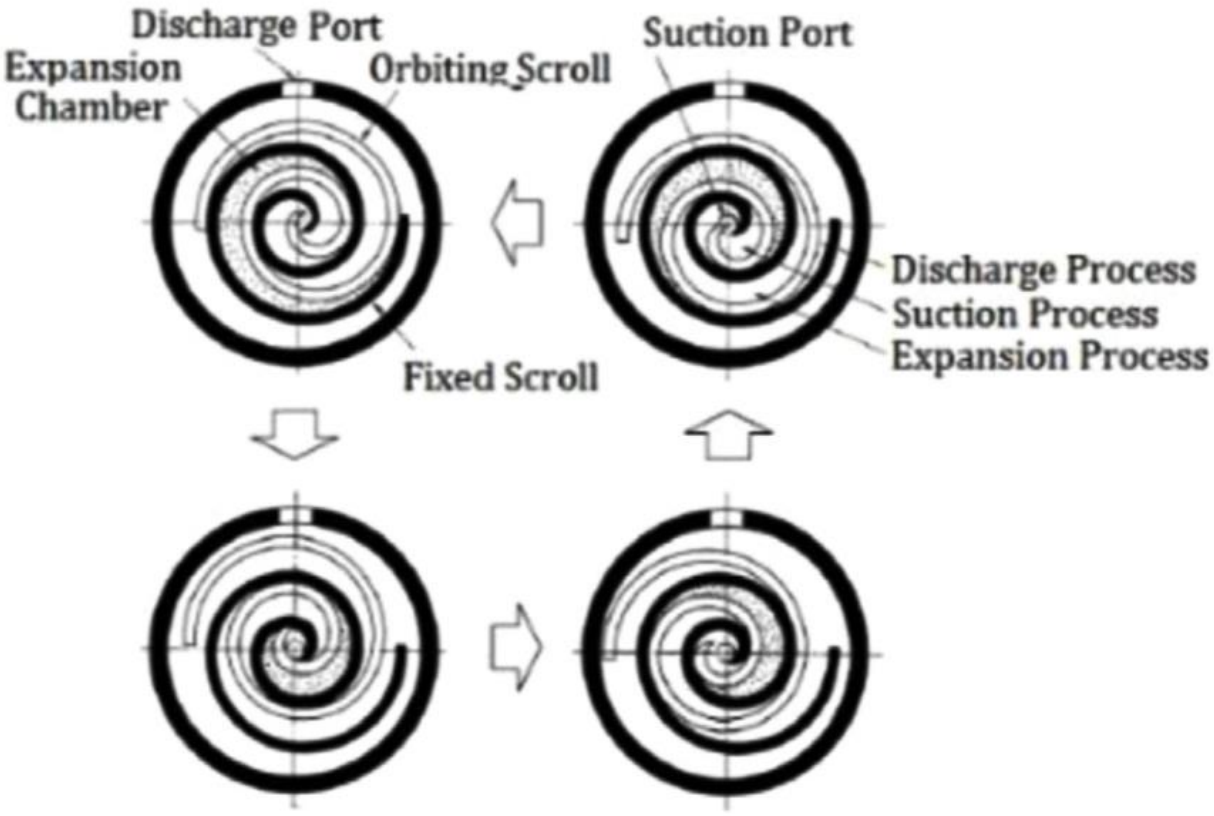

Figure 6: Scheme of the scroll expander

- Final selection of the expander

Above different solutions for the expander have been analysed. Here, some of the values reported previously are compared and discussed and the reasons of the selection are clarified.

The criteria for choosing in this kind of work are mainly the cost and availability of the machine and the performances.

Turbo-machines have been excluded mainly due to the high cost, the limited availability and the immaturity of this technology for small scale systems.

Screw expanders have been excluded owing to the cost and very small size of the system studied.

Piston expanders present values of pressure ratio that are too high for the conditions of the expander. Therefore, they have been excluded even though they present many characteristics that are suitable for this work, such as cost, availability, rotational speed and performances.

Vane expanders and scroll expanders have similar features. The performances are similar like the costs. They are both suitable for this study. Nevertheless, in this particular case, a scroll expander has been chosen owing to the fact that it was available in the laboratory due to previous studies.

It is an open drive scroll with a built-in pressure ratio of 2,3 and a swept volume of 121,9 cm^3.

2.3 CONCLUSIONS

In this chapter the ORC prototype available in the laboratory of the NTUA in Athens and its component are described. The selection of the scroll expander has been made owing to its cost and availability since the fact that the heat input presents a low quality and an important cost for an expander with better performances is not justified. The hypothesis of the models are reported and in most cases they have been validated experimentally.

The models of the ORC and of the expander are described in the following chapters and the methodology and the hypothesis that they use are the ones described in the chapter 3.

3 METODOLOGY

In this paragraph the methodology used to study the ORC cycle and the expander is explicated and the hypothesis are reported.

EES models are utilized to simulate the operation of the ORC cycle before and of the expander after.

The approach is sequential-modular:

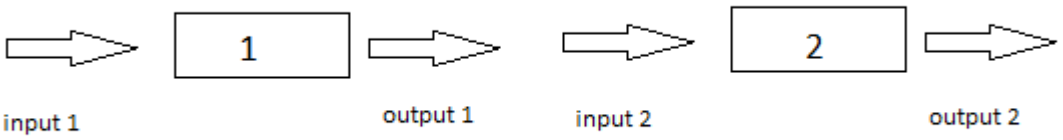

Figure 7: Sequential-modular approach

Output 1 becomes Input 2

For example: Suppose that the component 1 is the expander and the component 2 is the condenser. Input 1 are the temperature, the pressure and the mass flow rate at the inlet conditions of the expander. Once calculated the Output 1, that consists of the temperature, the pressure and the mass flow rate at the outlet conditions of the expander, this output becomes the Input 2 and, therefore, the temperature, the pressure and the mass flow rate at the inlet conditions of the condenser.

The models are made of various equations that belong to the following categories:

- equations that concern mass and energy balances of each component
- equations that express the performance features of each component
- equations of the physical properties and equations of state
- particular experimental equations of the unit

The hypothesis and the characteristics of the models are:

- The models are at steady state and zero-dimensional.

- The mass flow rate is imposed by the pump.

- The T_{in} and the mass flow rate of the water of the hot circuit are known. The pressure of the water of the hot circuit is 2,5 bar. The input heat is calculated. The maximum temperature of the cycle is imposed by the heat balance of the evaporator. The minimum allowed outlet temperature of the water of the hot circuit is 20°C. It is used to calculate the maximum heat that can be exploited by the cycle in order to compute a total recovery efficiency. The maximum heat input obtained is 125,2 kW. However, the problems connected with a low temperature such as the thermal stress need to be very accurately considered due to the location of the unit on a ship.

- The efficiency of the plate heat exchanger of the hot circuit is 0,93 at the design conditions. This value is very high but this fact can be explained by the great number of plates compared to the heat load. In fact, there are 90 plates when to ensure a good heat exchange 70 plates would have been enough. Furthermore, this value has been validated experimentally. In off-design conditions the value of the efficiency remains almost constant as the heat load decrease while it gets lower as the heat load increase. In particular, for values of mass flow rate higher than the design mass flow rate the following equation describes the evolution of the efficiency:

$$\varepsilon = \varepsilon_{dp} * \left(\frac{m}{m_{DP}} \right)^{-0,1}$$

- The expander inlet pressure that is the evaporator exhaust pressure is usually supposed fixed but it can be imposed by the expander itself. In fact, the pressure is a function of the density at the inlet conditions of the expander and it depends on the mass flow rate (imposed by the pump) and the features of the expander (swept volume, built-in volume ratio, rotational speed). However, in this last case the temperature at the inlet conditions of the expander must be fixed.

- The simulations are made keeping constant the condensation pressure when it is not specified in another way.

- The power of the auxiliary components is supposed constant as the load of the cycle changes and it is 0,5 kW.

- Sub-cooling is supposed to lower the temperature of the working fluid of 2°C.

- The η_{el} and η_{mec} of the pump are supposed constant, respectively 0,85 and 0,85

- The η_{el} and η_{mec} of the expander are supposed constant, respectively at 0,95 and 0,94 in the model of the ORC. The η_{mec} is calculated from the model of the expander.

4 MODEL OF THE ORC

In this chapter the EES model of the ORC prototype described above is presented. Then, different configurations are simulated so as to have a general idea of the influence of some parameters on the whole cycle. Then, the results obtained by the model are compared to the ones obtained experimentally to assess the validity of the model.

4.1 PRESENTATION OF THE EES MODEL

In this paragraph the EES model of the cycle is analysed. It is a zero-dimensional model of the ORC prototype. The EES model is used to study the evolution of the power plant in different working conditions. The model is divided into many parts:

- waste heat
- computation of the high pressure and filling factor
- expander
- condensation
- sub-cooling
- pump
- powers and cycle efficiency
- calculation of other parameters

Waste heat

In this part the temperature and the mass flow rate of the heat source are given:

$T_{[0]}$ = 363 K = 90°C

$m_{hotcirc}$ = 1,5 kg/s

The maximum temperature of the cycle is calculated from these parameters knowing the evolution of the efficiency of the heat function as a function of $\frac{m}{m_{DP}}$

$\varepsilon_{th} = \frac{(h[1]-h[5])}{(h[0]-h[5])}$

h[1] is the enthalpy of the working fluid at the inlet conditions of the expander

h[0] is the enthalpy of the water of the hot circuit at the inlet conditions of the evaporator

h[5] is the enthalpy of the working fluid at the outlet conditions of the pump

From this equation h[1] is calculated and then T[1] is calculated.

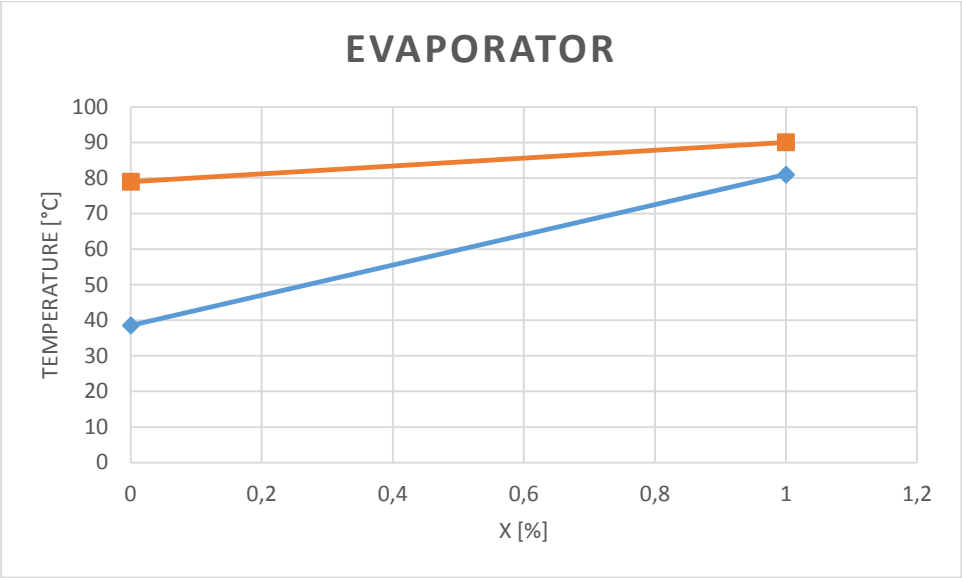

Figure 8: Heat exchange in the evaporator

The input heat is calculated by the mass flow rate of the working fluid and the difference of enthalpies:

$Q_{in} = m_{circ} * (h_1 – h_5)$

m_{circ} is calculated from the rotational speed of the pump as showed in the following part.

The outlet temperature of the hot water is calculated from the heat flow rate:

$Q_{in} = m_{hotcirc} * cp_{water} \ (T_{[0]} – T_{out})$

<u>Computation of high pressure and filling factor</u>

In this section the rotational speeds of the pump and the expander are fixed. The nominal values are:

$N_{pump} = 960$ and $N_{exp} = 1500$

N_{pump} is used to calculate the volume mass flow rate with the following equation:

$$V_{circ} = \frac{Npump - 22,86}{46,705}$$

The mass flow rate is calculated from the volume flow rate:

$m_{circ} = V_{circ} * \rho_{in,p}$

$\rho_{in,p}$ is the density at the inlet conditions of the pump.

The equation for the computation of V_{circ} is experimental.

In order to evaluate the theoretical mass flow rate the filling factor is needed. This parameter is, at this point, a function of only the rotational speed of the pump. The filling factor is the ratio between the measured mass flow rate and the mass flow rate theoretically displaced by the expander. Its value increases with internal leakage and supply cooling down, while it decreases with the supply pressure drop. The expression of the filling factor is:

$f = \frac{m_{circ} * \nu}{Vh}$

Vh = swept volume

$f = (7 * 10^{-11} * N_{exp}^3) - (3 * 10^{-7} * N_{exp}^2) + (0{,}0002 * N_{exp}) + 1{,}4346$

Once calculated the filling factor the theoretical mass flow rate can be calculated.

$m_{circ} = m_{th} * f$

Either the T[1] or the P[1] are fixed. Usually the high pressure is fixed and the temperature is calculated from the heat balance as explained before. Otherwise, with the maximum temperature fixed, the pressure is computed using the equation of state

P_1 = pressure of R134a with temperature = T_1 and density = $\rho_{in,e}$

The density of the working fluid at the inlet conditions of the expander is calculated from the theoretical mass flow rate. This parameter, together with the temperature at the same conditions, can be used to calculate the high pressure of the cycle.

$m_{th} = \frac{Nexp * Vh * \rho in,e}{rv,in}$

rv,in = built-in volume ratio

Once temperature and pressure are both known, the enthalpy is computed.
In the simulations it is specified each time which parameter is fixed and which one is calculated.

Expander

The expander is described and analysed accurately in the chapter 4 of this work. At this point the isentropic efficiency of the expander is considered as a simple function of the pressure ratio. This function is divided in two parts:

- For low values of rp (< 4,5), it can be round off

$\varepsilon_{T,is} = -(0{,}0029 * rp^4) + (0{,}0514 * rp^3) - (0{,}3164 * rp^2) + 0{,}7957 * rp - 0{,}0548$

- For high values of rp (> 4,5)

$\varepsilon_{T,is} = -0{,}0229 * rp + 0{,}7217$

The isentropic efficiency is : $\frac{h1-h2}{h1-h2is}$

$\varepsilon_{T,glob} = \varepsilon_{T,is} * 0{,}893$

0,893 is the electromechanical efficiency, supposed constant at this point

Condensation

The condensation pressure is fixed at 9,5 bar. Therefore, using the high pressure fixed or calculated before, the pressure ratio is computed.

$rp = \frac{P1}{P2}$

The temperature at the outlet conditions of the condenser is easily evaluated by the condensation pressure due to the fact that these two are mutually correlated.

Sub-cooling

After the condensation the working fluid passes through the sub-cooler. We assume that the pressure remains the same while the temperature decreases by 2 degrees. Sub-cooling heat is calculated by the mass flow rate and the difference of enthalpies, as the input heat.

$Q_{sc} = m_{circ} * (h_3 - h_4)$

Pump

Then there is the pump, that improves the pressure of the fluid from the condensation pressure to the maximum pressure of the cycle. The global efficiency of the pump is a function of the rotational speed. The electromechanical efficiency is supposed constant at 0,7225. The equations are the following:

$\varepsilon_{P,glob} = -4*10^{-11}*N\_pump^3 - 8*10^{-8}*N\_pump^2 + 0{,}0005*N\_pump - 8*10^{-5}$

$\varepsilon_{P,glob} = \varepsilon_{P,is} * \varepsilon_{P,el}$

$$\varepsilon_{P,is} = \frac{h5,is - h4}{h5 - h4}$$

Powers and efficiency

The net power is defined as the difference between the power of the expander and the power of the pump:

$P_{net} = P_{exp} - P_{pump} - 0{,}5$

0,5 is the power of the auxiliaries

$P_{exp} = m_{circ} * (h_1 - h_2)$

$$P_{pump} = m_{circ} * (h_5 - h_4) = \frac{Vcirc * (p5 - p4)}{\varepsilon P,is}$$

The thermal efficiency of the cycle is:

$$\varepsilon_{th} = \frac{Pnet}{Qin}$$

Calculation of other parameters

In this section some other parameters are calculated in order not to analyse the cycle only using the efficiency and the net power.
The pressure ratio is important due to its effect on the isentropic efficiency of the expander, mainly, and to understand how the cycle works in very different conditions. It has already been defined in the condensation section.
Another parameter is the isentropic enthalpies difference. It is the difference between the

enthalpy at the inlet conditions of the expander and the enthalpy that we would obtain if the expansion was isentropic. This parameter is the denominator in the equation of the isentropic efficiency.

$\Delta h_{is} = h_1 - h_{2,is}$

Another important parameter is the total isentropic efficiency, that is the ratio between the net power and the isentropic enthalpies difference described above. It is useful to have an idea about how much of the maximum theoretical work, considering that the pump does not consume any energy, can be exploited as output.

$$\varepsilon = \frac{Pnet}{mcirc * (h1 - h2,is)}$$

4.2 EXPERIMENTAL STUDY OF THE CYCLE

In this section the EES program of the cycle previously described is used to simulate the evolution of the ORC in different working conditions. First of all the nominal point and the values obtained in this condition are reported. After various simulations are carried out, starting from the design point and changing only one parameter per time so as to analyse its influence on the overall performances of the cycle. Then, some curves of the cycle are accomplished. Finally, the results obtained with the EES model are compared to the ones obtained experimentally in order to evaluate the validity of the model.

4.2.1 DESIGN POINT

The inputs in the nominal conditions are:

Variables	Values
N_pump	960 rpm
N_exp	1500 rpm
p_evap	25 bar
p_cond	9,5 bar
T_in_wat	363 K
m_wat	1,5 kg/s
p_wat	2,5 bar

Table 1: Inputs of the ORC model at the design point

The outputs obtained in these conditions are:

Variables	Values
delta_h_is	18,77 kJ/kg
EtaT_glob	57,66%
Eta_cycle	3,26%
EtaP_glob	37,08%
Eta_is_tot	43,68%
F	1,296
m_circ	0,3899 kg/s
P_net	2,321 kW
P_pump	1,398 kW
P_exp	4,219 kW
V_circ	0,0003344 m^3/kg
Total recovery efficiency	1,85%

Table 2: Outputs of the ORC model at the design point

4.2.2 BRIEF ANALYSIS OF THE PERFORMANCE OF THE CYCLE

In this paragraph a brief analysis of the evolution of some parameters is carried out. Different configurations are considered. The design point has been defined in the previous paragraph. Starting from these conditions, all the variables remain steady, but one at a time changes. The aim is to study the influence of the variable that changes on the performances of the cycle.

For this analysis some important simplifying assumptions are considered due to the fact that, at this point, only a first overview is required.
The isentropic efficiency of the expander is fixed at 0,65, the global efficiency of the pump is fixed at 0,3 and the filling factor is fixed at 1,1.

The parameters studied in the graphs are:

- P_out, electric output power
- P_pump, pump electric power
- P_exp, expander electric power
- Eta_is_tot, total isentropic efficiency
- Eta_th, thermal efficiency
- Eta_rec_tot, total recovery efficiency

The most important parameter is the output power. In fact, in spite of the fact that the thermal efficiency is important to be considered, the heat input is a waste heat flow rate and that means that the expenditures on the fuel are the same anyway. Therefore, the efficiency that should be considered is not the thermal efficiency but the total recovery efficiency.

Three cases are analysed:

- The condensation temperature ranges from 10 to 35°C
- The temperature at the inlet conditions of the expander ranges from 78 to 84°C
- The high pressure ranges from 20 to 27 bar

4.2.2.A CONDENSATION TEMPERATURE VARIABLE

In this part the condensation temperature varies in the range 10-35°C. This temperature is mutually correlated to the condensation pressure.

Graphs of the performances are reported as functions of the pressure ratio.

The power is:

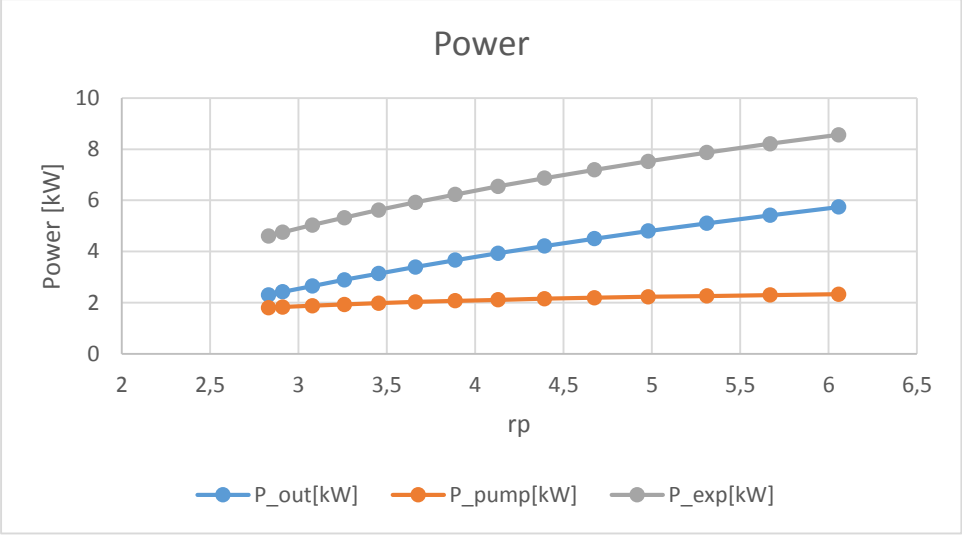

Figure 9.A: Powers of the ORC with condensation temperature variable

The total recovery efficiency:

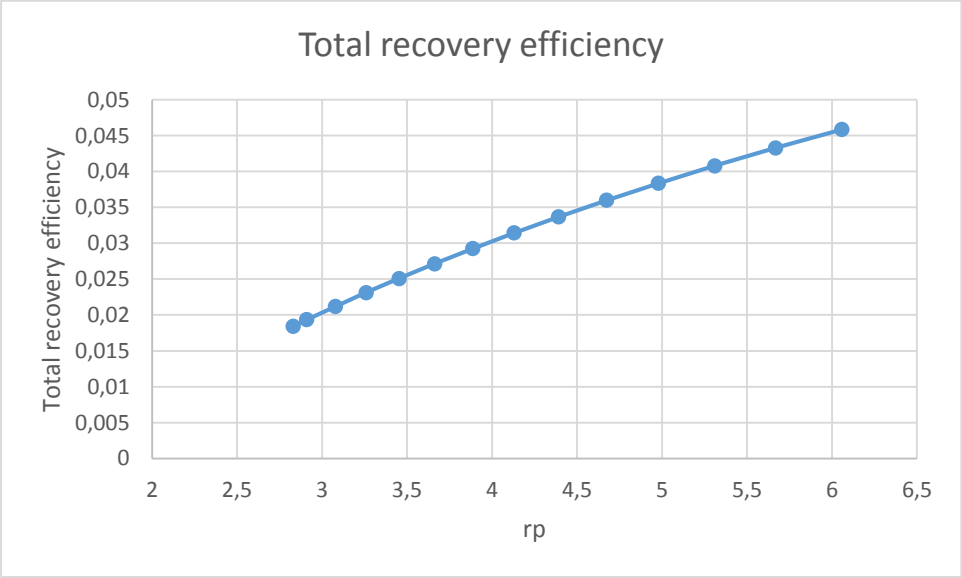

Figure 9.B: Total recovery efficiency of the ORC with condensation temperature variable

The total isentropic efficiency:

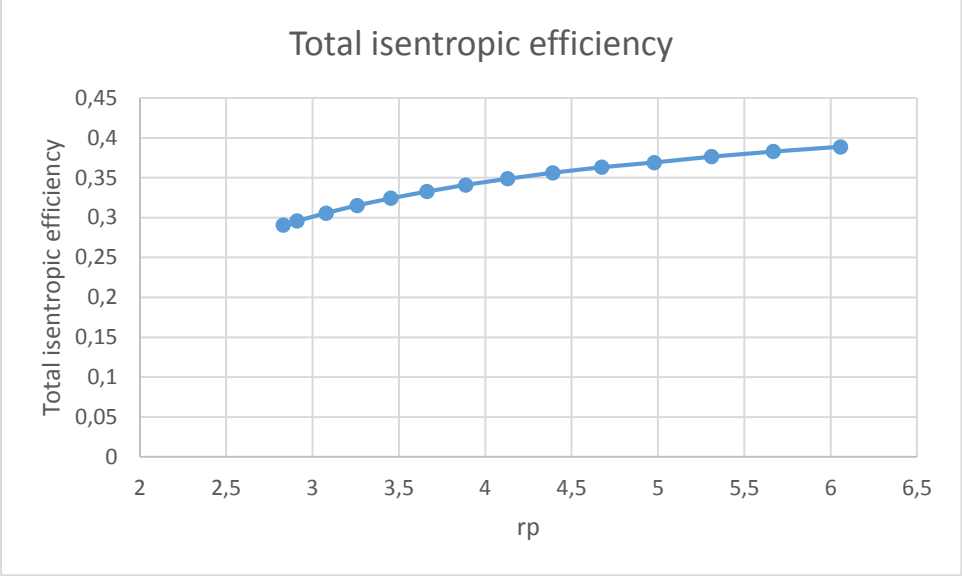

Figure 9.C: Total isentropic efficiency of the ORC with condensation temperature variable

The thermal efficiency:

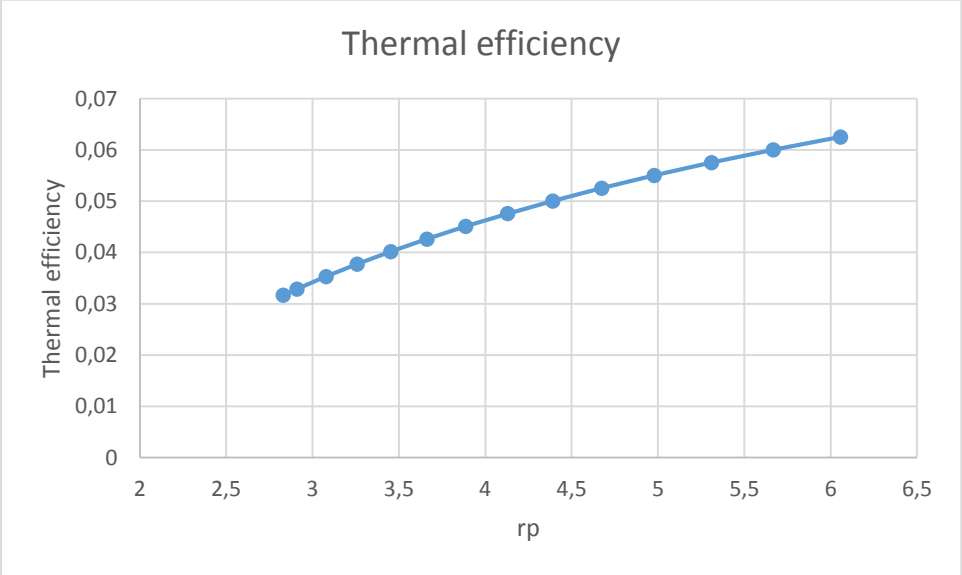

Figure 9.D: Thermal efficiency of the ORC with condensation temperature variable

The evolution of the output power and of the total recovery efficiency is the same owing to the fact that the maximum heat, that is the denominator of the efficiency, is fixed and the numerator is the output power. As it can be seen from the graphs, the pressure ratio is very important for the output of the power plant. The P_out increases highly with the rp, because the expander can take advantage of the greater available enthalpy difference, while the rise of the pump power is lower and the power of the auxiliaries is supposed constant. The net power reaches more than 6,2 kW as the pressure ratio is around 6 while in the design point conditions its value is 2,321 kW. The maximum total recovery efficiency is obtained as the pressure ratio is around 6 and its value is about 4,6%.
The isentropic efficiency of the scroll remains constant so that the total isentropic efficiency is not affected if the rp is far from the design point.
The trend of the thermal efficiency is the same as the net power and the other efficiencies, as expected.

The heat input is highly affected by the alteration of the condensation temperature.

Q=72,88 kW rp=2,829

Q=91,77 kW rp=6,056

That means that with higher values of pressure ratio the heat source is used in a better way.

4.2.2.B HIGH PRESSURE VARIABLE

In this part the high pressure ranges from 20 to 27 bar. The studied parameters are the same of the previous case.

Graphs of the performances are reported as functions of the high pressure.

The power is:

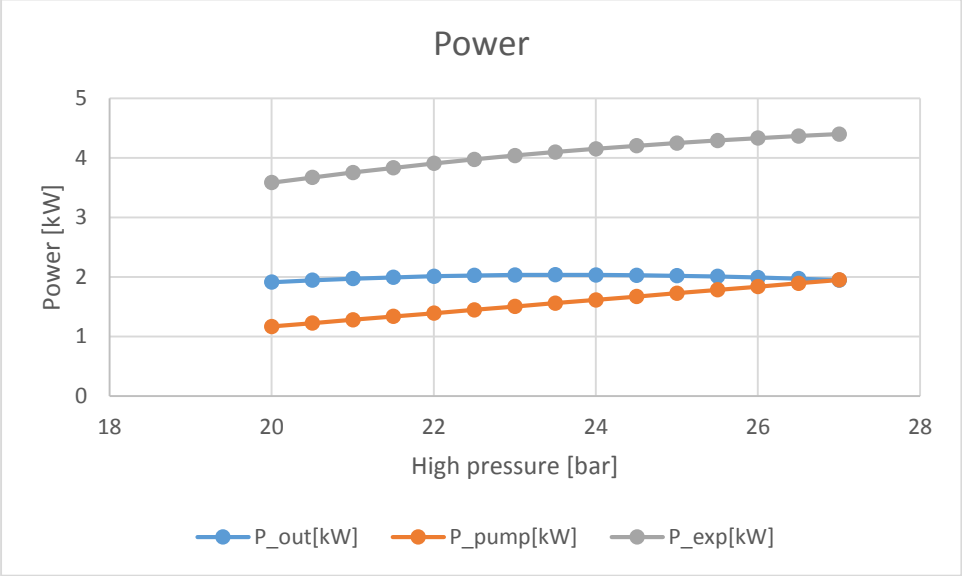

Figure 10.A: Powers of the ORC with high pressure variable

The total recovery efficiency is:

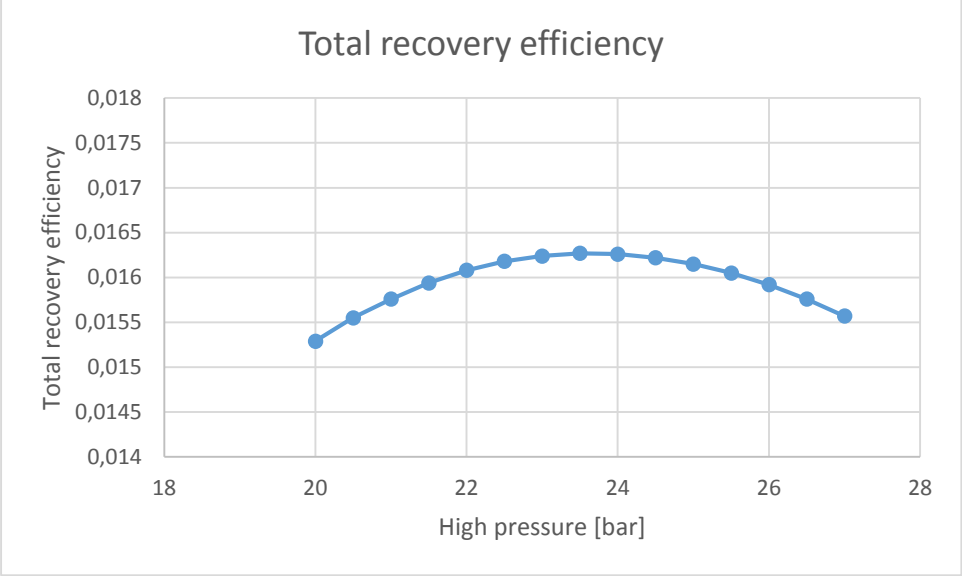

Figure 10.B: Total recovery efficiency of the ORC with high pressure variable

The total isentropic efficiency is:

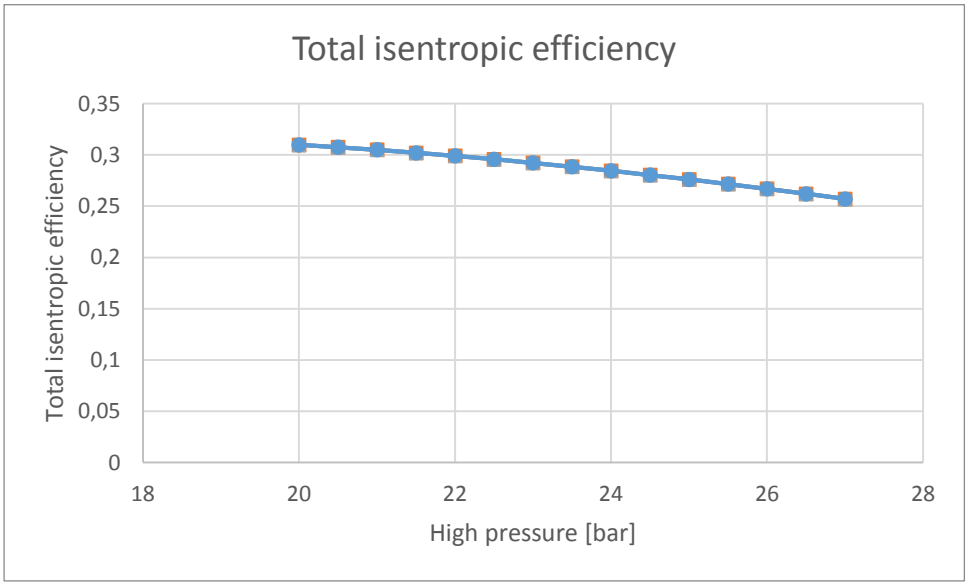

Figure 10.C: Total isentropic efficiency of the ORC with high pressure variable

The thermal efficiency is:

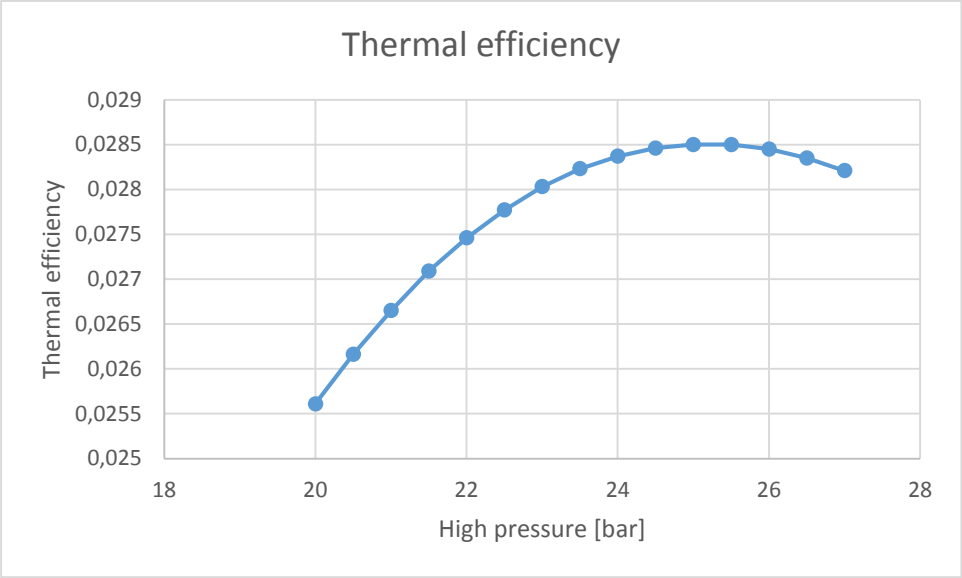

Figure 10.D: Thermal efficiency of the ORC with high pressure variable

The net power and the total recovery efficiency raise until the high pressure reaches the value of 23,5 bar and then they lower. It must be considered the fact that the input heat decreases as the high pressure increases owing to the lower latent heat. At 23,5 bar correspond a heat input of 72,15 kW and a thermal efficiency of 2,82 %. With values of high pressure higher than 23,5 bar, the increase of the power of the pump is greater than the one of the expander. With a high pressure of 20 bar the input heat is 74,72 kW but the thermal efficiency of 2,56% is too low to obtain the highest value of net power and total recovery efficiency. The opposite problem is with a high pressure of 25,5 bar that corresponds to the maximum value of the thermal efficiency, 2,85%, but a heat input of 70,48 kW.

4.2.2.C INLET EXPANDER TEMPERATURE VARIABLE

In this case the inlet expander temperature ranges from 78 to 84°C. The studied parameters are the same of the previous cases. In this case, the inlet expander temperature is not calculated by the heat balance at the evaporator since it is fixed as input. The high pressure is maintained constant at 25 bar.

Graphs of the performances are reported as functions of the inlet expander temperature.

The power is:

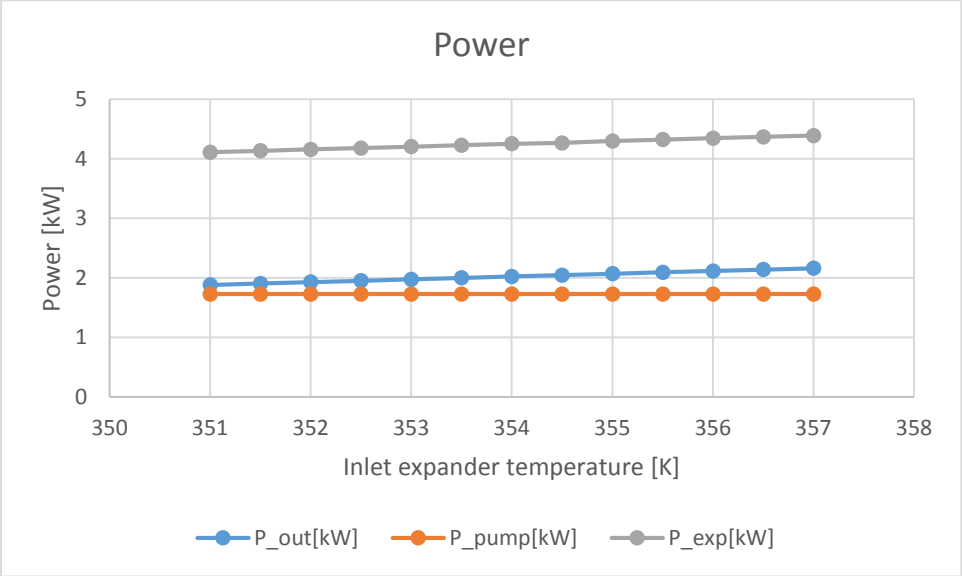

Figure 11.A: Powers of the ORC with inlet expander temperature variable

The total recovery efficiency is:

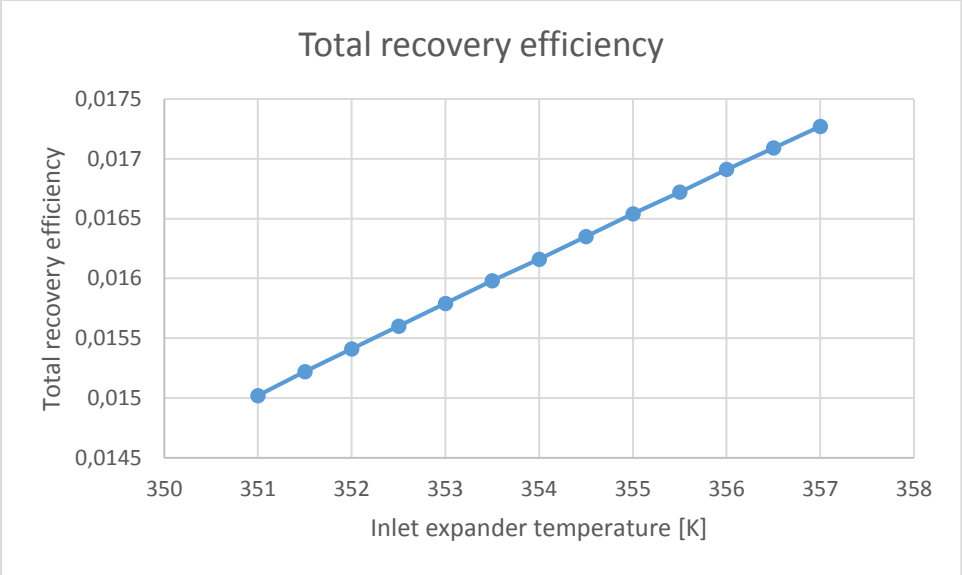

Figure 11.B: Total recovery efficiency of the ORC with inlet expander temperature variabl

The total isentropic efficiency is:

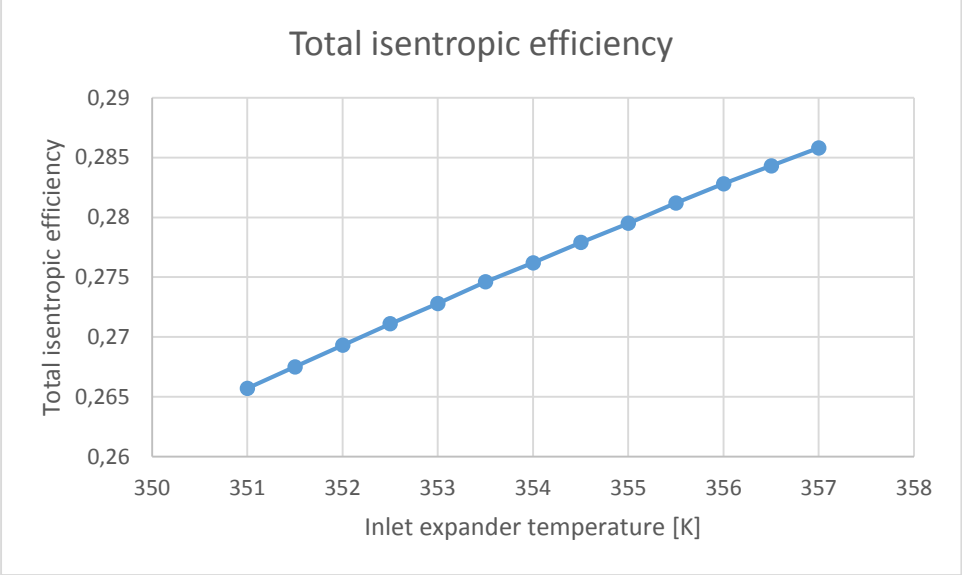

Figure 11.C: Total isentropic efficiency of the ORC with inlet expander temperature variable

The thermal efficiency is:

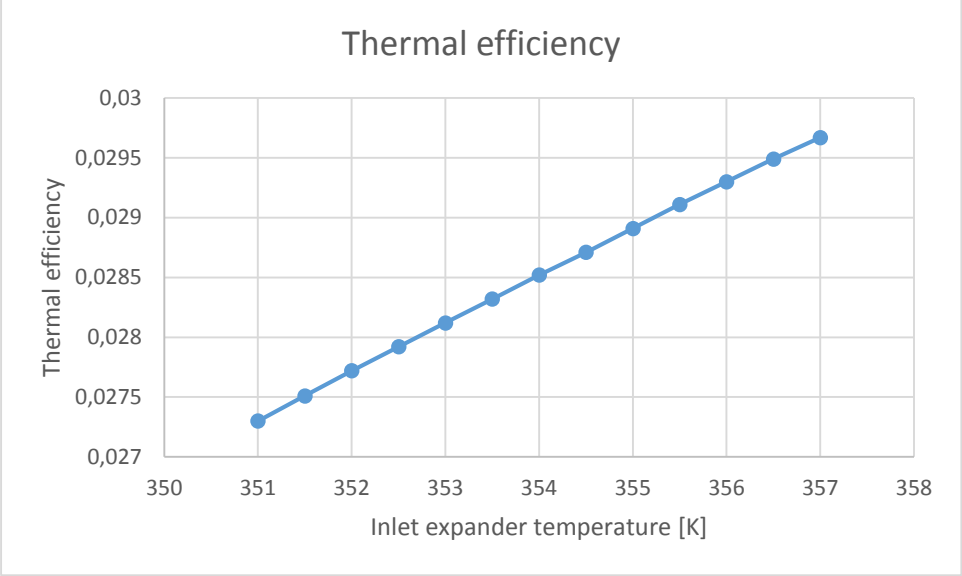

Figure 11.D: Thermal efficiency of the ORC with inlet expander temperature variable

Like the first case, all the performances analysed increase as the studied parameter increases. The power of the pump is constant while the power of the expander and, therefore, the net power raise as the inlet temperature increases. This influences every performance. The maximum values of the net power and the total recovery efficiency are, respectively, 2,16 kW and 1,73% as the inlet temperature is 84°C.

4.2.2.D CONCLUSIONS

A simplified overview of the performances of the cycle has been carried out.
Despite the fact that the values are not very accurate, some important considerations can be made. The most affective parameter is the pressure ratio as it can be noticed from the graphs in the section 3.2.2.A. In fact, increasing the pressure ratio, lowering the condensation pressure, influences highly the power that can be obtained by the ORC unit. Both the heat input and the thermal efficiency of the cycle raise as the pressure ratio grows and, consequently, the increase of the net power is very important. The problems associated with high values of pressure ratio are analysed in the chapter 5.

The same considerations can be made with the inlet expander temperature. Indeed, as this temperature raise, the output power increase due to the increase of the heat input and the thermal efficiency. Nevertheless, the gain is much lower than the previous case. In this case, to obtain a higher temperature at the outlet conditions of the evaporator it is sufficient to modify the heat exchanger. In fact, it is a plate heat exchanger and it can be modified only adding more plates so as to improve its efficiency and obtain a higher temperature of the working fluid at the outlet conditions of the evaporator. As said before, the increase of the performances and of the net power in particular, are low and, therefore the cost for more plates must be evaluated together with the increase of the power.

In the section 3.2.2.B the performances achieved varying the high pressure are represented. This case is different from the other two owing to the fact that the net power increases with the raise of the high pressure until 23,5 bar and then it decreases. Unlike the other two cases, the heat input gets lower as the high pressure grows. The evolution of the thermal efficiency is different too because its value reaches a maximum at 25,5 and then it lowers.

A compromise between heat input and thermal efficiency must be found so as to maximize the total recovery efficiency and, therefore, the output power. The high pressure is an input in the study but in the practice it is modified changing the rotational speed of the expander.

4.2.3 DEFINITION OF PUMP AND SCROLL PERFORMANCES AND CONSTRUCTION OF THE CURVES

In this section, the efficiency of the scroll and of the pump and the filling factor are described. Furthermore, some curves of the cycle are achieved using the EES model. In the first part, the simplifying assumptions used in the section 3.2.2 are now corrected so as to obtain more accurate values. The aim of this section is the definition of the three performances mentioned above and the study of some parameters, in particular the power of the scroll, in order to complete the analysis of the section 3.2.2 before focusing on the expander in the chapter 4.

First of all, the isentropic efficiency of the scroll and of the pump and the filling factor are studied and their functions are reported in graphs. The isentropic efficiency of the pump has been obtained experimentally on this particular ORC unit. The trends of the isentropic efficiency of the scroll and of the filling factor are common trends for this kind of scroll and power plant. The isentropic efficiency of the scroll and the filling factor are calculated accurately in the chapter 4. The maximum value of the isentropic efficiency of the scroll is supposed 0,65 and the evolution of the curve of the efficiency as a function of the pressure ratio is achieved using the one in [32].

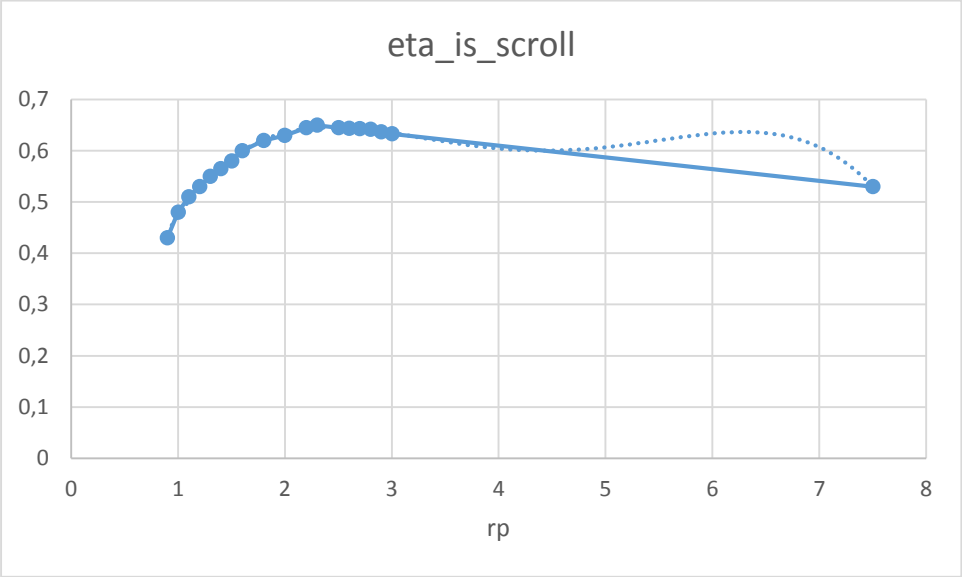

Figure 12: Isentropic efficiency of the scroll in the ORC model

The filling factor is a function of the expander rotational speed and its evolution is reported in the following graph:

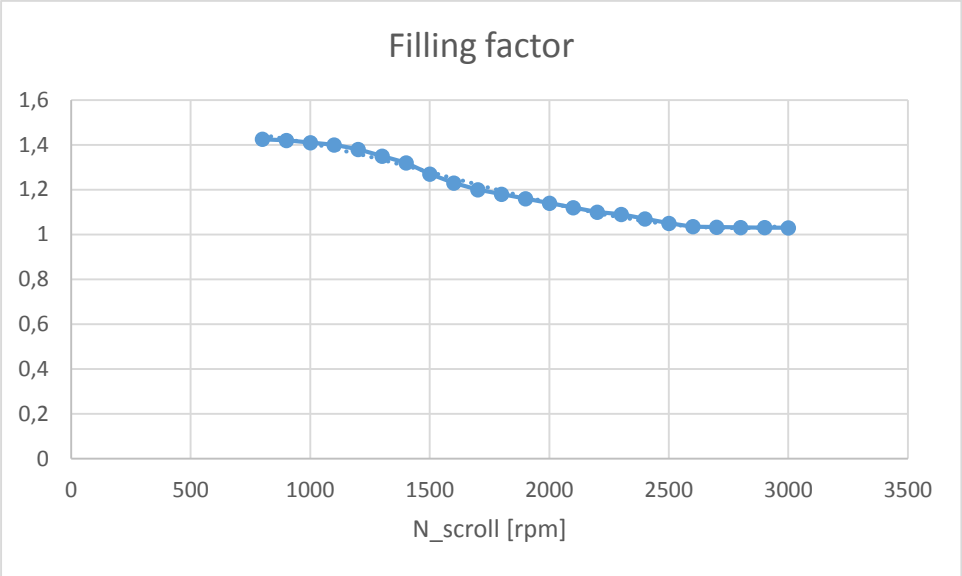

Figure 13: Filling factor in the ORC model

The global efficiency relative to the pump of this power plant is represented as a function of the rotational speed of the pump. It is the product of the isentropic efficiency of the pump and the electromechanical efficiency, that is supposed constant at 0,7225. The evolution of the global efficiency of the pump is:

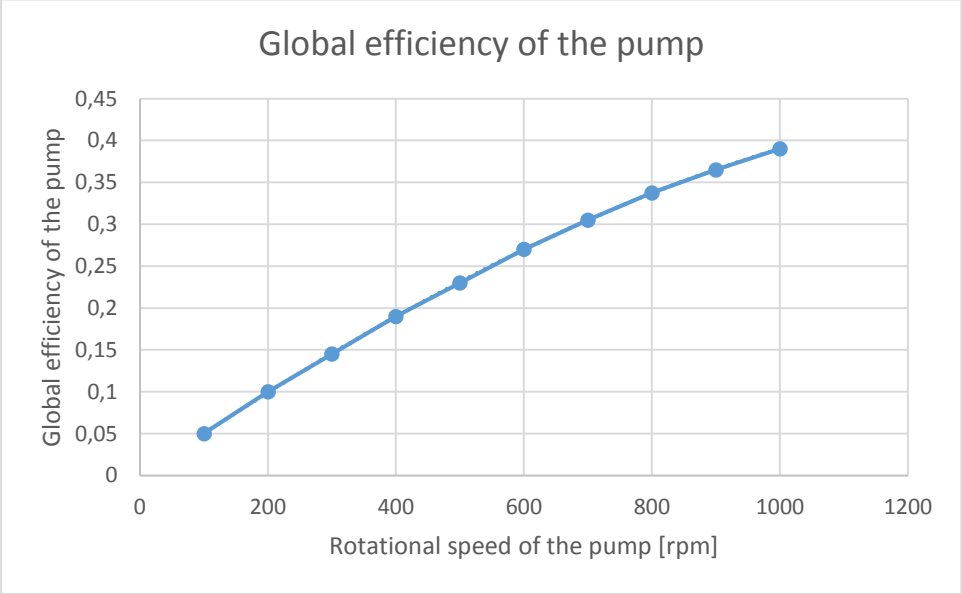

Figure 14: Global efficiency of the pump

The graph corresponds to the nominal pressure ratio that is 2,63. When the pressure ratio is different from the nominal one the values obtained in the curve are multiplied for $(r_p / r_{p,dp})^{0,02}$

The performances analysed in the curves are functions of the rotational speed of the pump, with either different values of the rotational speed of the expander (1000, 1500, 2000, 2500 rpm) or different values of the inlet expander temperature (79, 81, 83, 85°C).

The examined performances are:

- High pressure

- Power of the scroll

- Power of the pump

- Net power

The high pressure in not an input in this case but it is calculated by the equation (3.6) while the inlet expander temperature is fixed at 82°C when the values are studied with different values of the rotational speed of the expander. The other values are at the design point.

All the calculations are carried out for different values of the built-in volume ratio: 2,1; 2,3; 2,5. The scroll expander in the unit presents a built-in volume ratio of 2.3. Analysing different values of built-in volume ratio provides the possibility of changing the scroll expander due to the fact that other expanders with built-in volume ratio of 2,1 and 2,5 are easy to acquire.

4.2.3.A High pressure

These curves are about the high pressure as a function of the rotational speed of the pump with different values of $r_{v,in}$: 2,1 , 2,3, 2,5.

On the left the high pressure is represented for different values of the rotational speed of the expander while on the right it is represented for different values of the inlet expander temperature.

$r_{v,in}$=2,1

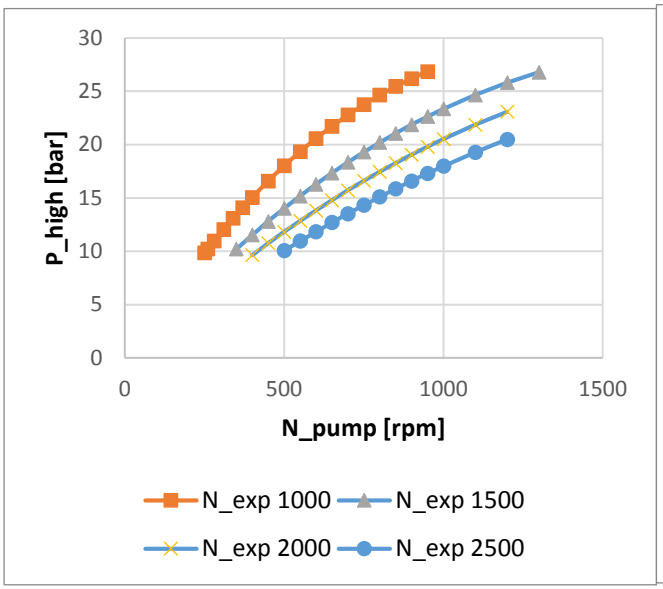

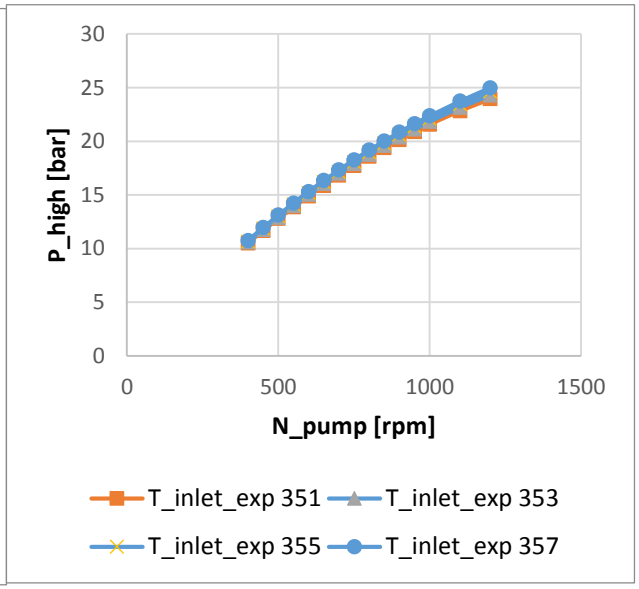

$r_{v,in}$=2,3

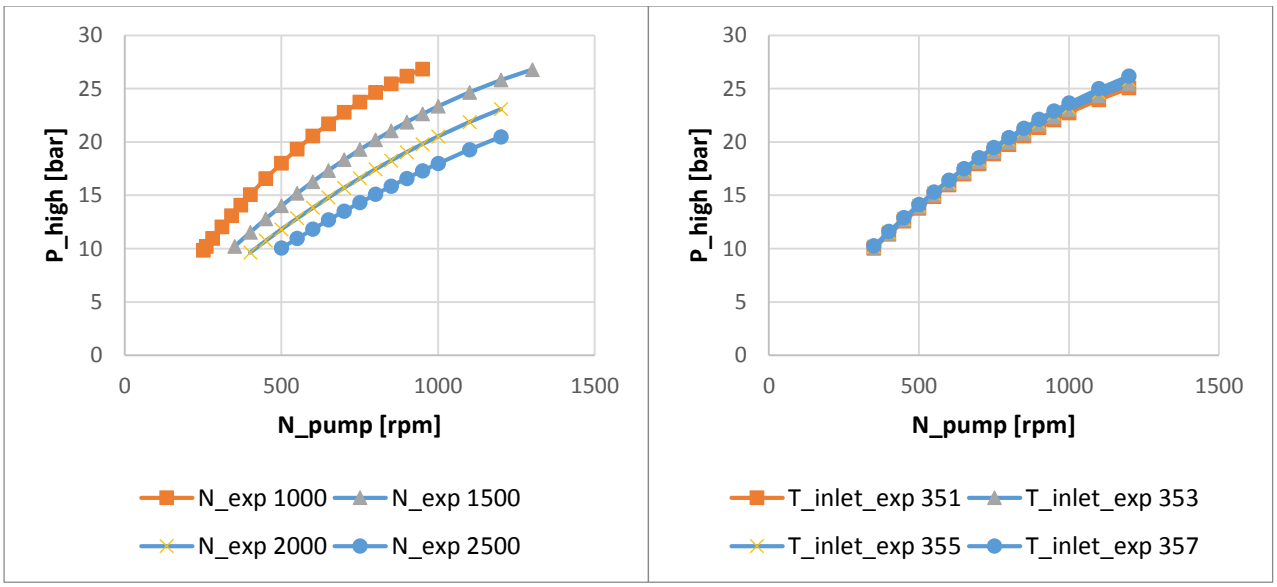

$r_{v,in}$=2,5

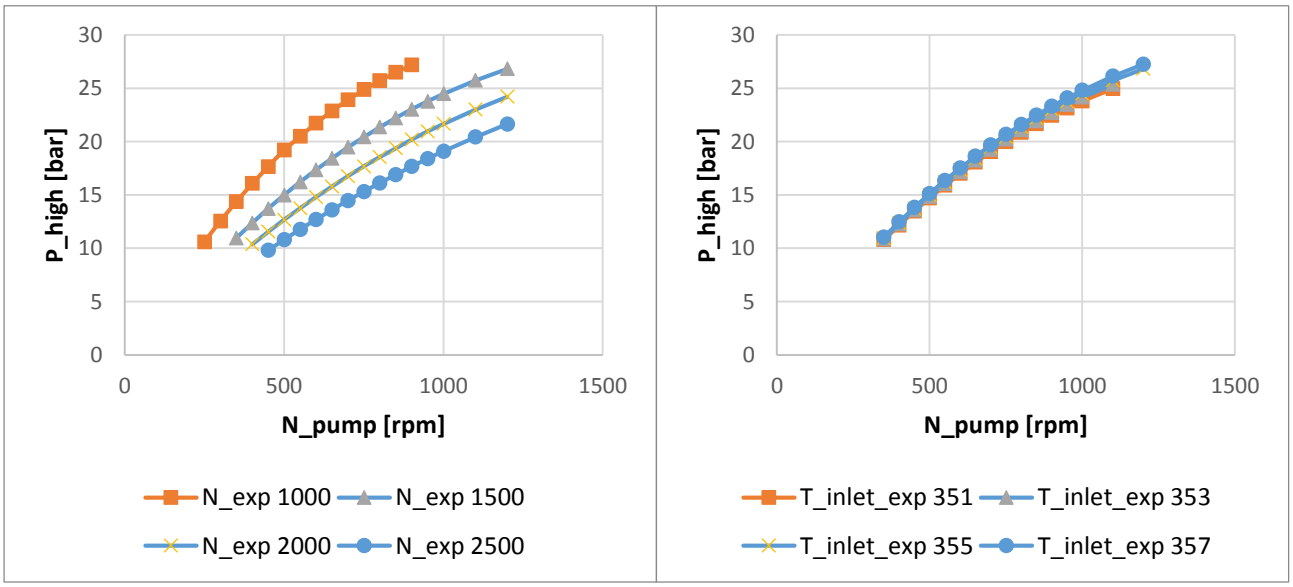

The change of the built-in volume ratio is not very effective for the high pressure.

The inlet expander temperature is not critical while varying the rotational speed of the expander is much more important.

4.2.3.B Power of the scroll, power of the pump and net power

This section deals with the curves of the scroll power. It is important to obtain these curves owing to the fact that the chapter 4 focuses on the expander.

$r_{v,in}$=2,1

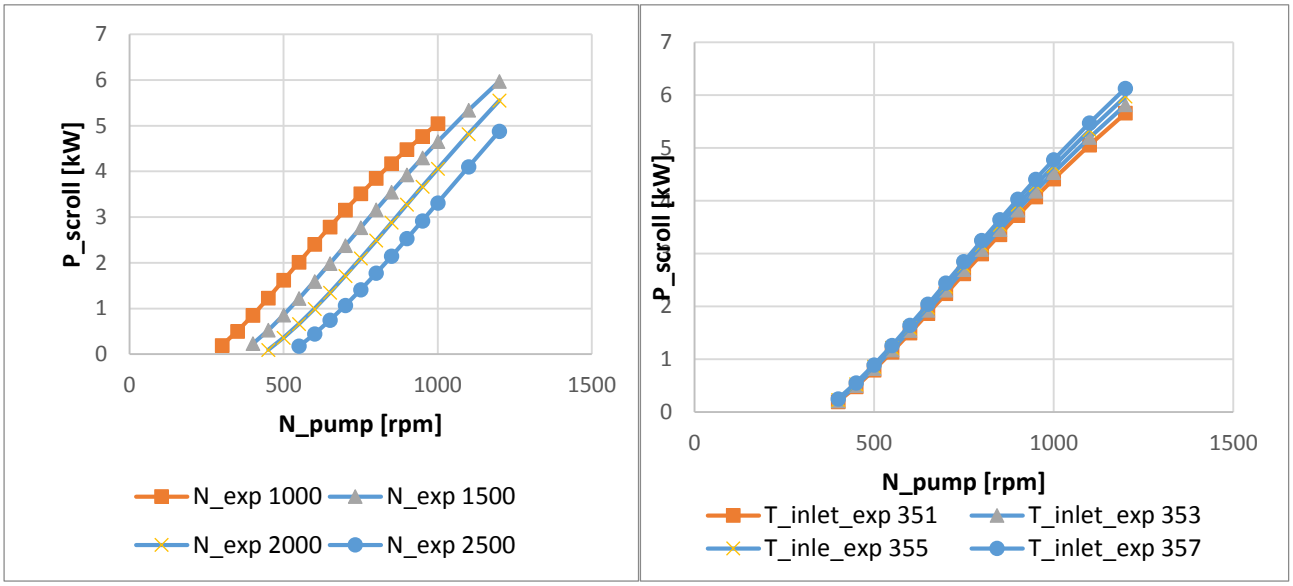

$r_{v,in}$=2,3

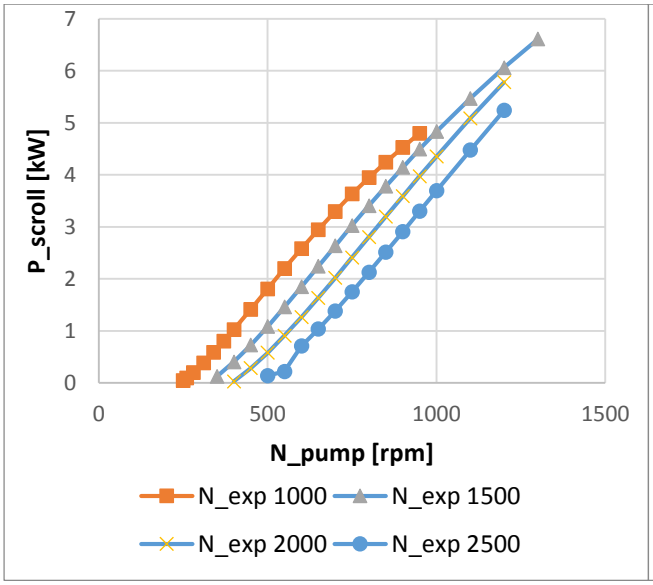

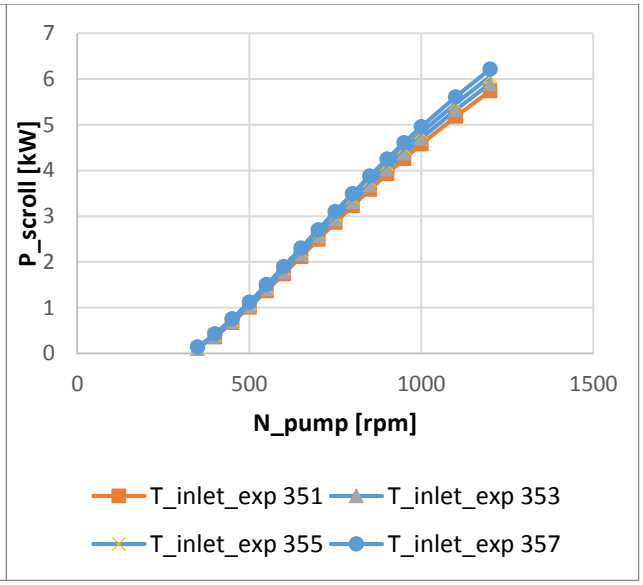

$r_{v,in}$=2,5

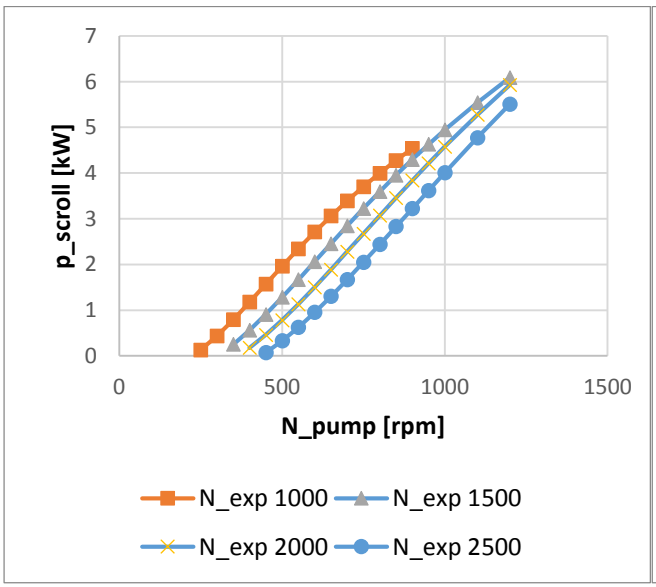

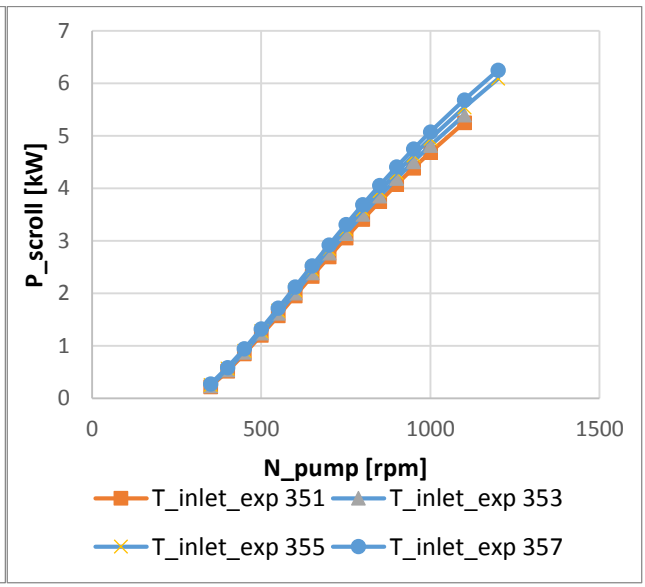

The following graphs are the curves of the power of the pump.

$r_{v,in}$=2,1

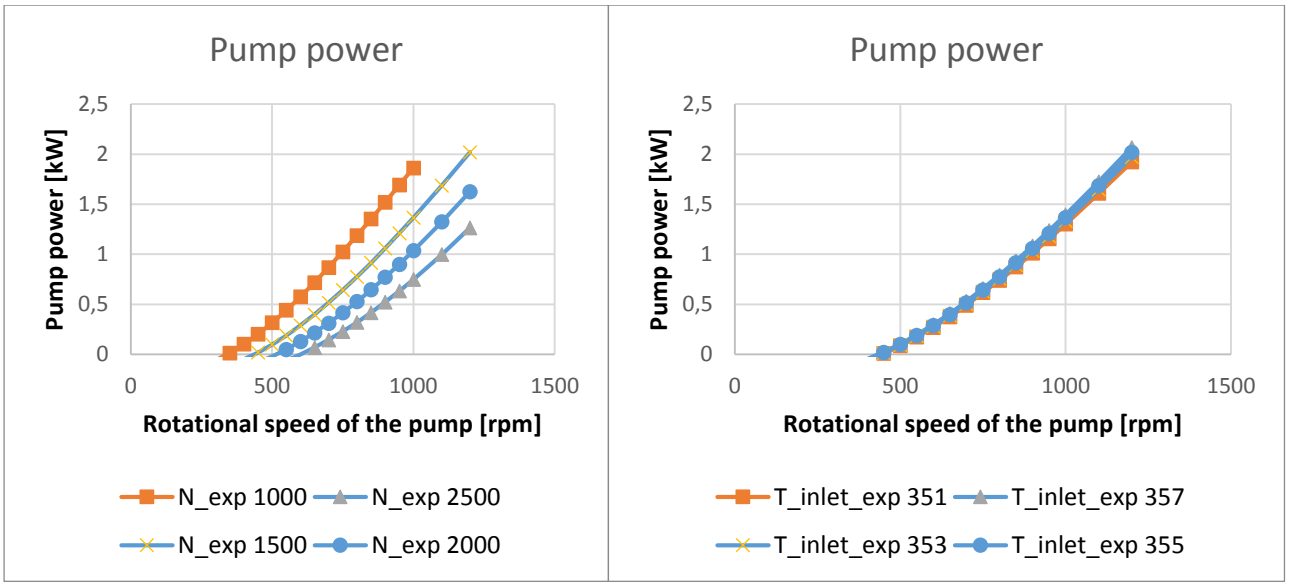

$r_{v,in}$=2,3

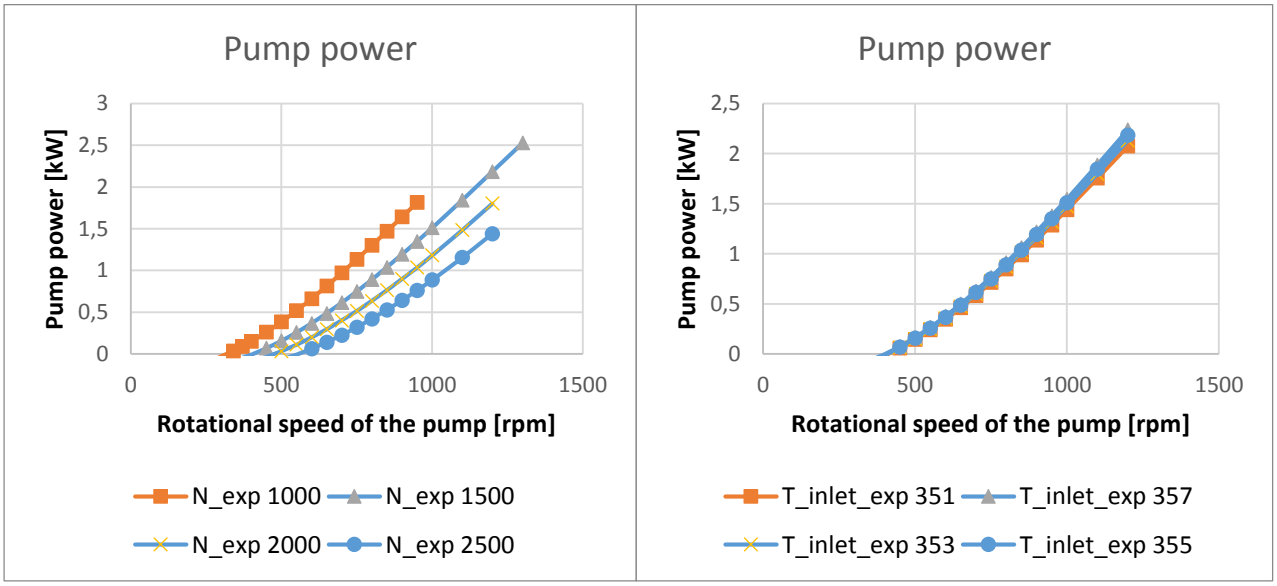

$r_{v,in}$=2,5

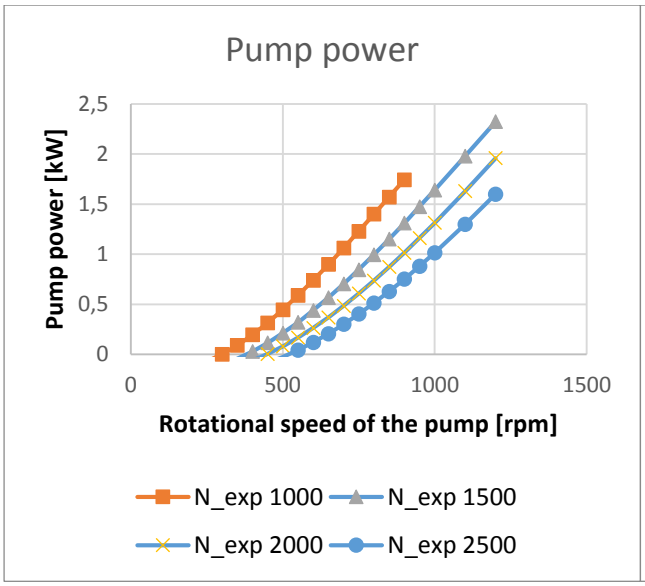

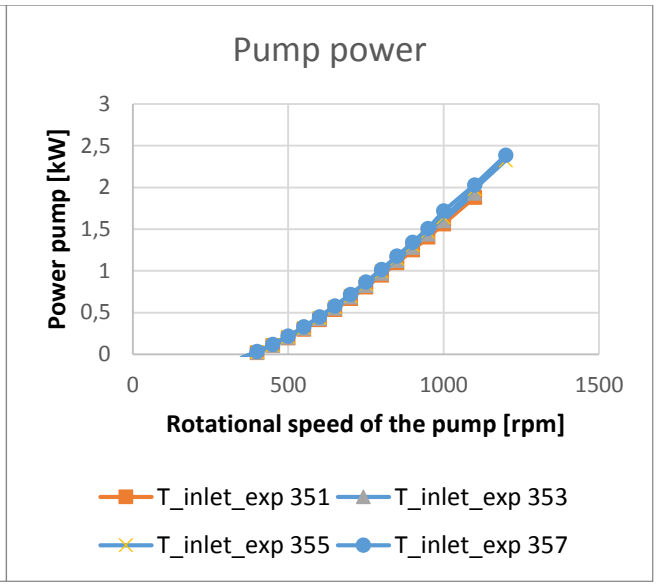

The curves of the net power are reported below:

$r_{v,in}$=2,1

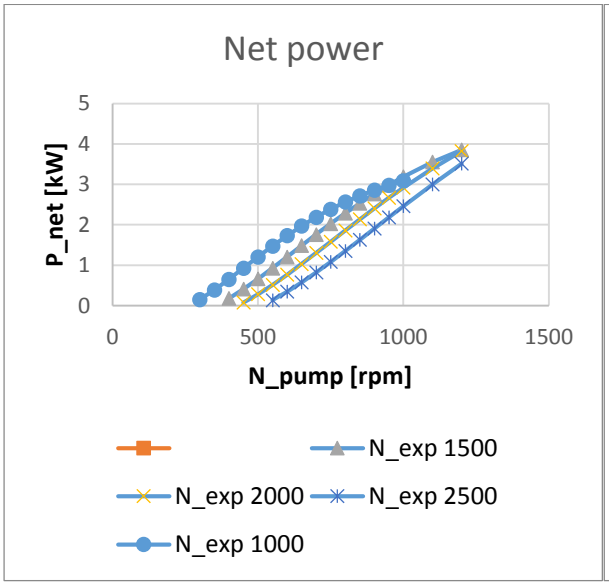

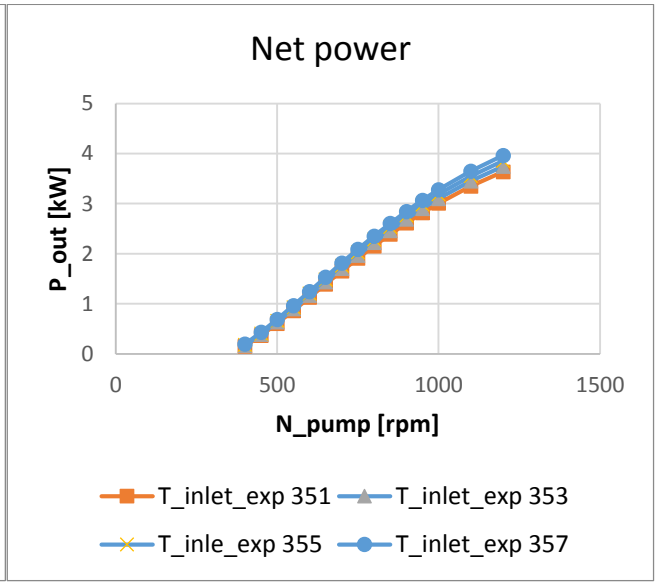

$r_{v,in}$=2,3

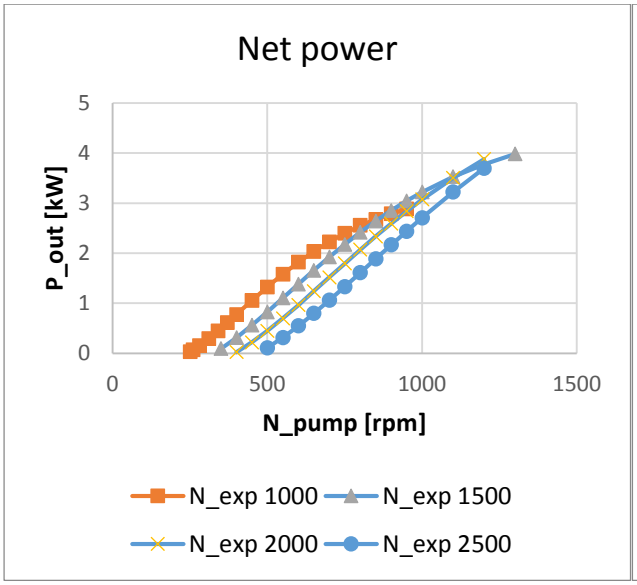

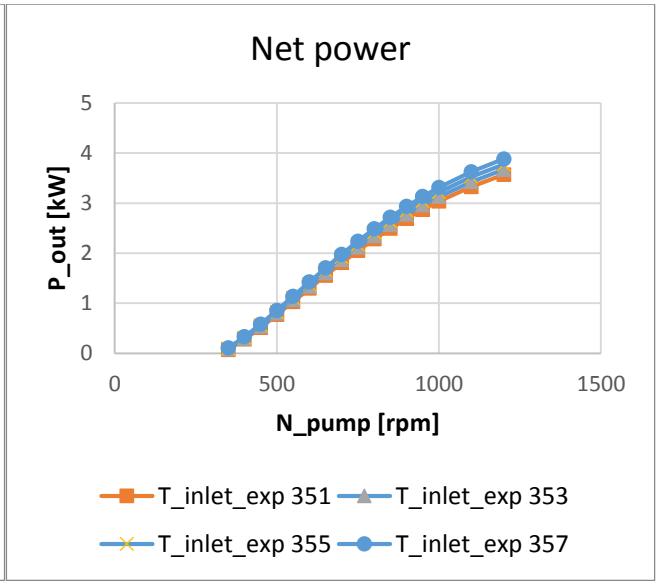

$r_{v,in}$=2,5

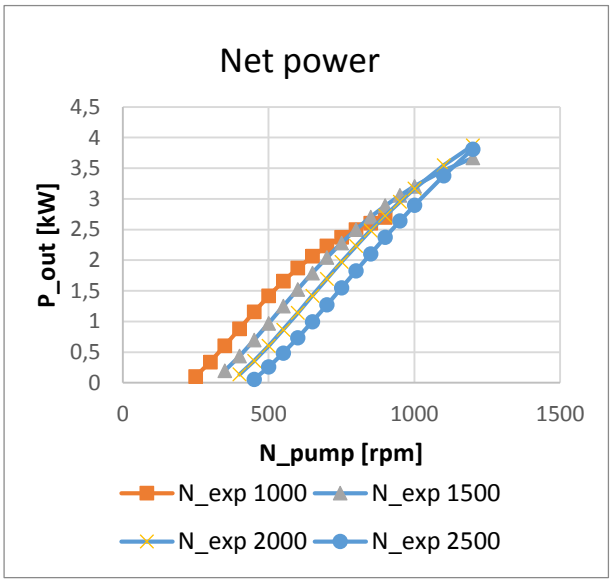

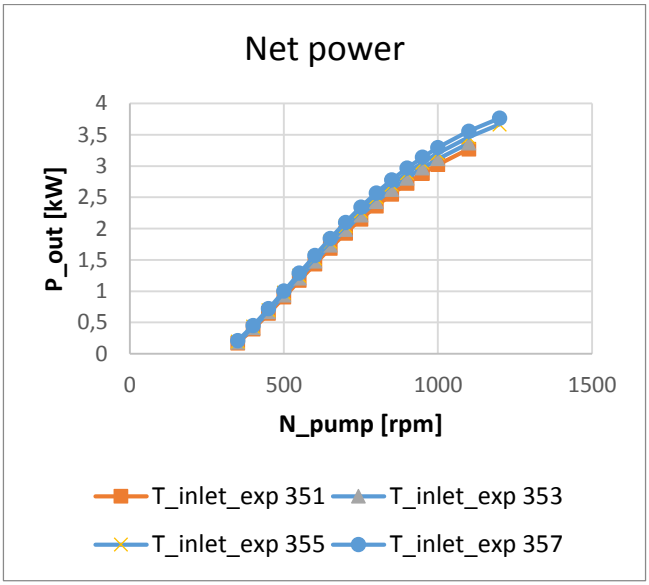

Like the case of the high pressure changing the rotational speed of the expander is more effective than changing the inlet expander temperature. Considering, the net power, that is the most important parameter in this study, with low values of the N_pump the P_out is higher as the N_exp is lower, in this case 1000 rpm. The problem is that the pump power grows more with small expander rotational speeds and at a certain point the net

power that can be obtained is greater with higher values of N_exp. In particular 2500 rpm as rotational speed of the expander becomes the best choice when the N_pump reaches about 1200 rpm. However, the rotational speed that ensures the best evolution of the net power, especially with built-in pressure ratio of 2,3 and the rotational speed of the pump around the value of the design point, is 1500 rpm, that corresponds to the value of the rotational speed of the expander at the design point.

*4.2.3.*C Conclusions

In this section the definition of the performances at the beginning is very important. As said before, the total isentropic efficiency of the pump is accurate and it related to this particular power plant. The efficiency of the scroll and the filling factor described in this section are compared in the chapter 4 with the ones achieved after the calibration of the model of the scroll expander.

Besides, the curves show that with a rotational speed of 960 rpm, that corresponds to the design point, the choice of the expander is justified by the values of the net power achieved.

4.2.4 COMPARISON WITH EXPERIMENTAL RESULTS

In this part the results achieved with the EES model described in the section 3.1 are compared to the experimental results so as to evaluate the accuracy of the model. 60 different settings are used to judge the model. In the first part of this section, the same study and graphs reported in 3.2.2 are carried out, using the efficiency of the scroll and of the pump and of the filling factor described in 3.2.3. The results obtained with these assumptions are the ones compared to the experimental values.

First of all, the graphs obtained with the new hypothesis are reported and the potential differences from the case 3.2.2 are commented.

- High pressure variable

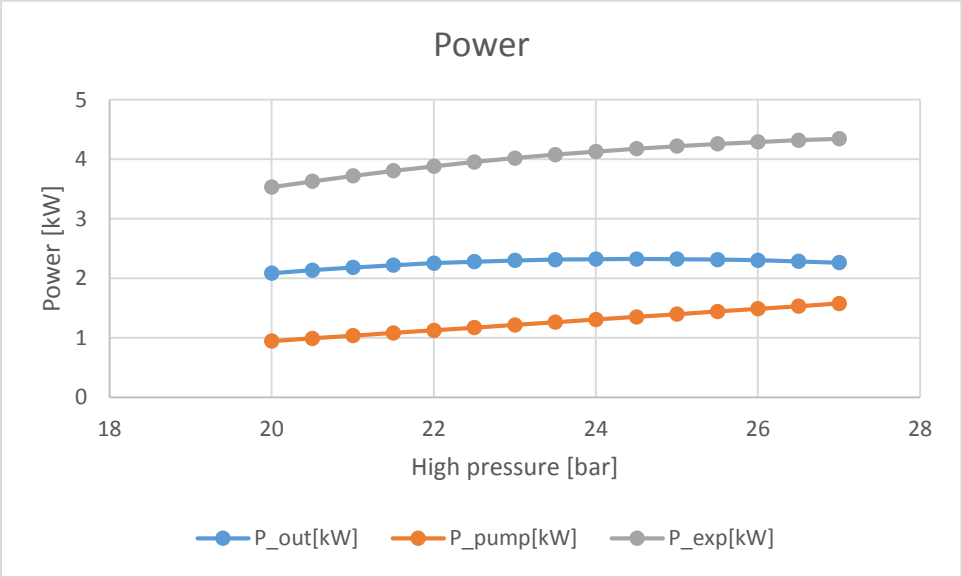

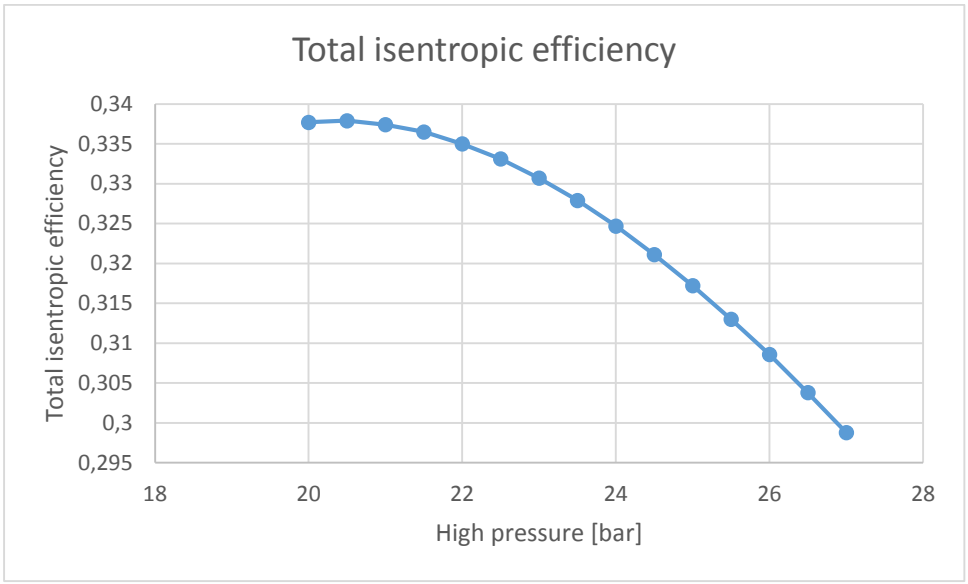

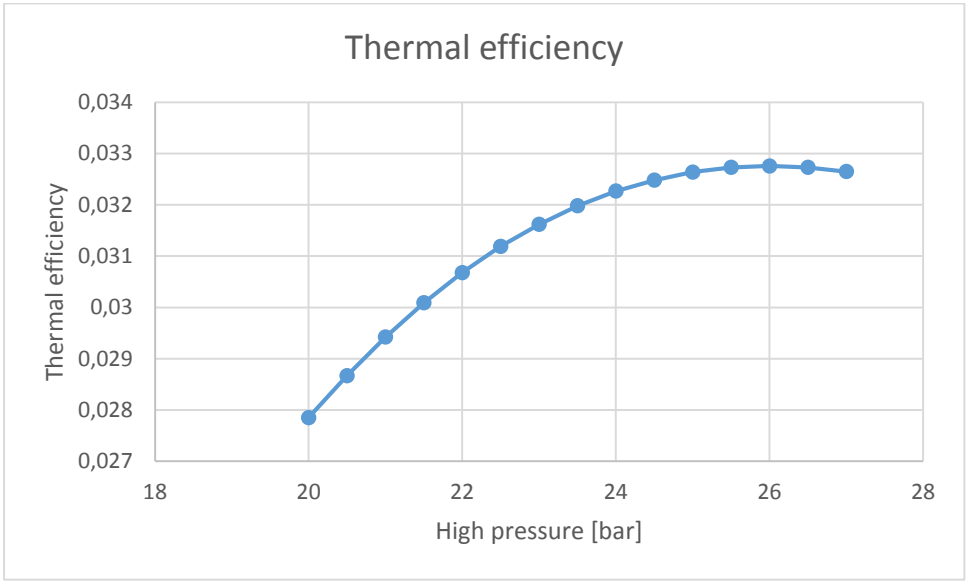

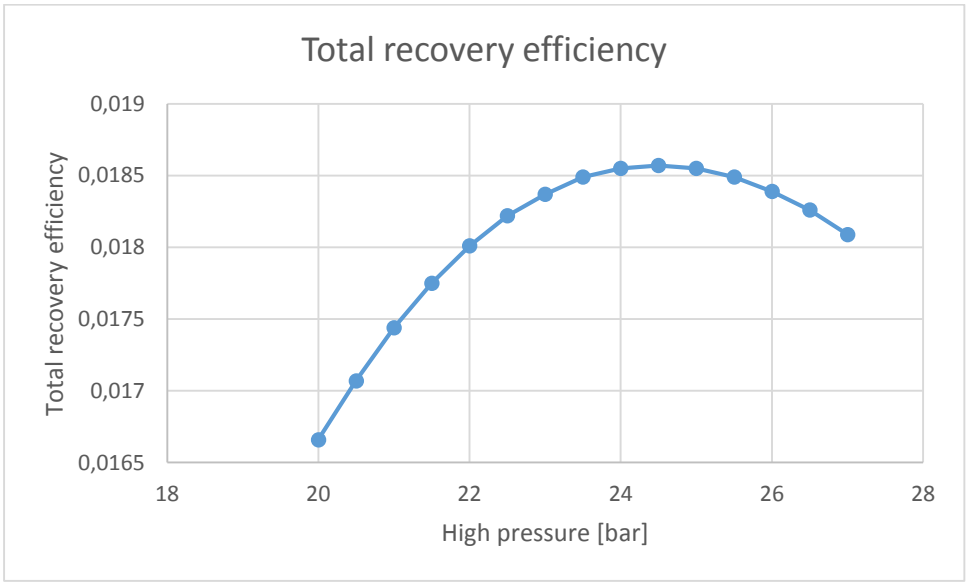

Figure 15: New performances of the ORC model with high pressure variable

The values of the performances are different and the values of high pressure that maximize the performances are different too. Nevertheless, the evolutions are very similar and the considerations made previously remain the same.

- Condensation temperature variable

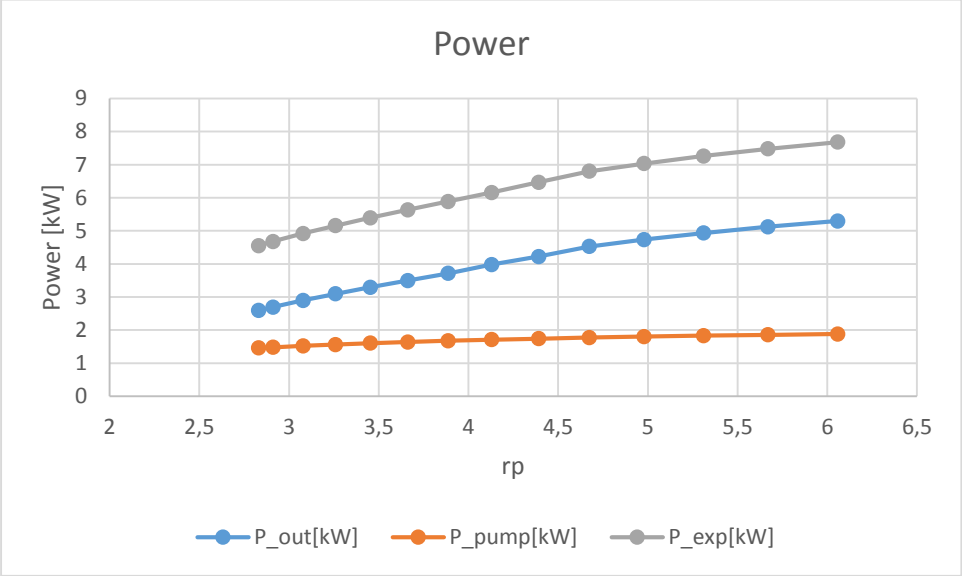

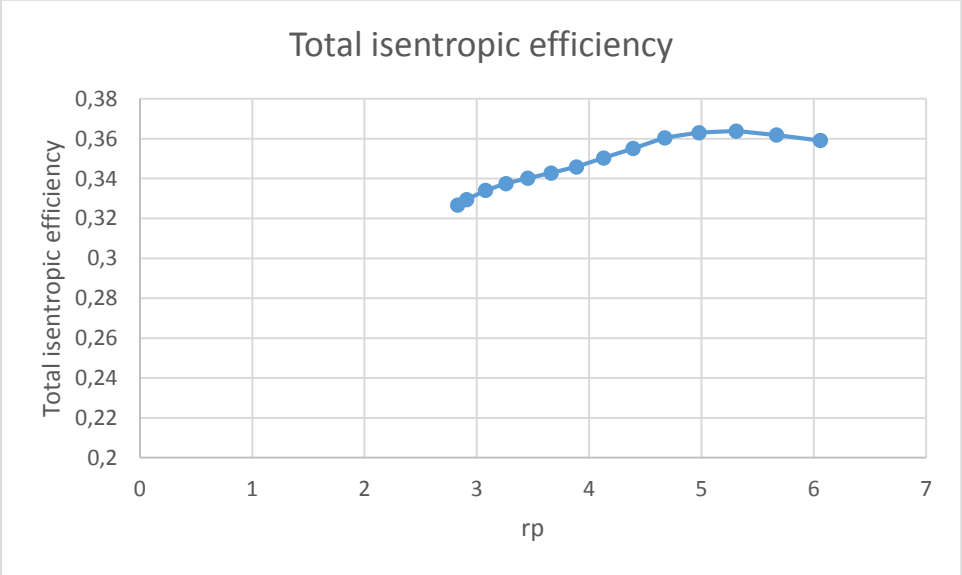

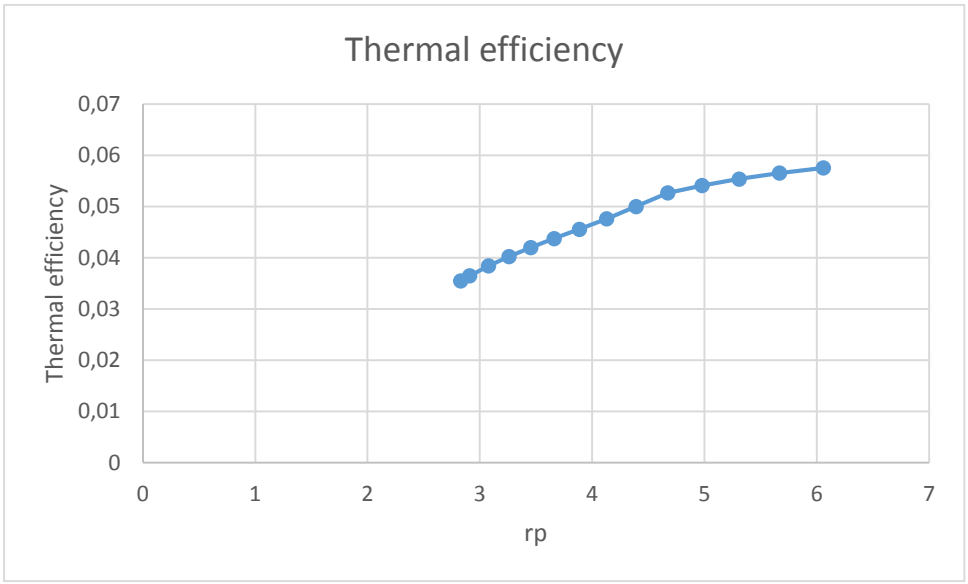

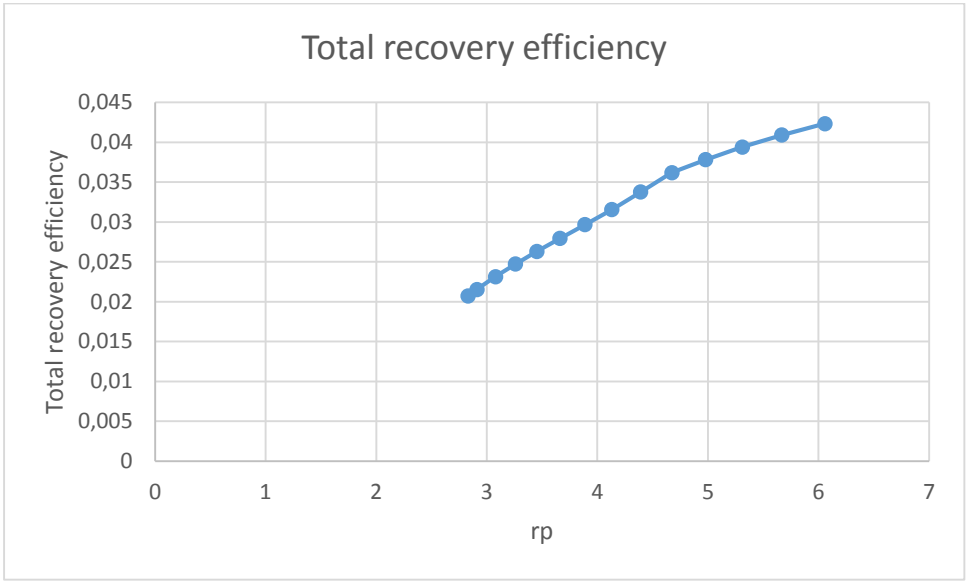

Figure 16: New performances of the ORC model with condensation temperature variable

As the previous case, the values are different but the evolutions and the considerations are the same.

- Inlet expander temperature variable

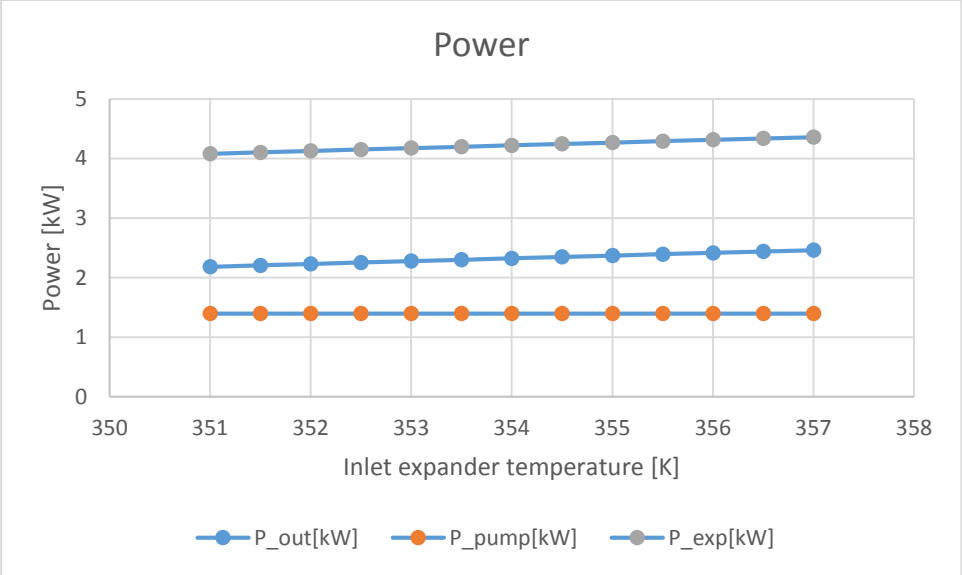

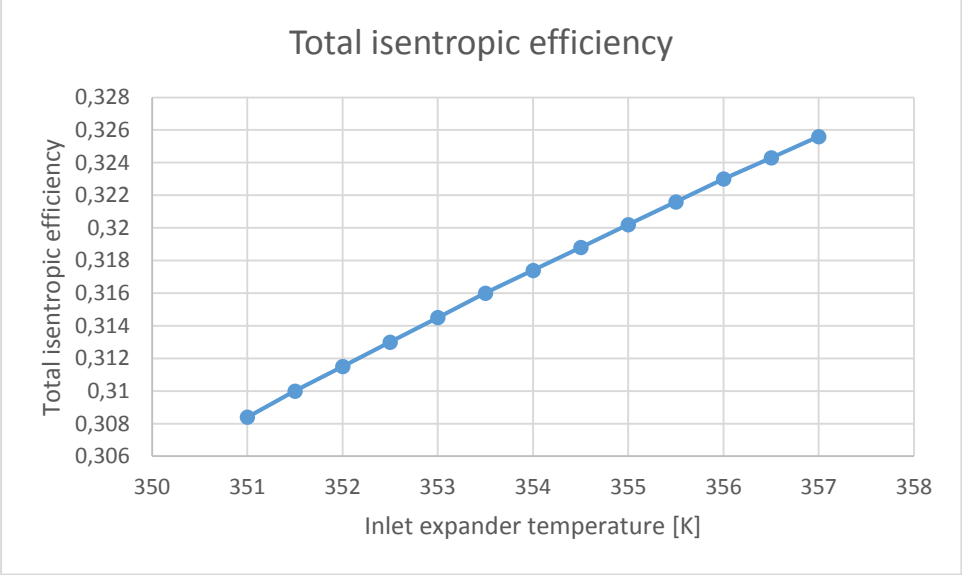

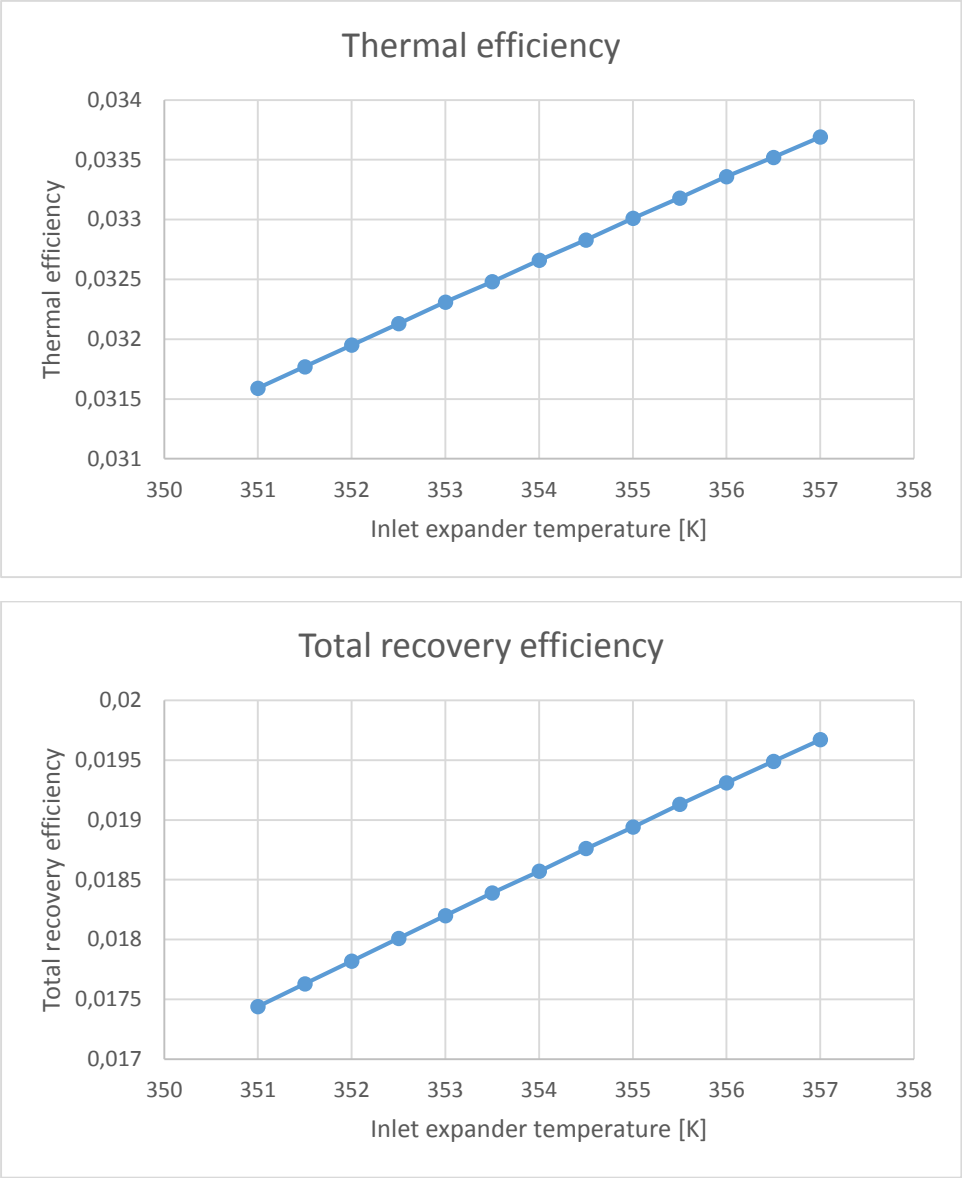

Figure 17: New performances of the ORC model with inlet exander temperature variable

Like the other two cases, the trends of the studied performances and the considerations made before remain the same. In conclusion, despite the fact that the values obtained before are not very accurate, the possible changes of the cycle mentioned before are viable options and they are studied in the chapter 5 of this work.

It's fundamental to compare the values obtained with the EES program with real values in order to value this work and to understand where the model can be improved.

The input heat is nearly the same with a maximum error of about 1% while the condensation heat of about 3%. The mass flow rate calculated from the rotational speed of the pump is very nearly the same in both the results and that confirms the accuracy of the equation provided in the EES program.

The filling factor presents a maximum deviation of 23% from the experimental data.

Regarding the powers of the scroll and the isentropic efficiency, some of the results show an error of less than 4% but there are some values that are quite different.

The pump power obtained with the model is similar and this means that the expression of the global efficiency of the pump is accurate. The thermal efficiency is affected by the low accuracy of the power of the expander.

In general the differences between the result are maximum 5-6%. The only variables that create problems in this comparison are the values regarding the scroll expander, in particular the power and the filling factor. In the next chapter the expander is analysed and an EES model of the scroll is realized in order to improve the accuracy of these variables.

4.3 CONCLUSIONS

The EES model of the ORC has been introduced and studied in this chapter. The experimental results are similar to the results obtained using the EES model described at the beginning of the chapter. The filling factor and the isentropic efficiency of the scroll are the only performances obtained by the EES model that are significantly different from the experimental results. Consequently, the chapter 4 deals with a detailed EES model of the expander so as to obtain more accurate values of these two parameters and therefore, of the power of the expander and of the net power. The assumptions made at the beginning, regarding the model, have been validated by the experimental results.

The study of the cycle in different configurations has shown that the design point does not correspond to the best configuration and that there are some possible developments in order to obtain higher values of the net power, that is the most important parameter to analyse. The parameter that affects mostly the performances of cycle is the pressure ratio. Nevertheless, it would mean changing deeply the existing power plant. Also the high pressure and the inlet expander temperature affect the performances of the cycle, even though less than the pressure ratio. Modifying these two parameter is however easier than modifying the pressure ratio. These developments are examined and evaluated more accurately in the chapter 5.

5 MODEL OF THE EXPANDER

In this chapter the model of the expander is studied. In the first part there is the presentation of the EES model and all the transformations are explained. Afterwards, the calibration of the model, used to obtain values that are as similar as possible to the experimental values, is described. Finally, the results are discussed and some important variables are compared with the previous cases.

5.1 PRESENTATION OF THE EES MODEL

In this section the EES model of the expander is described.
The model of the expander is a semi-empirical model, obtained from the one proposed by Winandy et al [33], the one by Quoilin et al. [34] and the one by [35]. The following figure shows the conceptual scheme of the scroll model.

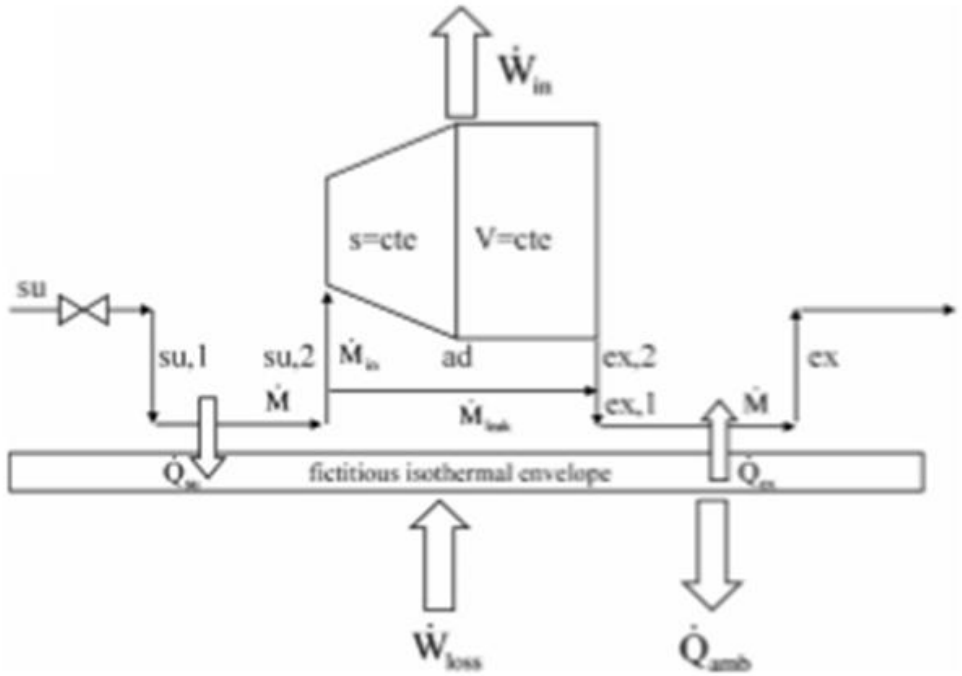

Figure 18: Conceptual scheme of the expander model

The evolution of the fluid through the expander is decomposed into the following consecutive steps:

- Adiabatic supply pressure drop l(su su,1)
- Isobaric supply cooling down (su,1 su,2)
- Adiabatic and reversible expansion to the "adapted" pressure imposed by the built-in volume ratio of the machine (su,2 ad)
- Adiabatic expansion at a constant machine volume (ad ex,2)
- Adiabatic mixing between supply and leakage flows (ex,2 ex,1)
- Isobaric exhaust cooling-down or heating-up (ex,1 ex)

To simplify the study, the supply pressure drop, the heat transfers, and the internal leakages are fictitiously dissociated from the actual expansion process. It is noted that the pressure losses at the expander exhaust line are neglected, as the pressure levels of the refrigerant at this point are much lower compared to the respective supply values which lead to high pressure losses.

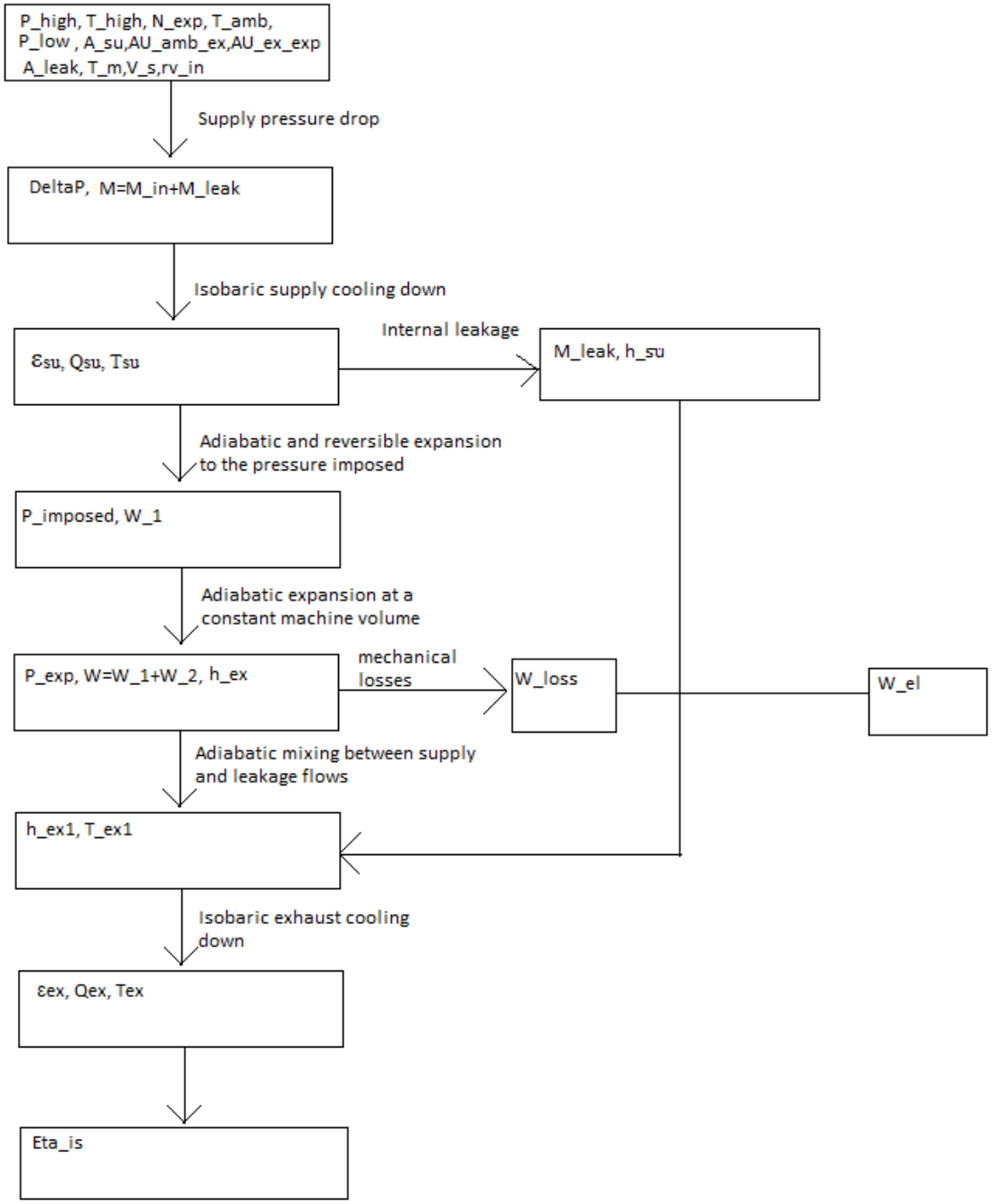

The flow chart reports the transformations that describe the EES model. These transformations are analysed singularly and the main equations of the model are reported.

0. Supply pressure drop (su su,1)

The supply pressure drop is ($P_{su} - P_{su,1}$) and considers the pressure losses encountered by the fluid from the suction line to the suction chamber. The pressure drops in the supply are modelled by reference to an isentropic flow in a simple nozzle. The fluid can also be considered as incompressible due to the occurrence of very low pressure drops (0-3%) which according to the theory of isentropic flows of ideal gases also implies low Mach numbers (0.01-0.1). Indicatively it is mentioned that even for Mach 0.3 the fluid's density alters just by 4% which justifies the assumption of the fluid as incompressible.

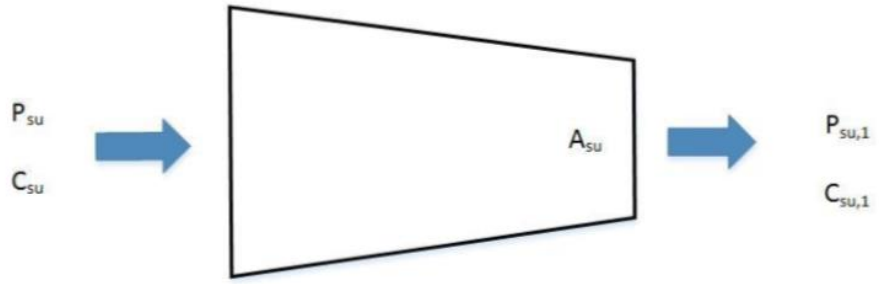

The area A_{su} has not a real meaning but an equivalent that simulates the procedure of the pressure drops in the current machine. Due to the steady-state nature of the model, this area represents an average value of the suction port effective area over the entire suction process (that extends over one shaft revolution).
This parameter is determined from experimental data, using the model calibration process that will be presented in the section 4.2.

The speed of the fluid at the expander inlet can be considered zero (C_{su}=0) and therefore we have the case of an isentropic flow in a nozzle from a buffer tank of pressure P_{su}. Using the equations of mass and energy conservation through the nozzle, for an adiabatic flow, we can obtain the equation of the mass flow rate entering the expander.

Energy conservation equation for an adiabatic flow

$$h_{su} + \frac{c_{su}^2}{2} = h_{su1} + \frac{c_{su1}^2}{2} \rightarrow h_{su} = h_{su1} + \frac{c_{su1}^2}{2}$$

Momentum conservation equation for an adiabatic flow

$$h_{su} + \frac{c_{su}^2}{2} = h_{su1} + \frac{c_{su1}^2}{2} \rightarrow h_{su} = h_{su1} + \frac{c_{su1}^2}{2}$$

$$P_{su1} = P_{su} - \Delta p_{su}$$

$$\dot{M} = \frac{\dot{V}_{su,1}}{v_{su}}$$

$$\dot{V}_{su1} = A_{su} \cdot c_{su}$$

Using these equations, the equation of the mass flow rate can be expressed:

$$\dot{M} = A_{su} \cdot \sqrt{2 \cdot \Delta P_{su} \cdot \rho_{su}}$$

Knowing the mass flow rate entering the expander, the pressure $P_{su,1}$ can be calculated by the previous equation.

There are two main phenomena that are responsible for these pressure losses:

- During part of the suction process, the expander suction port is blocked by the tip of the orbiting scroll, reducing the effective suction port area. This phenomenon is presented in the following figure.

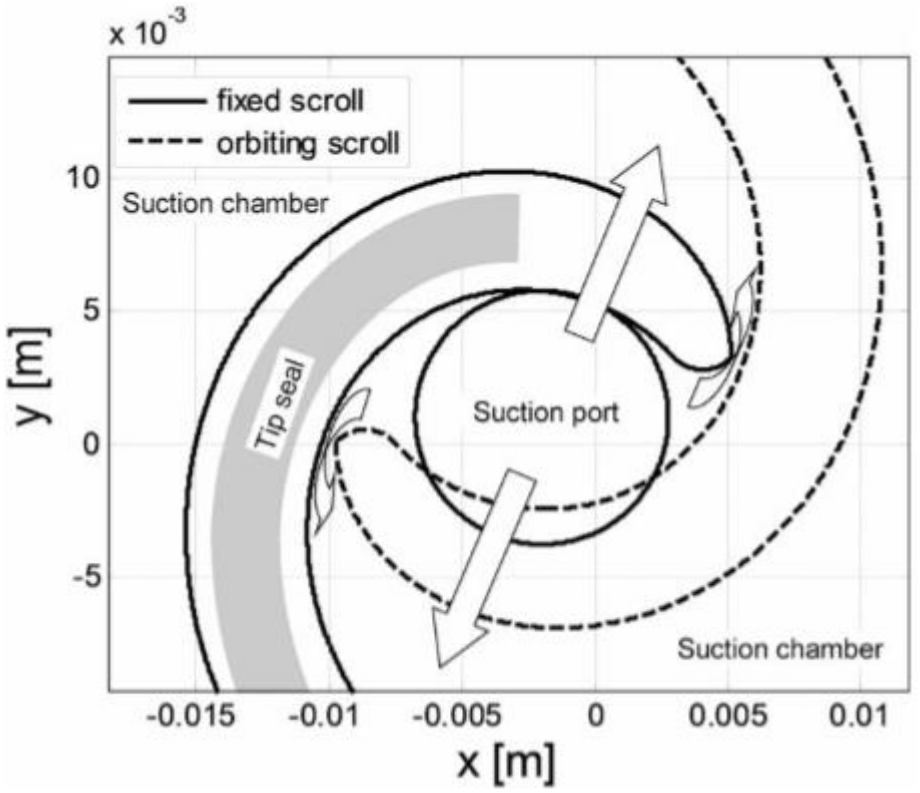

Figure 19: Representation of the suction chambers at the end of the suction process[34]

- At the end of the suction process, the flow passage between the central portion of the suction chamber and the two adjacent crescent-shaped portions is progressively reduced to zero. Nevertheless, the tip seal does not extend to the end of the scrolls, which increases the flow between the central and the adjacent chambers and attenuates the supply pressure drop.

1. Isobaric supply cooling (su,1 su,2)

Owing to the fact that the expander's shell is at lower temperature than the incoming fluid there is a heat transfer from the fluid to the shell.

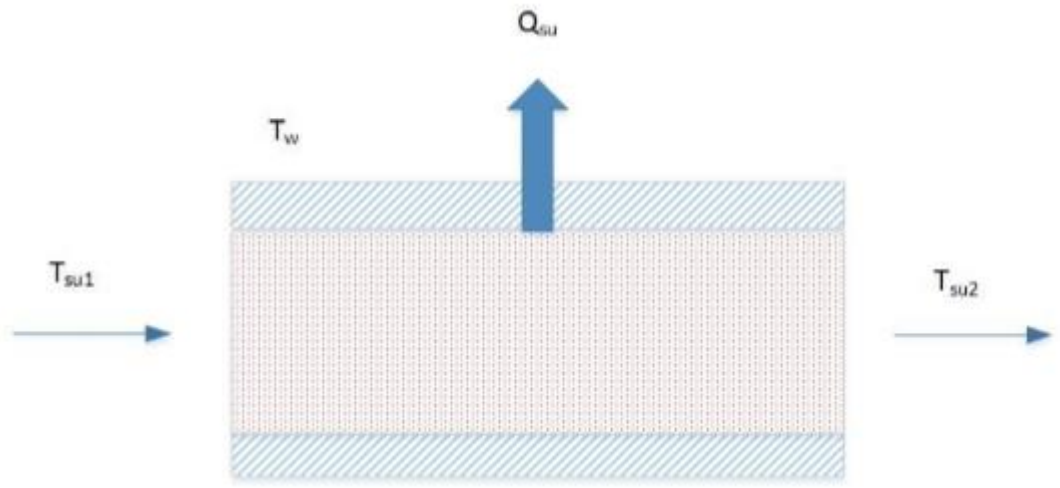

The supply heat transfer is computed by introducing a fictitious metal envelope of uniform temperature T_w (wall). This fictitious envelope represents the metal mass associated to the expander shell, the fixed and the orbiting scrolls. The heat flow can be calculated as:

$$\dot{Q}_{su} = \dot{M} \cdot C_p \cdot (\dot{T_{su2}} - T_{su1})$$

$$\dot{Q}_{su} = \varepsilon_{su} \cdot \dot{M} \cdot C_p \cdot (T_w - T_{su1})$$

The ε-NTU method is used so that the efficiency is computed as:

$$\varepsilon_{su} = 1 - e^{-\frac{AU_{su}}{\dot{M} \cdot C_p}}$$

The heat transfer coefficient AU_{su} (W/K) alters according to the mass flow rate. Therefore a nominal mass flow rate M_n and a respective nominal heat transfer coefficient $AU_{su,n}$ are defined.

The evolution of the heat transfer coefficient can be approximated as:

$$AU_{su} = AU_{su_n} \cdot \left(\frac{\dot{M}}{\dot{M}_n}\right)^{0,8}$$

The value of the nominal mass flow rate M_n is chosen arbitrarily, it usually takes values in the same magnitude as the expected real mass flow rate. The value of the $AU_{su,n}$ is defined by the model calibration procedure. The equation that describes the evolution of the heat transfer coefficient can be justified by the Reynolds' analogy for a turbulent flow through a pipe by assuming that the fluid properties, not included in this expression, remain unchanged. The rest thermodynamic properties can be retrieved from the refrigerant's properties assuming that the pressure remains steady between these two points.

2. Internal leakage

There are two different leakage paths in a scroll compressor/expander: the radial leakage is due to a gap between the bottom or the top plate and the scrolls and the flank leakage results from a gap between the flanks of the scrolls [36]. All the possible paths are lumped into one unique fictitious leakage clearance, whose cross-sectional area A_{leak} is a parameter to identify and it is very important to analyse accurately. The leakage flow rate can be computed by reference to the isentropic flow through a simply convergent nozzle, whose throat area is A_{leak}. The pressure at the inlet of the nozzle is $P_{su,2}$. The throat pressure corresponds to the maximum between exhaust and critical pressures:

$$P_{thr,leak} = MAX(P_{ex,2}, P_{crit,leak})$$

The value of the critical pressure is calculated by considering the refrigerant vapour as a perfect gas:

$$P_{crit,leak} = P_{su,2}\left[\left(\frac{2}{\gamma+1}\right)^{\left(\frac{\gamma}{\gamma-1}\right)}\right]$$

This hypothesis is very closed to the real situation and it does not affect the results of this study.

Like for the supply pressure drop, we combine the mass and energy conservation equations so as to express the leakage mass flow rate:

$$\dot{M}_{leak} = \frac{A_{leak}}{v_{thr,leak}}\sqrt{2(h_{su,2} - h_{thr,leak})}$$

The mass flow rate entering the expander is made up of the internal mass flow rate M_{in} and the leakage mass flow rate M_{leak}.

$$\dot{M} = \dot{M}_{in} + \dot{M}_{leak}$$

The internal mass flow rate is the volume flow rate $V_{s,exp}$ divided by the specific volume of the fluid $\nu_{su,2}$ after the pressure drop and the cooling down, both described above. The volume flow rate is the swept volume $V_{s,exp}$ multiplied by the expander rotational speed N. The swept volume in expander mode is equal to the one in compressor mode $V_{s,cp}$ divided by the built-in volume ratio of the machine $r_{v,in}$.

$$\dot{M} = \dot{M}_{in} + \dot{M}_{leak} = \frac{\dot{V}_{s,exp}}{v_{su,2}} + \dot{M}_{leak} = \frac{N \cdot V_{s,exp}}{v_{su,2}} + \dot{M}_{leak} \qquad = \frac{N}{v_{su,2}} \cdot \frac{V_{s,cp}}{r_{v,in}} + \dot{M}_{leak}$$

3. Internal expansion (su,2 ex,2)

The cycle of this expander is made up of three processes: suction, expansion and discharge.

- Suction: the working fluids flows from the suction line into the suction chamber. At the end of this process, the suction chamber ceases to be in communication with the suction line.
- Expansion: as soon as the suction process is completed, the expansion initiates.
- Discharge: it initiates when the discharge chambers enter in communication with the discharge line.

The internal power produced by the expander is the summation of these three processes:

$$\dot{W}_{in} = \dot{W}_{suc} + \dot{W}_{expan} + \dot{W}_{dis}$$

$\dot{W}_{in}$ = internal power

$\dot{W}_{suc}$ = suction power

$\dot{W}_{expan}$ = expansion power

$\dot{W}_{dis}$ = discharge power

Besides, due to the fact that the internal expansion process (su,2 ex,2) is assumed adiabatic, $\dot{W}_{in}$ can be expressed as function of the difference of enthalpies:

$$\dot{W}_{in} = \dot{M}_{in}(h_{su,2} - h_{ex,2})$$

Now the three addends of the summation are analysed separately.

3.1 Suction power

To achieve the equation of the suction power, we use the equation of the energy balance across the suction chamber, between the beginning and the end of the suction process. The equation that we obtain is the following:

$$\dot{W}_{suc} = \dot{M}_{in}(h_{su,2} - u_{su,2}) = \dot{M}_{in}P_{su,2}v_{su,2} = P_{su,2}\dot{V}_{s,exp}$$

3.2 Expansion power

The expansion process is assumed to be adiabatic and reversible. Through the energy balance between the beginning and the end of the process we obtain the following expression for the expansion power:

$$\dot{W}_{expan} = \dot{M}_{in}(h_{su,2} - P_{su,2}v_{su,2} - h_{ad} + P_{ad}v_{ad})$$

3.3 Under and over-expansion

Under-expansion occurs when the pressure ratio imposed by the machine ($P_{su,2}/P_{ad}$) is lower than the pressure ratio imposed by the working system ($P_{su,2}/P_{ex,2}$). The pressure in the expansion chambers at the end of the expansion process P_{ad} is higher than the pressure in the discharge line. The modelling assumes that there is no pressure drop through the discharge point, as mentioned before. Some fluid has to flow out of the discharge chambers so as to balance the pressures in the discharge chambers and in the discharge line. We assume that the balance is achieved instantaneously as soon as the expansion chambers open onto the discharge line. The energy balance over the discharge chamber can be expressed as:

$$\left(\dot{M}_{in} - \Delta\dot{M}_{in}\right)u_{ex,2} - \dot{M}_{in}u_{ad} = -\Delta\dot{M}_{in}h_{ex,2}$$

Over-expansion occurs when the conditions are the opposite: the pressure ratio imposed by the machine is higher than the one imposed by the system. The energy balance in this case can be expressed as:

$$(\dot{M}_{in} + \Delta\dot{M}_{in})u_{ex,2} - \dot{M}_{in}u_{ad} = \Delta\dot{M}_{in}h_{ex,2}$$

There is not work associated directly to the under and over-expansion.

3.4 Discharge power

Like the case of the suction, we use the equation of conservation of energy between the beginning and the end of the process to obtain:

$$\dot{W}_{dis} = -(\dot{M}_{in} \pm \Delta\dot{M}_{in}) P_{ex,2}\, v_{ex,2} = -r_{v,in} P_{ex,2} \dot{V}_{s,exp}$$

3.5 Total internal power

Using the equations of the suction, expansion and discharge processes described above, we can achieve the internal power:

$$\dot{W}_{in} = \dot{M}_{in}[(h_{su,2} - h_{ad}) + v_{ad}(P_{ad} - P_{ex,2})]$$

4. Adiabatic mixing between supply and leakage flows (ex,2 ex,1)

The leakage internal flow after skipping the expansion is then mixed adiabatically with the mass flow rate from the discharge chamber of the expander. This process is shown in the following figure:

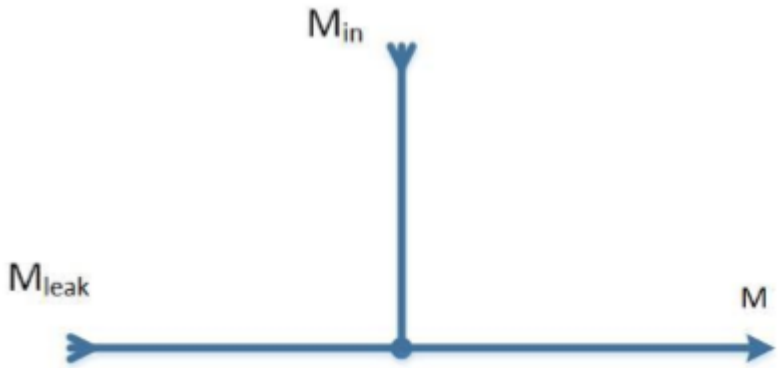

There are two inputs and one output and the equation that describes the adiabatic mixing is the following:

$$\dot{M}_{in} \cdot h_{ex} + \dot{M}_{leak} \cdot h_{su2} = \dot{M} \cdot h_{ex1}$$

The pressure is assumed to remain constant during the process.

5. Exhaust heat transfer

In the most cases the working fluid is at a lower temperature than the expander's shell. Consequently, this heat transfer is usually a heating and it occurs from the shell to the fluid. The equation of the heat transfer is expressed as:

$$\dot{Q}_{ex} = \dot{M} \cdot C_p \cdot (\dot{T_{ex2}} - T_{ex1})$$

As in the case of the supply heat transfer we use the ε-NTU method to compute the heat flow:

$$\dot{Q}_{ex} = \varepsilon_{ex} \cdot \dot{M} \cdot C_p \cdot (T_w - T_{ex1})$$

$$\varepsilon_{ex} = 1 - e^{-\frac{AU_{ex}}{\dot{M} \cdot C_p}}$$

Another analogy with the supply cooling is the fact that the heat transfer coefficient AU_{ex} varies according to the mass flow rate. Therefore, we need to define a nominal heat transfer coefficient $AU_{ex,n}$ that corresponds to the nominal mass flow rate M_n. The evolution of the heat transfer coefficient is assumed to be:

$$AU_{ex} = AU_{ex_n} \cdot \left(\frac{\dot{M}}{\dot{M}_n}\right)^{0,8}$$

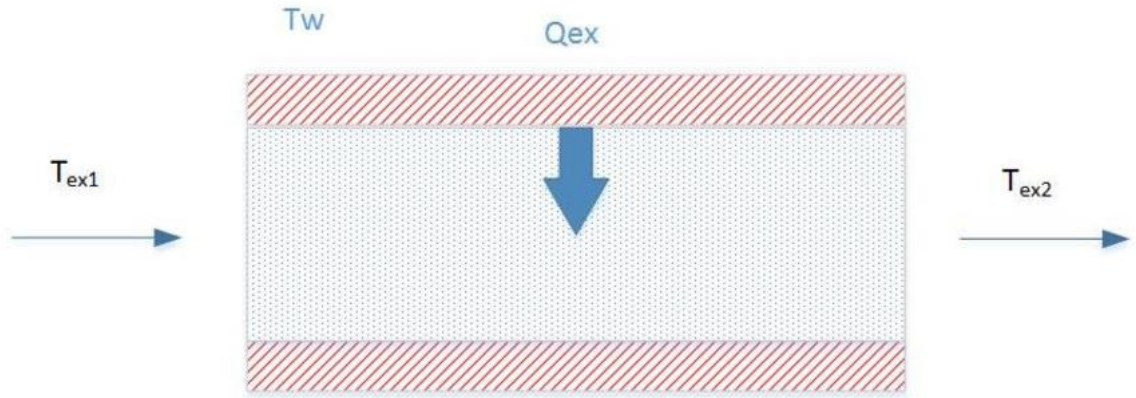

The main heat transfers that occur inside this kind of expander affect

- The expander shell and the fluid in the supply and exhaust pipes
- The scroll (fixed and orbiting) and the fluid in the suction, expansion and discharge chambers
- Between the shell and the ambient

6. Mechanical losses

The work produced by the expander W_{in} is not fully available to the shaft due to the mechanical losses W_{loss}. These losses are mainly caused by friction losses in the reciprocating mechanism, between the springs and the jacket as well as in the bearings of the crankshaft.

$$\dot{W}_{sh} = \dot{W}_{in} - \dot{W}_{loss}$$

According to [37] the friction losses of the machine are separated into:

- Losses depended on the cylinder load (cylinder pressure)

- Losses depended on the speed of the piston

In this model we simplify and we gather up all these losses in one factor: T_{loss}, mechanical loss torque. This parameter needs to be computed through the calibration. It is assumed that this parameter is independent of the rotational speed and the pressure. The shaft powers is, th us, defined as:

$$\dot{W}_{sh} = \dot{W}_{in} - 2 \cdot \pi \cdot N_{rot} \cdot T_{loss}$$

The mechanical efficiency of the expander is defined as:

$$\eta_m = \frac{\dot{W}_{sh}}{\dot{W}_{in}}$$

For this kind of expanders the mechanical efficiency is usually around 0,85.

7. Overall heat balance

A unique value of the temperature T_w was assumed to prevail at the machine shell in order to describe the heat transfer between the expander's shell and the fluid in a simple way. This temperature can be found by the thermal equilibrium of the expander in steady state operation. The expander's heat losses to the environment are described by introducing a total heat transfer coefficient AU_{amb} between the envelope and the ambient:

$$\dot{Q}_{amb} = AU_{amb} \cdot (T_w - T_{amb})$$

T_{amb} is the temperature of the ambient and $AU_{ambi\ s}$ the heat transfer coefficient of the ambient. As the others heat transfer coefficients, AU_{amb} is computed by the calibration of the model. The mechanical losses can be considered as heat released to the machine so that we can yield the overall heat balance of the expander:

$$\dot{W}_{loss} - \dot{Q}_{ex} - \dot{Q}_{su} - \dot{Q}_{amb} = 0$$

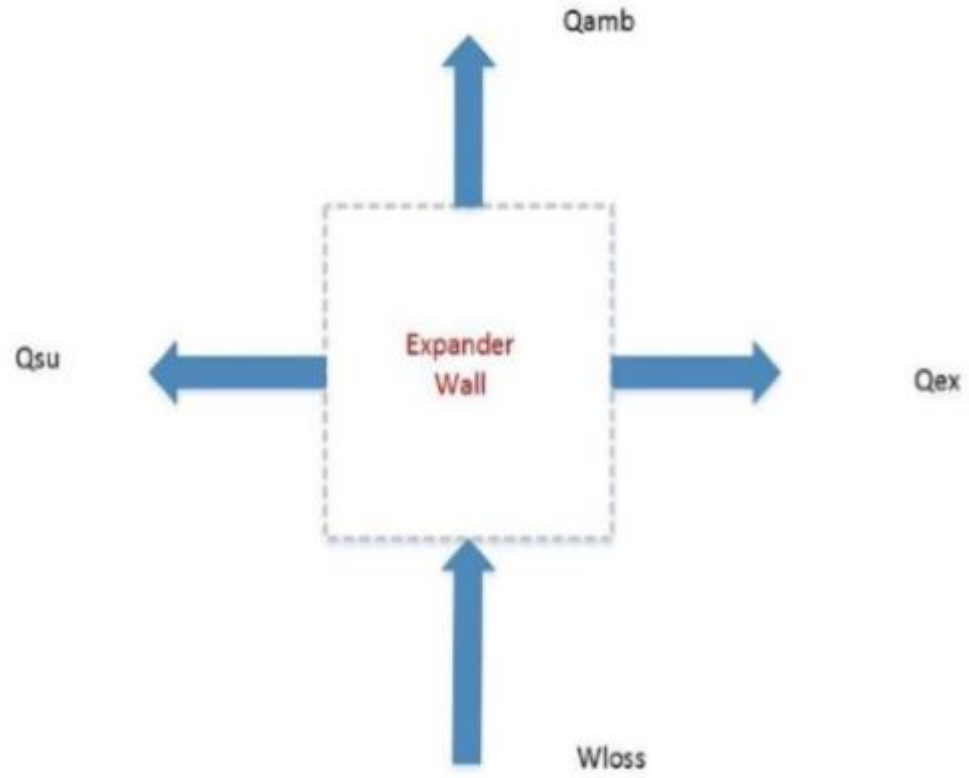

The value of the temperature of the expander's shell T_w is computed by the supply and exhaust heat transfers between the shell and the refrigerant as well as between the shell and the environment and by the mechanical losses.

8. Efficiency

The isentropic efficiency is one of the most important parameters for the analysis of the expander. This efficiency is the ratio between the real work obtained and the maximum work achievable by the expander in isentropic conditions.

$$\eta_{is} = \frac{W_{sh}}{\dot{M} \cdot \left(h_{su} - h_{ex_{is}}\right)}$$

$h_{ex,is}$ is the enthalpy at the end of the ideal isentropic expansion up to the exhaust pressure P_{ex}.

5.2 CALIBRATION

In this section the calibration of the model of the expander is explained and the analysed parameters are identified.

The model described above uses many parameters to analyse the different processes which occur inside the expander. These parameters need to be computed so as to make the EES correspond as much as possible to the actual operation of the real expander. The identification of these parameters is the so-called calibration of a semi-empirical model: knowing the experimental data (inputs and outputs) allows us to understand how to change the guess values of the parameters in order to obtain an EES model that suits the real expander.

With the calibration we need to compute the following variables:

- AU_{amb}

- AU_{ex}

- AU_{su}

- A_{leak}

- A_{su} (d_{su})

- T_{loss}

- V_s

- $r_{v,in}$

The deviation from the experimental values is identified using the error:

$$Error = \sqrt{\sum_{1}^{N}\left(\frac{\dot{M}_{calc}-\dot{M}_{exp}}{\dot{M}_{exp}}\right)^2} + \sqrt{\sum_{1}^{N}\left(\frac{\dot{W}_{sh_{calc}}-\dot{W}_{sh_{exp}}}{\dot{W}_{sh_{exp}}}\right)^2} + \sqrt{\sum_{1}^{N}\left(\frac{T_{ex_{calc}}-T_{ex_{exp}}}{T_{ex_{exp}}}\right)^2}$$

For N experimental points the variances between the experimental and the calculated values of the mass flow rate, the shaft power and the outlet temperature, which are the main model outputs, are summed. In this case N=20. Using this method the parameters are determined in order to minimize the Error. Having many experimental points allows

for a better model calibration while the computational cost rises. The process of the model calibration can be schematized as:

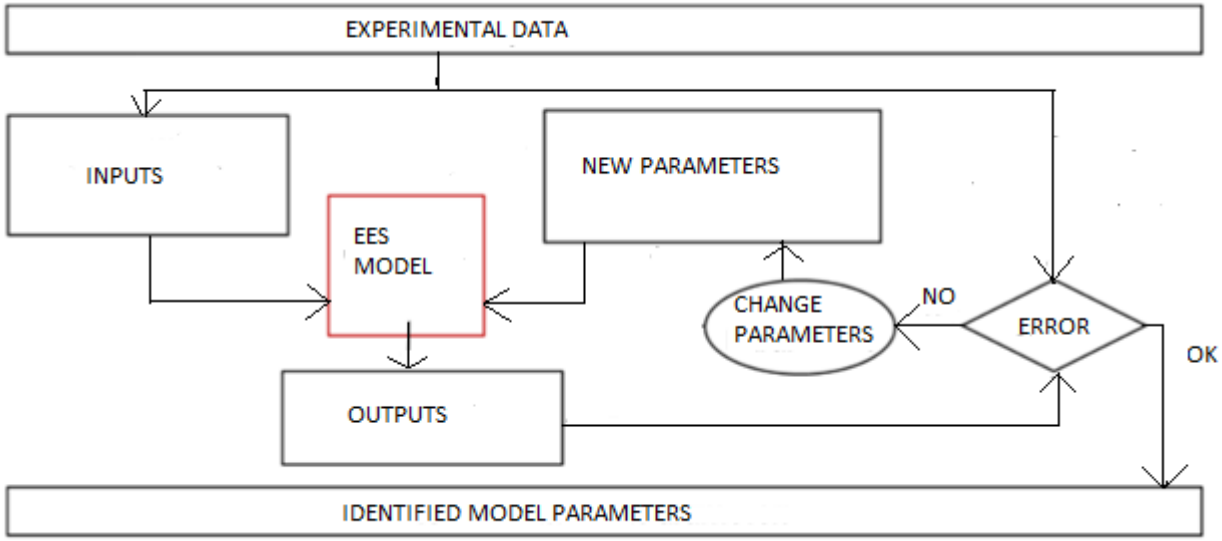

The maximum total error must be lower than 20%.

The error is made up of three terms:

$$\sqrt{\sum_{1}^{N}\left(\frac{\dot{M}_{calc}-\dot{M}_{exp}}{\dot{M}_{exp}}\right)^{2}}$$, that corresponds to the error correlated to the mass flow rate

$$\sqrt{\sum_{1}^{N}\left(\frac{T_{ex_{calc}}-T_{ex_{exp}}}{T_{ex_{exp}}}\right)^{2}}$$, that corresponds to the error correlated to the outlet temperature

$$\sqrt{\sum_{1}^{N}\left(\frac{\dot{W}_{sh_{calc}}-\dot{W}_{sh_{exp}}}{\dot{W}_{sh_{exp}}}\right)^{2}}$$, that corresponds to the error correlated to the outlet power and that is usually the most critical.

The total error obtained with the calibration is 19,5 % and it is divided in:

- 3 % is the error of the mass flow rate

- 3,5 % is the error of the temperature

- 13 % the error of the power

The following graphs allow us to understand the validity of the calibration. In fact, the values computed with the EES model are very similar to the ones obtained experimentally.

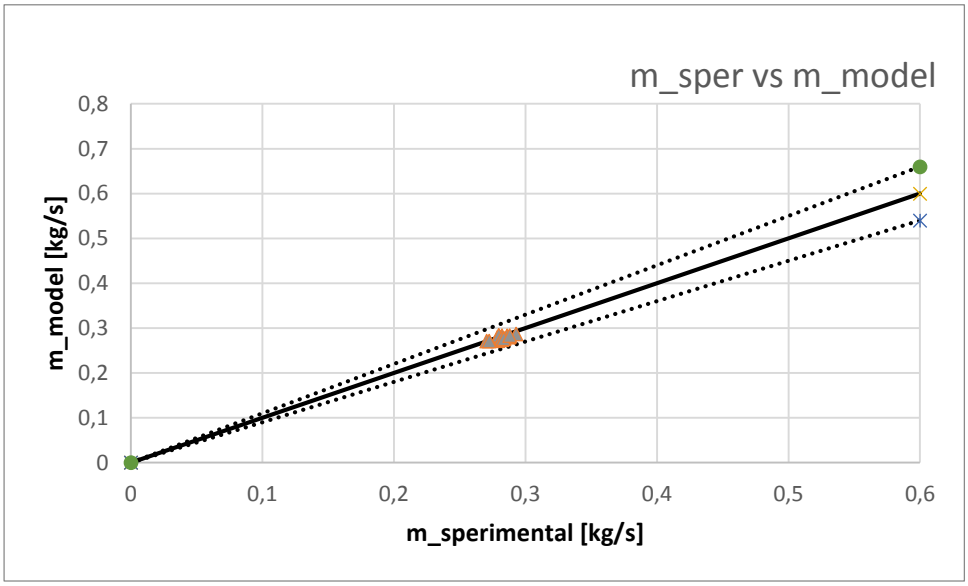

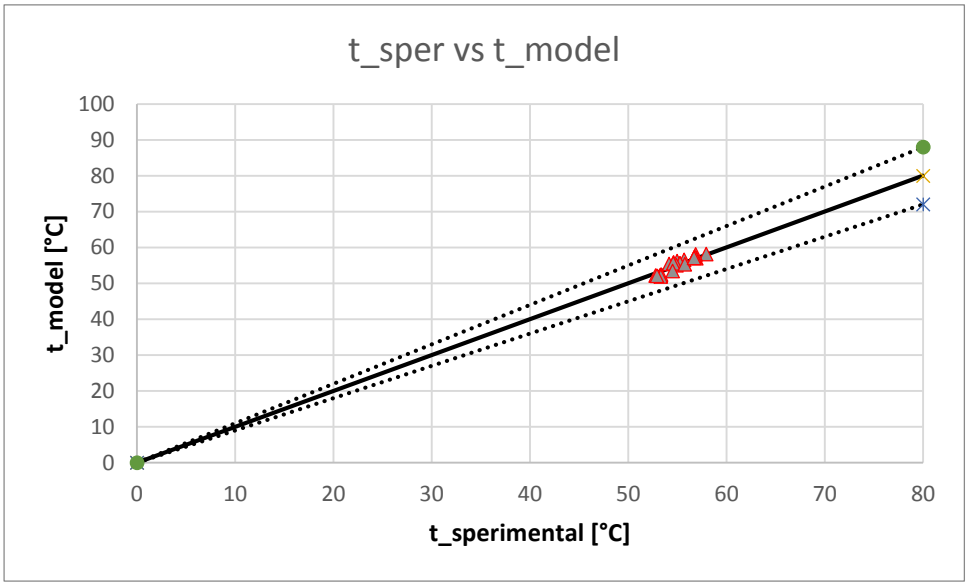

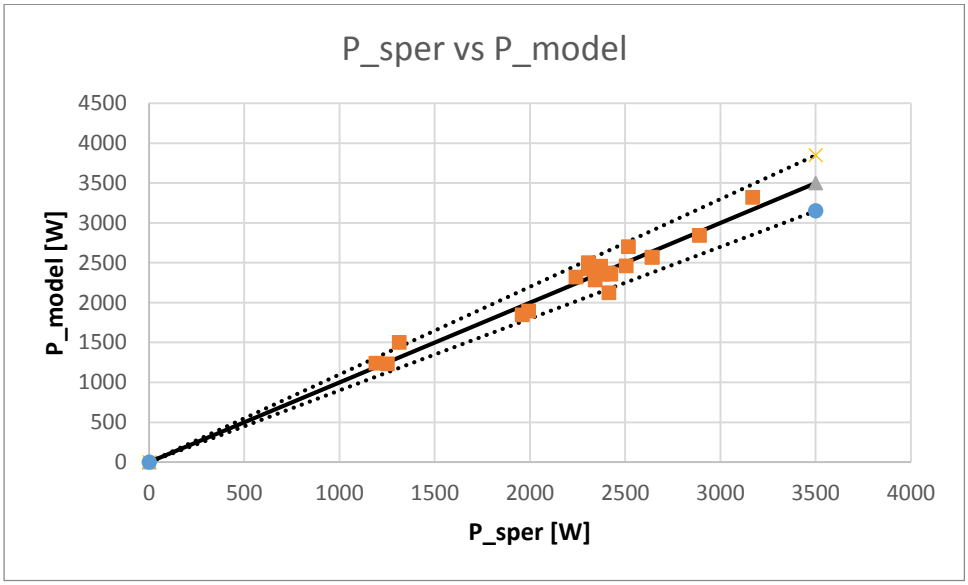

Figure 20: Errors obtained with the calibration of the model

The continuous lines represent an error between the experimental results and the obtained results of 0% while the dashed lines represent an error of 10%. The errors for the mass and the temperature are very low and they are never closed to the lines of 10%. Conversely, the power presents higher errors and in two cases the value is out of the dashed lines.

The values of the power are calculated with a mechanical efficiency calculated by the model and an electric efficiency assumed 0,95 as before. The evolution of the mechanical efficiency is described in 4.3.3

5.3 RESULTS AND COMPARISON

In this section, the performances obtained with the calibrated model are reported and discussed. In particular, in the first part, the isentropic efficiency of the expander is studied in different conditions. This efficiency and the filling factor are compared to the results obtained with the previous EES model. The mechanical efficiency obtained with the new model is reported and analysed. At the end of this part the power of the expander is compared to the one obtained before in the same 3 studies of 3.2.3.

5.3.1 ISENTROPIC EFFICIENCY

In this part, the isentropic efficiency calculated using the EES model of the expander is analysed and compared with the values computed by the previous EES model. The evolution of this performance in different conditions is described through some graphs.

The design point is at a high pressure of 25 bar, a temperature of 82°C and a rotational speed of the scroll of 1500 rpm. The effects of changing alternately the high pressure, the temperature at the inlet conditions of the scroll and the rotational speed is analysed separately. The isentropic efficiency is studied as a function of the pressure ratio.

In the first case only the high pressure changes and there are four cases: 24; 25; 26 and 27 bar. It can be noticed from the curves that greater values of pressure correspond to greater values of the isentropic efficiency of the scroll. The maximum values obtained are respectively 65.02% with a high pressure of 24 bar and a pressure ratio of 3,2, 66.04 % with a high pressure of 25 bar and a pressure ratio of 3,333, 67.34 % with a high pressure of 26 bar and a pressure ratio of 3,467, 68.79 % with a pressure ratio of 27 bar and a pressure ratio of 3,6. Increasing the high pressure from 25 bar to 27 bar improve the maximum value of the isentropic efficiency of 2,75%. However, greater is the value of the high pressure, more important is the decrease of the isentropic efficiency distancing from the pressure ratio that maximize the efficiency even though the differences are low.

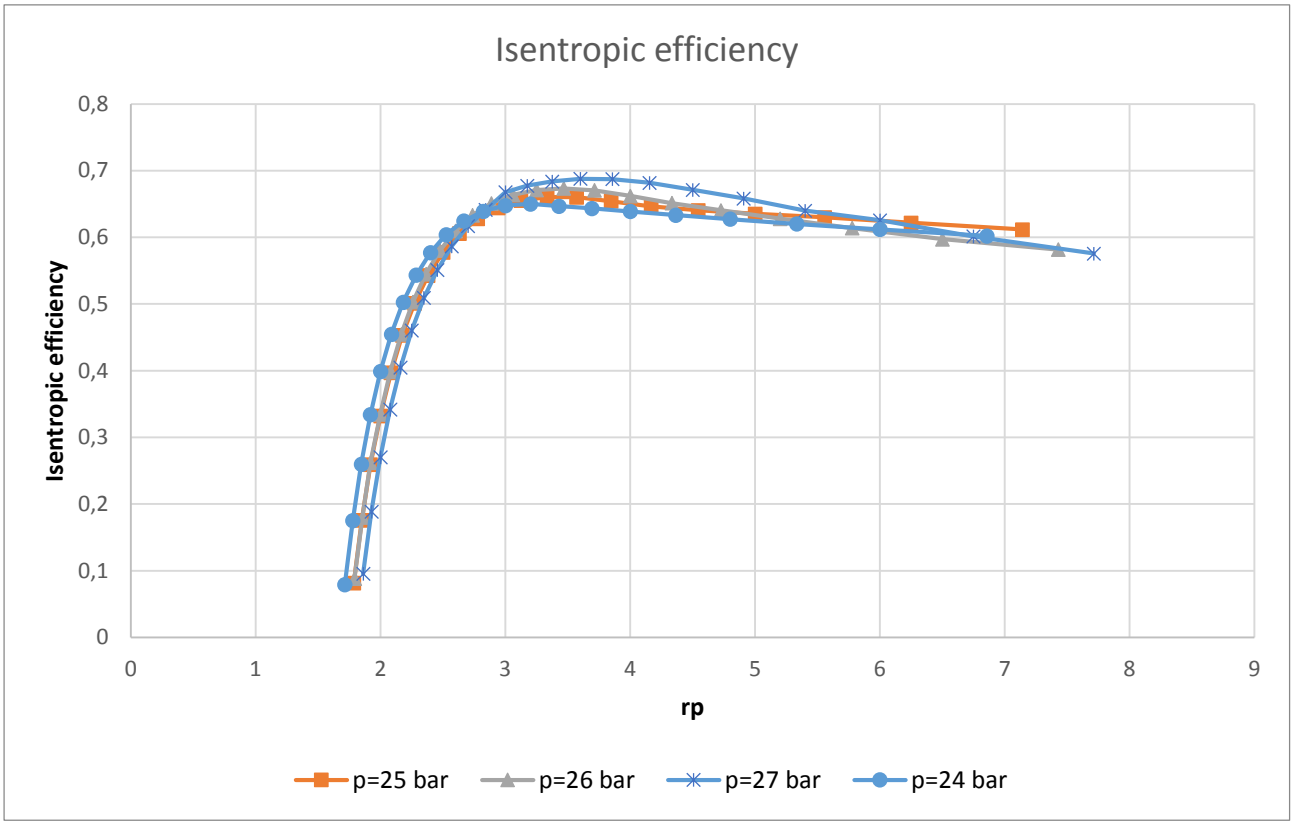

Figure 21: Isentropic efficiency with different values of the high pressure

In the second case the scroll inlet temperature varies and four cases are studied: 78, 80, 82 and 84°C. This variable affects quite significantly the isentropic efficiency of the expander. In particular, more its value, less the isentropic efficiency. It is interesting to notice that the maximum value of the isentropic efficiency of the scroll gets greater as the temperature gets lower. In fact, the maximum value is obtained as the inlet temperature is 78°C and it is 67,91%. When the inlet temperature is 84°C the maximum value obtained is 65,36% so that the difference is 2,55%.

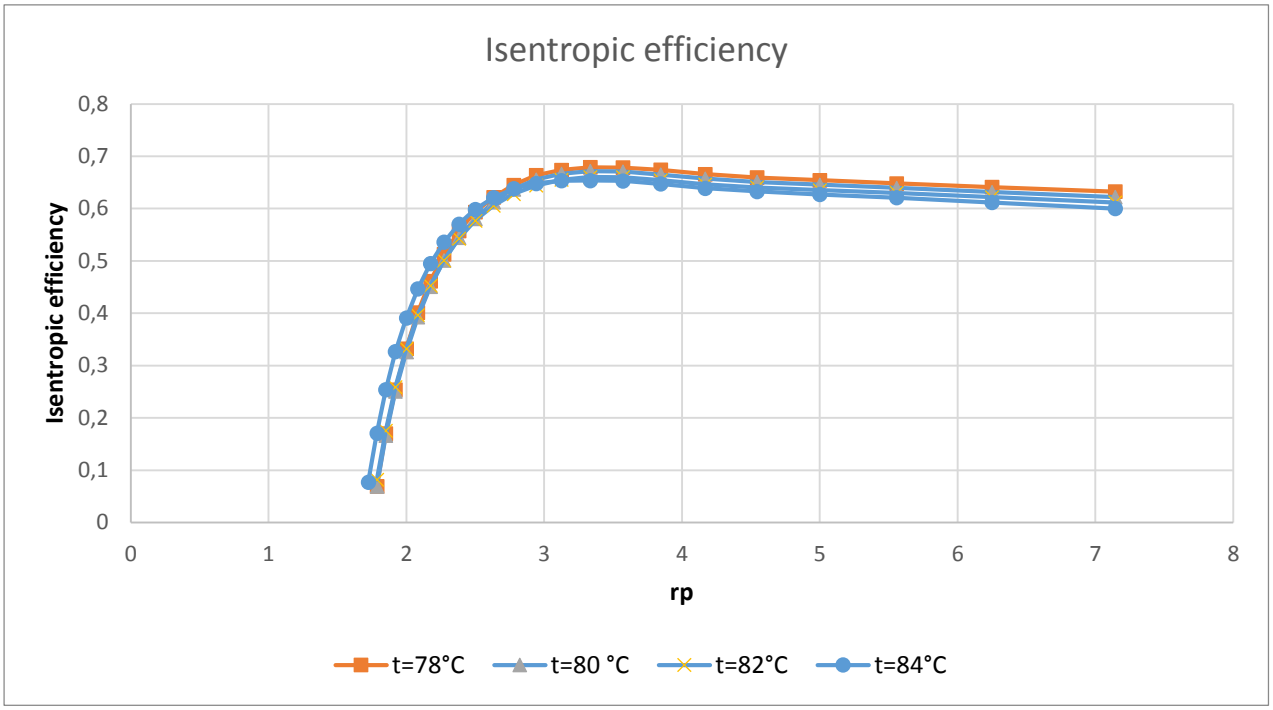

Figure 22: Isentropic efficiency with different values of the inlet expander temperature

In the third and last case the rotational speed changes and four cases are examined: 1300; 1400; 1500 and 1600 rpm. The maximum value is obtained as the rotational speed is 1300 rpm and it is 67,66% while with 1600 the maximum value obtained is 65,27

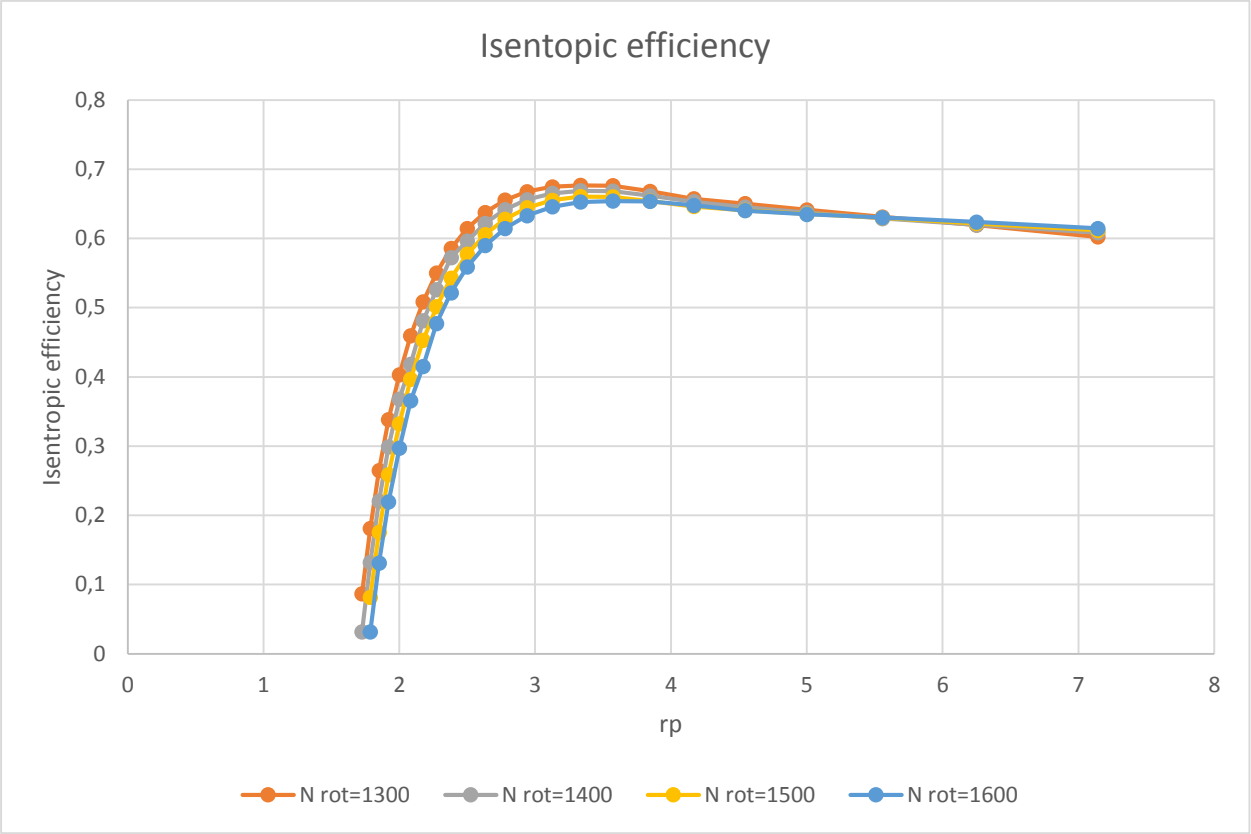

Figure 23: Isentropic efficiency with different values of the rotational speed

With a high pressure of 27 bar, an inlet temperature of 78°C and a rotational speed of 1300 rpm we obtain an isentropic efficiency of 69,3%.

For the comparison with the isentropic efficiency obtained with the first EES model we consider the curve with high pressure 25 bar, temperature of 82°C and rotational speed of 1500 rpm.

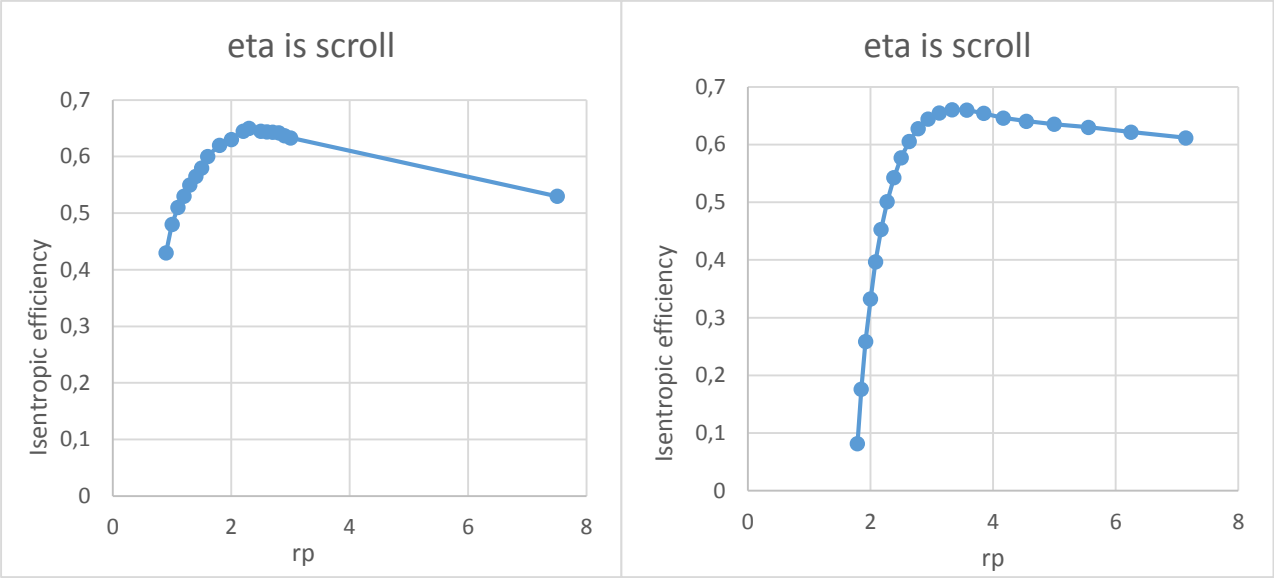

Figure 24: Comparison of the isentropic efficiency with different EES models

The maximum values are very similar: 65% in the first case and 66,04 % in the second one. Besides, the evolutions are quite the same although in the left case the decrease of the efficiency is more important as the pressure ratio improves.

5.3.2 FILLING FACTOR

A comparison between the filling factor obtained with the new EES program and the one obtained from the one in 3.2.3 is presented in this paragraph. The conditions are the same in both cases: high pressure 25 bar and inlet temperature of 82°C while the rotational speed varies from 700 to 3000 rpm.

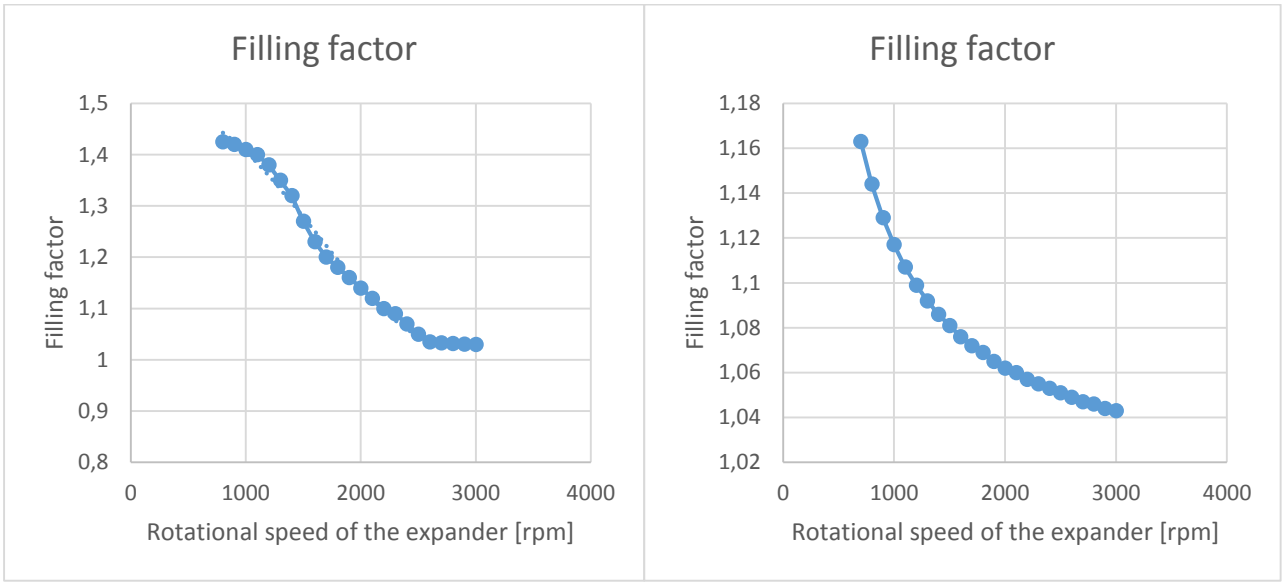

Figure 25: Comparison of the filling factor with different EES models

The difference is very important between the two graphs. Both values and evolution are far. In the first case the maximum value is 1,43 and the lowering of the filling factor is quite big until an inflection point, then it gets more constant. In the second case the maximum value is 1,163 and the evolution is more continuous; the value of the filling factor lowers gradually less as the rotational speed gets greater.
The only similarities are:

- The filling factor gets lower as the rotational speed improves
- With high values of rotational speed of the scroll its values are almost constant and very closed to 1.

5.3.3 MECHANICAL EFFICIENCY

Before analysing the power of the expander, there is a comparison between the mechanical efficiency obtained with the model of the scroll and the one assumed before. In the previous model the mechanical efficiency is assumed constant at 0,94. In the new model it is described as a function of the rotational speed of the expander as shown by the following curve:

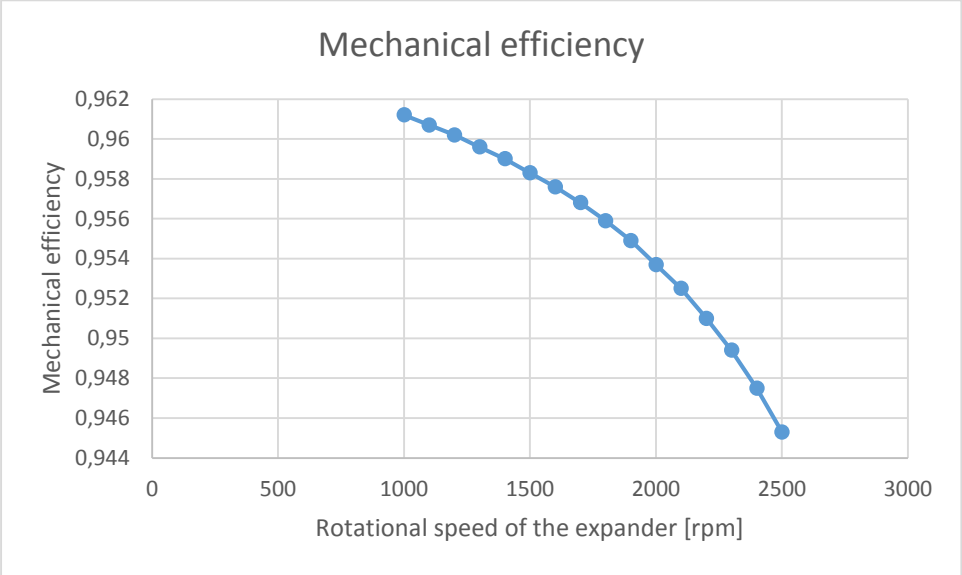

Figure 26: Mechanical efficiency obtained with the calibrated model

The value of the mechanical efficiency ranges from 0,961 to 0,945. Therefore, the assumption made before is quite valid. As expected, the efficiency lowers as the rotational speed increases, even though its value remains high.

5.3.4 POWER OF THE EXPANDER AND NET POWER

In this section the power of the expander calculated after the model calibration and the one obtained with the preceding model are compared.

Three cases are analysed, as in 4.2:

- Condensation temperature variable
- High pressure variable
- Temperature at the inlet conditions of the expander variable

- CONDENSATION TEMPERATURE VARIABLE

The condensation temperature varies in the range 10-35°C. It is mutually correlated to the condensation pressure. The power is represented as a function of the pressure ratio. The high pressure is fixed at 25 bar, while the condensation pressure changes with the condensation temperature. The evolution of the power is described by the following graph:

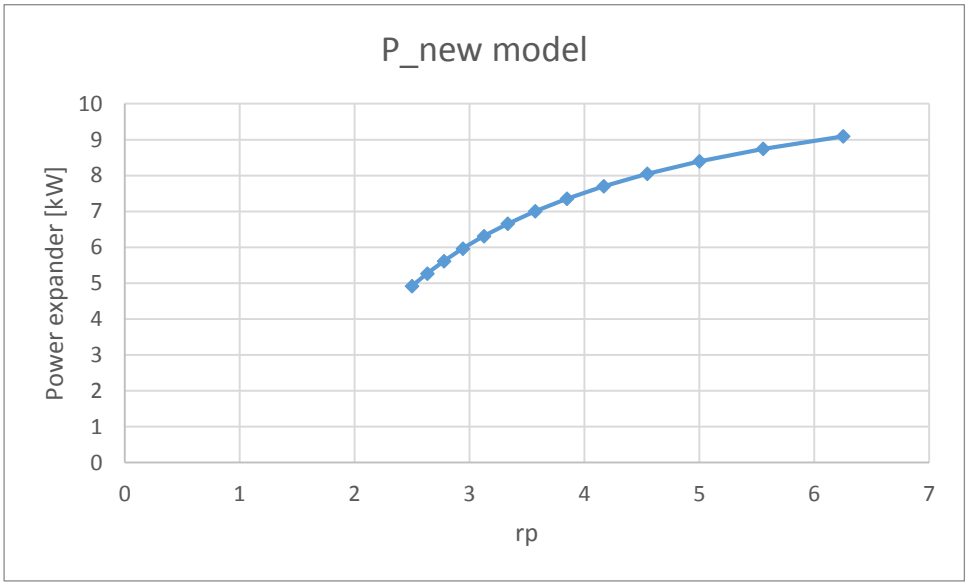

The comparison with the results obtained previously is:

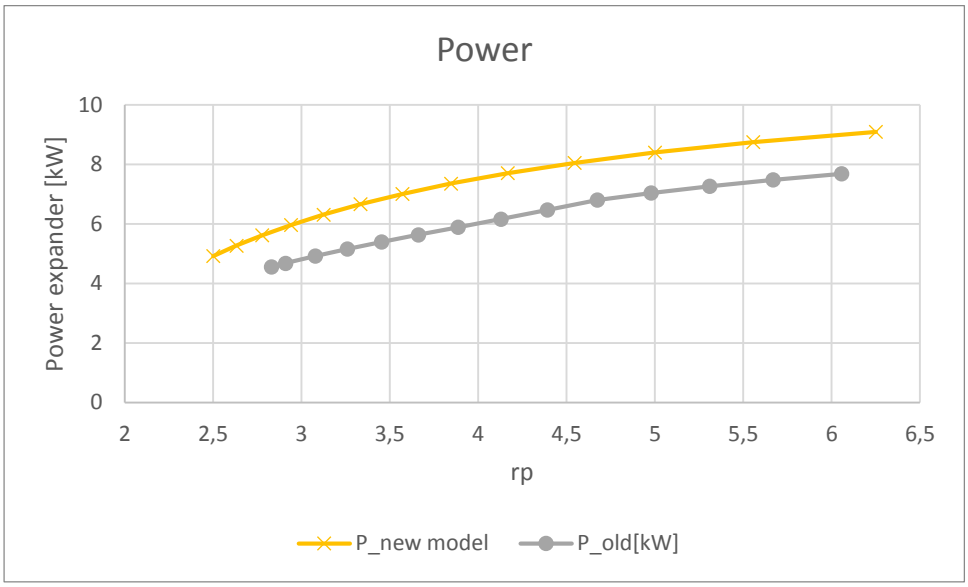

The trend is very in this comparison, especially with high values of pressure ratio. The values of the power achieved with the detailed model are higher compared to the previous ones. The evolution of the results obtained with the old model is more similar to a straight line as rp is lower than 5.

- HIGH PRESSURE VARIABLE

The high pressure ranges from 20 to 27 bar while the condensation pressure remains 9,5 bar.

The power is represented as a function of the high pressure.

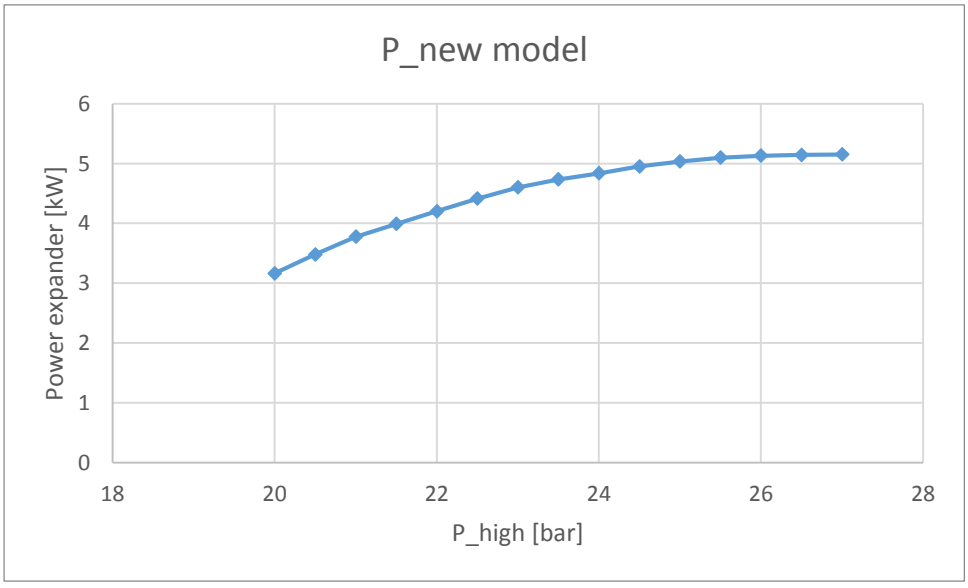

The comparison is:

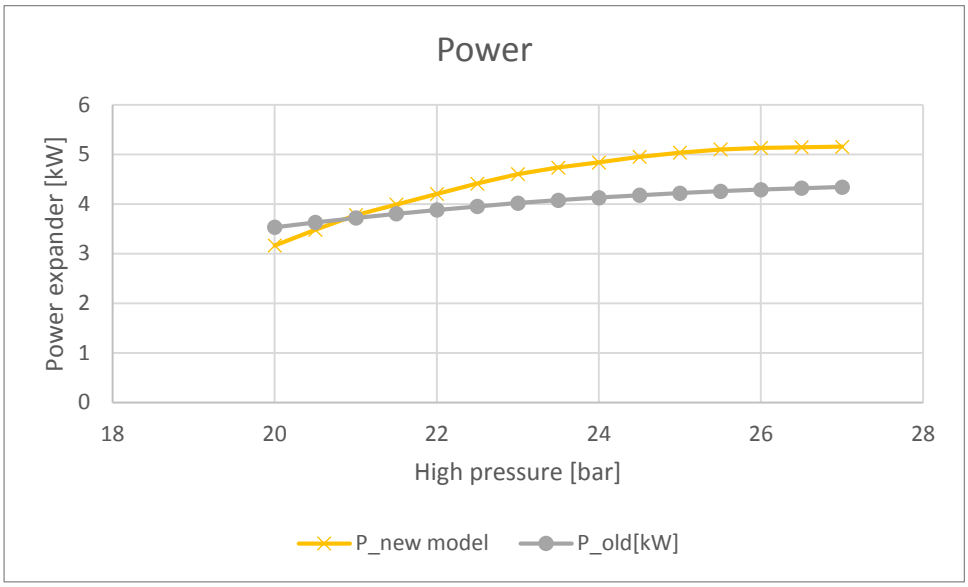

In this case the evolution and the values are quite different. Despite the fact that both the model have an increasing trend, the evolutions are quite different. In the old model the values of the power vary less than 1 kW from 20 bar to 27 bar, while in the new model the difference is around 2 kW. It means that the influence of the high pressure is much greater in the second case so that this parameter gets more important.

- TEMPERATURE AT THE INLET CONDITIONS OF THE EXPANDER VARIABLE

In this comparison the temperature at the inlet conditions of the scroll ranges from 78 to 85°C. The power is studied as a function the inlet temperature.

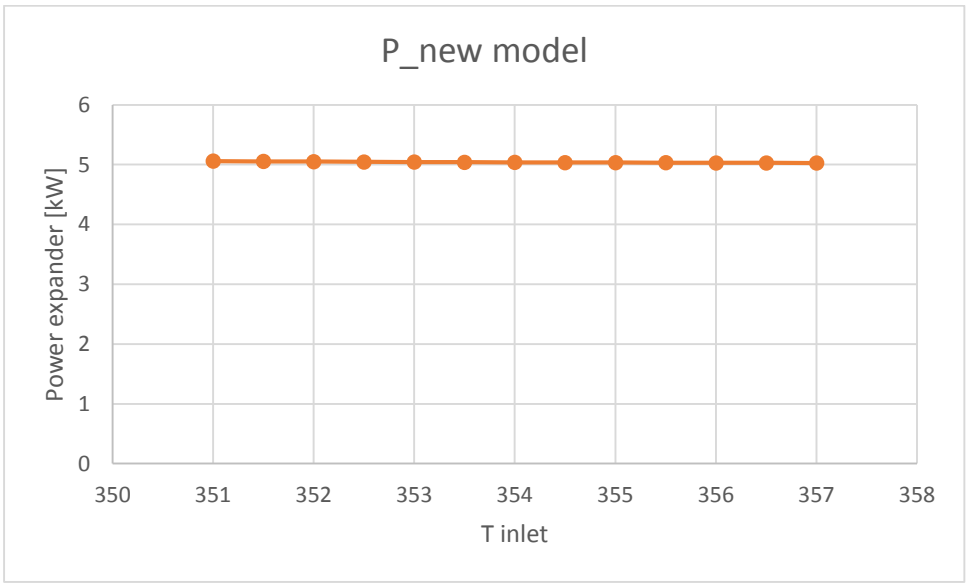

The comparison is:

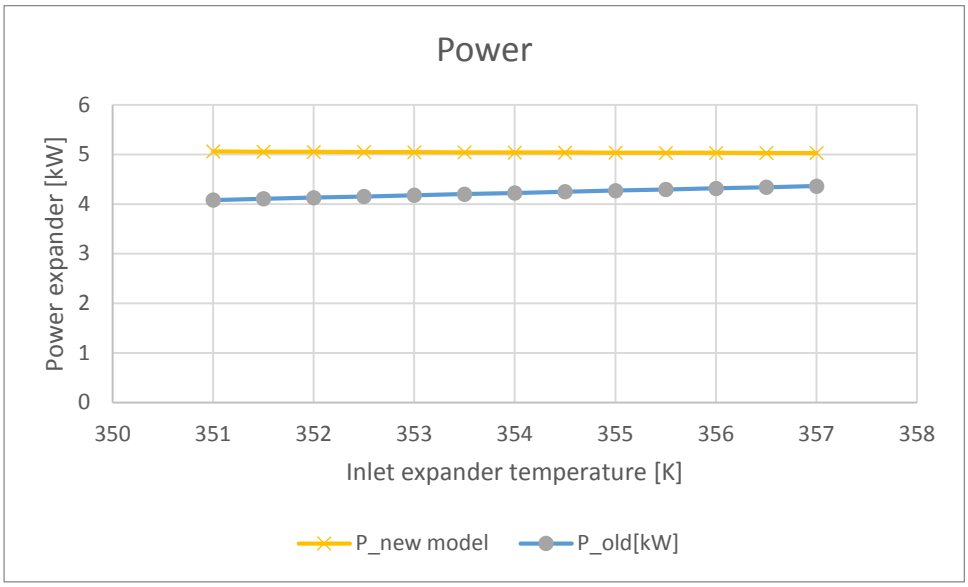

The comparison shows a difference between the trends. The results of the old model reveal an increase as the inlet temperature improves. Conversely, the new model has a decreasing trend even though the values are almost constant. The two models obtain similar results as the inlet temperature gets higher.

The net power is studied for the same three cases and using the power of the pump obtained before.

- CONDENSATION TEMPERATURE VARIABLE

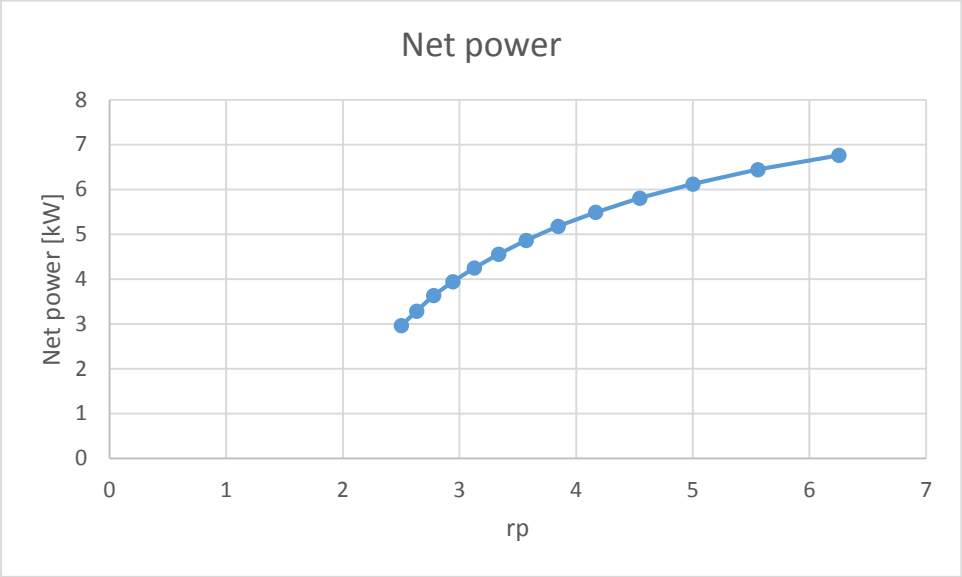

- HIGH PRESSURE VARIABLE

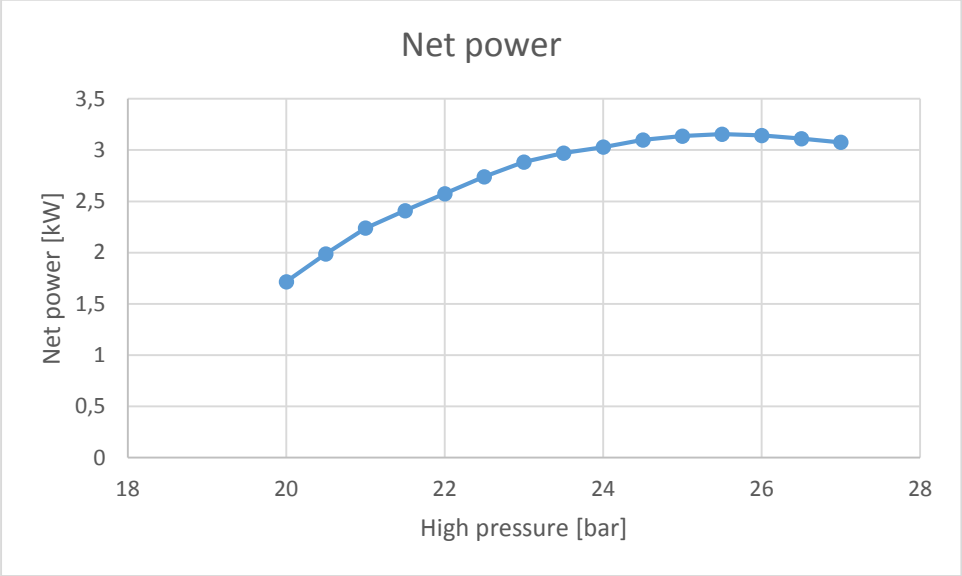

- TEMPERATURE AT THE INLET CONDITIONS OF THE EXPANDER VARIABLE

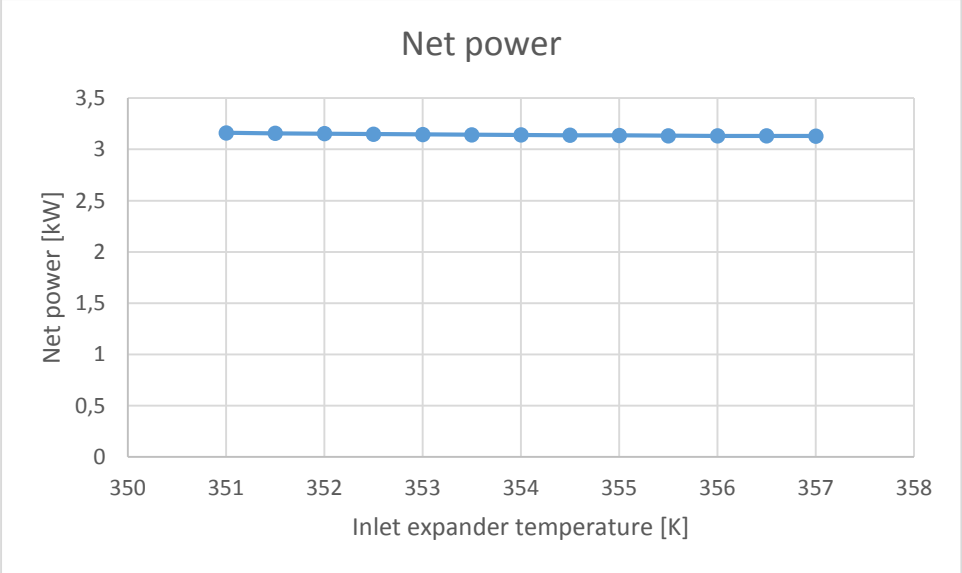

Despite the values are different, the considerations about the net power are the same made in the chapter 3. The only difference is that the inlet expander temperature does not affect significantly the net power that can be considered almost constant as the temperature varies in this range.

5.4 CONCLUSION

In this chapter, the scroll expander has been studied accurately and some assumptions made before have been corrected. The results obtained with the calibration are very similar to the experimental values as shown by the graphs in 4.2. At the design point, the net power obtained is 3,13 kW that corresponds to a total recovery efficiency of 2,5% while before the net power was 2,32 kW that corresponds to a total recovery efficiency of 1,85%. The realization of this model of the expander is fundamental for the study since the most important parameter is the net power. The consideration made at the end of the chapter 3 can be reconsidered after the realization of the EES model of the expander. Regarding the pressure ratio and the high pressure, the values are different but the conclusions are still valid and further developments are evaluated in the next chapter. For the inlet expander temperature, instead, the considerations are completely different since the fact that the expander and net power are only a very little affected by the change of this parameter.

6 FURTHER DEVELOPMENTS

In this chapter the possible developments mentioned in the previous chapters are analysed. The aim is to obtain the maximum net power from the waste heat. The studies of the ORC system and the scroll expander have shown the possibility of changing the working conditions so as to increase the net power. At the design point, the net power is 3,13 kW that corresponds to a total heat recovery of 2,5%. Two possible developments are analysed in this chapter:

- increasing the pressure ratio

- increasing the mass flow rate of the working fluid and, therefore, the heat input

The problems connected with these developments are considered and some solutions are proposed.

6.1 PRESSURE RATIO

In this section, the possibility of changing the pressure ratio is taken into account. The problems regarding the operation with high values of pressure ratio are considered. The graphs obtained before have shown that the increase of the pressure ratio affects strongly the value of the net power of the cycle. The increase of the power is constant with the increase of the pressure ratio. However, it must be considered that high values of pressure ratio mean low values of condensation pressure and, therefore, low values of the condensation temperature. With a pressure ratio of 6,25 the condensation temperature would be 10°C. In this case, the temperature of the water of the condensation circuit would be too low.

6.1.1 PROBLEMS OF R134a

As just mentioned, R134a is not suitable to operate with high values of pressure ratio due to the fact that it would require very low temperature of the water of the cold circuit. In addition to that this organic fluid presents another problem related to the GWP. R134a is a very well-known fluid due to its wide use in these last years. It took CFC-12's place in the domestic refrigeration and in the vehicles air conditioning. This refrigerant belongs to the HFC and its ODP is zero. However, it presents some problems that can't be ignored and that will probably lead us to substitute it. The main problem is its high value of GWP (global warming potential), that is around 1300.

Regarding the vehicles air conditioning, from the 1st of January 2011 the MAC (mobile air condition systems) legislation entered into force and since then it has been forbidden the use of refrigerants with GWP higher than 150 in new vehicles. Therefore, new vehicles could not use R134a anymore. This means that another refrigerant needed to be found.

6.1.2 OTHER WORKING FLUIDS

In this section some other organic fluids are analysed and evaluated as substitutes of R134a. The fluids taken into account in this part are the following:

- R1234yf
- R1234ze
- R245fa

R134a presents the following characteristics:

Saturation temperature at 25 bar: 77,5°C

Saturation temperature at 4 bar: 9°C

A high pressure of 25 bar and a low pressure of 4 bar correspond to a pressure ratio of 6,25 that is the maximum value analysed in the work.

R1234yf has substituted the R134a for the new vehicles air conditioning since the 1st of January 2011. In fact, it belongs to the HFO, that present low values of GWP, and its value is 6. However, the characteristics of this fluid are very similar to the ones of R134a and the problems about the temperature of condensation with high pressure ratios remains. In fact, a condensation pressure of 4 bar corresponds to a temperature of about 7 °C. The saturation temperature at 25 bar is 79,5°C. Therefore, with the same pressure ratio the temperatures are not suitable.

R1234ze has a low value of GWP and a low level of flammability with high temperatures. The values of temperature obtained are:

Saturation temperature at 25 bar: 90,5°C

Saturation temperature at 4 bar: 18°C

In this case the value of the condensation temperature is higher and it could be considered. Nevertheless, the value of the saturation temperature at 25 bar is too high. This means that the high pressure would be lower and the pressure ratio would decrease.

R245fa is nearly a non-toxic fluid. It presents values of flammability that must be analysed accurately for this marine ORC. It has no ODP and its value of GWP is 950. Despite the fact that this value is lower than the GWP of R134a, it is still very high compared to the other two fluids analysed above. The values obtained are:

Saturation temperature at 25 bar: 133°C

Saturation temperature at 4 bar: 55 °C

The value of the saturation temperature at 4 bar suggests the possibility to lower the condensation pressure. In fact, with a condensation pressure of 1,5 bar the condensation temperature is higher than 25°C. The saturation temperature at 25 bar is too high for the waste heat in this work. With a high pressure of 7,5 bar and a low pressure of 1,5 the values of saturation temperature are, respectively 78 and 25°C, and they correspond to a pressure ratio of 5 that cannot be reached by the other fluids. However, a further study must be carried out so as to determine the real opportunity of changing the working fluid. Indeed, changing the working fluid affects many characteristic of the cycle and the pressure is only one of the many variables that must be considered. The analysis in this chapter is only a suggestion based on the results obtained in this work.
The following table summarizes the characteristics of the fluid taken into account in this section

FLUID	ODP	GWP	SATURATION TEMPERATURE AT 25 BAR [°C]	SATURATION TEMPERATURE AT 4 BAR [°C]
R134a	0	1300	77,5	9
R1234yf	0	6	79,5	7
R1234ze	0	7	90,5	18
R245fa	0	950	133	55

Table 3: Working fluids

6.2 MASS FLOW RATE OF THE WORKING FLUID

In this section the problem of the heat input is analysed. The maximum heat that can be exploited from the water flow rate is assumed to be 125,2 kW that corresponds to the condition in which the outlet temperature of the water of the hot circuit is 20°C. As shown in the study in 3.2.2.A the heat input increases as the pressure ratio increases. With a pressure ratio of about 6 the heat input is around 91 kW. Consequently, the heat input is far from the maximum value. The problem is the mass flow rate of the working fluid, too low to exploit the available heat input. The nominal rotational speed of the pump is 960 rpm and it corresponds to a mass flow rate of 0,3899 kg/s and at the design point it corresponds to a net power of 3,13 kW and a heat input of 71,13 kW. At the same conditions, with a rotational speed of the pump of 1200 rpm the net power is 3,651 kW and the heat input is 88,1 kW, while with a rotational speed of 1400 the net power is 4,175 kW and the heat input is 101,7 kW. The heat input at the nominal conditions is too low compared to the maximum available heat due to the fact that the mass flow rate of R134a with the nominal value of the rotational speed of the pump is only 0,3899 kg/s. In order to obtain rotational speeds around 1400 rpm so that the heat input and, therefore, the net power are higher, the pump must be studied and possibly changed. In spite of the fact that the cost of this kind of pump is not high, changing the pump must be considered accurately.

7 CONCLUSIONS

The aim of this work is the study of the power plant and in particular of the expander, that is a key element that affects highly the performances of the whole cycle. The ORC system in the laboratory of the NTUA in Athens has been described and the methodology used in this work has been defined, together with all the assumptions. The selection of the expander of the cycle has been analysed and the scroll has been identified as the most suitable option regarding the cost and the availability more than the performances.

Two EES model have been realised, explained and used so as to simulate the evolution of some performances of the ORC. The most important parameter that must be considered is the electric net pump, that is the output of the power plant.

The total recovery efficiency has been defined in order to understand how the available heat is used. Despite the fact that the values of the total recovery efficiency are very low, the heat input is a waste heat flow rate and the temperatures are very low. The thermal efficiency of the ORC has a relative importance and it is not a parameter that influences highly the decisions on the working conditions.

The main work of this thesis has been made on the EES model of the scroll expander. In fact, the values of net power of the expander achieved with the first model are quite far from the experimental results and the considerations on the whole cycle could be misunderstood so that the conclusions could be wrong. The calibration of the model of the scroll expander has been used to reduce as much as possible the gap between results obtained from the EES model and the experimental results. 20 cases have been considered and the errors achieved are very low. The net power obtained at the design conditions after the calibration is 3,13 kW.

From this work, it has been carried out that the parameter that affects more the performances of the cycle is the pressure ratio. The best working conditions are far from the design point due to the fact that the power plant exploits only a little part of the available heat. The best conditions are the ones that correspond to high values of pressure ratio. With R134a and high values of pressure ratio, the condensation temperature is too low and it is not possible to operate in these conditions. An analysis of the possibility of changing the working fluid has been carried out in the chapter 5. R1234yf has shown the same problems of R134a; R1234ze has shown an evaporation temperature too high and, therefore, the pressure ratio cannot be very high; R245fa presents characteristics that are different from the other working fluids. With this last fluid it can be reached a pressure ratio of 5. However it has a level of flammability that is higher than the other fluids and the level of pressures analysed to obtain a pressure ratio of 5 are quite different from the ones studied in this work.

The heat input can be improved increasing the mass flow rate of the working fluid so that to exploit a greater part of the available heat. Nevertheless, in this case, the change of the pump must be considered.

Raising the heat input determines a decrease of the outlet temperature of the water of the hot circuit. In this work, the maximum available heat has been considered the one corresponding to an outlet temperature of the hot water of 20°C. This value and the value of the minimum outlet temperature allowed must be analysed with the particular conditions of the location of the ORC power plant on the ship.

REFERENCES

[1] Basic Principles of Ship Propulsion, MAN Diesel & Turbo SE, Copenhagen, Denmark, December 2011.

[2] Kalli, J., Karvonen, T., Makkonen, T., 2009, Sulphur content in ships bunker fuel in 2015, Technical Report, Helsinki, Finland: Ministry of Transport and communications.

[3] Larsen, U., Sigthorsson, O., Haglind., F., 2014, A comparison of advanced heat recovery power cycles in a combined cycle for large ships, Energy, vol. 74

[4] Gan, S., Ng, H.K., Pang. K.M., 2011, Homogeneous Charge Compression Ignition (HCCI) combustion: implementation and effects on pollutants in direct injection diesel engines. Applied Energy ,vol 88

[5] Yao, M., Zheng, Z., Liu, H., 2009, Progress and recent trends in homogeneous charge compression ignition (HCCI) engines. Progress in Energy and Combustion Science 2009, vol. 35

[6] Zheng, M., Reader, G.T., 2004, Energy efficiency analyses of active flow aftertreatment systems for lean burn internal combustion engines, Energy Conversion and Management, vol. 45

[7] Lu, X., Shen, Y., Zhang, Y., Zhou, X., Ji, L., Yang, Z., 2011, Controlled three-stage heat release of stratified charge compression ignition (SCCI) combustion with a two-stage primary reference fuel supply. Fuel, vol. 90

[8] Shu, G., Liang, Y., Wei, H., Tian, H., Zhao, J., Liu, L.,, 2013, A review of waste heat recovery on Two-stroke IC engine aboard ships, Renewable Sustainable Energy Review 2013, vol. 19

[9] Larsen, U., Sigthorsson, O.,Haglind., F., 2014, A comparison of advanced heat recovery power cycle for a marine Diesel engine, Energy, vol. 74

[10] Larsen, U., Nguyen, T. Knudsen, T. Haglind, F., 2014, System analysis and optimisation of a Kalina split-cycle for waste heat recovery on large marine diesel engines, Energy, vol. 64

[11] MAN, Diesel & Turbo, Denmark, 2012, Waste heat recovery systems (WHRS). URL: www.mandieselturbo.com [accessed 30.08.13].

[12] Bounefour,Ouadha, 2014, Thermodynamic analysis and thermodynamic analysis and working fluid optimiazation of a combined ORC-VCC system using waste heat from a marine diesel engine, Proceedings of the ASME 2014 International Mechanical Engineering Congress and Exposition IMECE2014 November 14-20, 2014, Montreal, Quebec, Canada.

[13] Yang, M.H., Yeh, R.H., 2014, Analyzing the optimization of an organic Rankine cycle system for recovering waste heat from a large marine engine containing a cooling water system, Energy Conversion and Management, vol. 88

[14] Jian Song, Yin Song* , Chun-wei Gu, Thermodynamic analysis and performance optimization of an Organic Rankine Cycle (ORC) waste heat recovery system for marine diesel engines

[15] Aris-Dimitrios Leontaritis, Platon Pallis, Sotirios Karellas, Aikaterini Papastergiou, Nikolaos Antoniou, Panagiotis Vourliotis, Nikolaos Matthaios Kakalis, and George Dimopoulos, 2015, Experimental study on a low temperature ORC unit for onboard waste heat recovery from marine Diesel engines.

[16] Jian Song, Yin Song, Chun-wei Gu, Thermodynamic analysis and performance optimization of an Organic Rankine Cycle (ORC) waste heat recovery system for marine diesel engines

[17] Dig Vijay Singh, Eilif Pedersen, A review of waste heat recovery technologies for maritime applications

[18] Francesco Baldi, , Ulrik Larsen , Cecilia Gabrielli, Comparison of different procedures for the optimisation of a combined Diesel engine and organic Rankine cycle system based on ship operational profile

[19] Charles Sprouse III, Christopher Depcik, Review of organic Rankine cycles for internal combustion engine exhaust waste heat recovery

[20] R. Zanelli, D. Favrat, 1994, Experimental investigation of a hermetic scroll expander generator, Proceeding of the International Compressor Engineering Conference at Purdue

[21] T. Yanagisawa, M. Fukuta, Y. Ogi, T. Hikichi, 2001, Performance of an oil-free scroll-type air expander, Proceedings of the IMechE Conference on Compressors and their Systems

[22] M. Kane, D. Larrain, D.Favrat, Y. Allani, 2003, Small hybrid solar power system, Energy 28

[23] J. Manzagol, P. d'Harboullè, G.Claudet, Gistau Baguer, 2002, Cryogenic scroll expander for Claude cycle with cooling power of 10 to 100 watts at 4.2 K, Proceedings of the Cryogenic Engineering Conference

[24] P. Gao, L. Jiang, L.W. Wang, R.Z. Wang, F.P. Song, 2014, Simulation and experiments on an ORC system with different scroll expanders based on energy and exergy analysis

[25] T. Yamamoto, T. Furuhata, N. Arai, K. Mori, 2001, Design and testing of the organic Rankine cycle, Energy 26

[26] G. Pei, J. Li, Y. Li, D. Wang, J. Ji, 2011, Construction and dynamic test of a small-scale organic Rankine cycle, Energy 36

[27] S.H. Kang, 2012, Design and experimental study of ORC and radial turbine using R245fa working fluid, Energy 41

[28] Wang XD, Zhao L, Wang JL, Zhang WZ, Zhao XZ, Wu W., 2010, Performance evaluation of a low-temperature solar Rankine cycle system utilizing R245fa, Sol Energy

[29] Badr O, Probert SD, O'Callaghan P, 1985, Multi-vane expanders: vane dynamics and friction losses, Appl Energy

[30] Subiantoro A, Yap KS, Ooi KT, 2013, Experimental investigations of the revolving vane (RV-1) expander, Appl Therm Energy

[31] Zhou N, Wang X, Chen Z, Wang Z, 2013, Experimental study on organic Rankine cycle for waste heat recovery from low-temperature flue gas, Energy

[32] S.Quoilin, 2015, Thermocycle: A Modelica library for the simulation of the thermodynamic systems

[33] E. Winandy, C. Saavedra, J. Lebrun, 2002, Eperimental analysis and simplified modelling of a hermetic scroll refrigeration compressor, Applied thermal Engineering 22

[34] Vincent Lemort, Sylvain Quoilin, Cristian Cuevas, Jean Lebrun, 2009, Testing and modelling a scroll expander integrated into an Organic Rankine Cycle, Applied Thermal Engineering

[35] N. P. Halm, 1997, Mathematical modeling of scroll compressors, Master Thesis, Purdue University, West Lafayette

[36] X. Kakatsios, 2006, Introduction to Heat and Mass Transfer, Symeon publishing group: Athens

[37] W. Z.Black, J. G.Hartley, 1985, Thermodynamics. Harper and Row, New York

Ringraziamenti

Voglio ringraziare prima di tutto il professor Andrea Lazzaretto, il quale mi ha aiutato a sviluppare e migliorare il lavoro oggetto di questa tesi.
Un ringraziamento particolare va a Sotirios Karellas, il quale mi ha seguito e aiutato durante il mio periodo ad Atene.
Voglio, inoltre, ringraziare l'ingegner Sergio Rech per gli utili consigli che mi ha dato al fine di migliorare questo lavoro.
Ringrazio anche la mia famiglia che mi ha supportato finanziariamente e moralmente.
Un caloroso ringraziamento va alla mia ragazza Giulia, che mi ha sopportato durante gli esami e la preparazione della tesi e ai miei amici ignoranti, che mi hanno sempre sostenuto nei momenti di difficoltà. Infine, ringrazio tutte le persone conosciute in Grecia, con le quali ho passato mesi bellissimi durante lo svolgimento del progetto Erasmus.